FUNCTIONAL AND MECHANISTIC INSIGHTS OF ARABIDOPIS THALIANA ARGONAUTE10 AND ITS COFACTOR RICE1 IN RNA SILENCING

A Dissertation

by

FUQU HU

Submitted to the Office of Graduate and Professional Studies of
Texas A&M University
in partial fulfillment of the requirements for the degree of

DOCTOR OF PHILOSOPHY

Chair of Committee,	Xiuren Zhang
Committee Members,	Dorothy Shippen
	Pingwei Li
	Alan Pepper
Head of Department,	Gregory Reinhart

August 2014

Major Subject: Biochemistry

ABSTRACT

Argonautes (AGOs) are central components in RNA-induced gene silencing complexes (RISCs) and control almost all aspects of developmental processes in eukaryotes. Study on AGO proteins not only elucidates the fundamental mechanism of RNA silencing but also provides a new opportunity for developing novel therapeutic strategies.

Arabidopsis thaliana encodes nine functional AGO proteins among which AGO10 is genetically involved in shoot apical meristem (SAM) development, yet the underlying mechanism remains elusive. Because AGO proteins recruit small RNAs (sRNAs) to execute their regulatory functions, we have managed to clone and sequence the sRNA library from AGO10-immunoprecipitates. We have found that AGO10 specifically binds with miR166/165, two miRNAs with a difference in a single nucleotide but targeting the same homeodomain transcriptional factors (*HD-ZIP III*). Further biochemical studies reveal that the strong preference of AGO10 to miR166/165 is due to the unique duplex structure of miR166/165. By a series of mutagenesis we were able to pinpoint the critical secondary structures which contribute to the specific AGO10-miR166/165 interaction.

We then took combination approaches of genetics and biochemistry to study the biological role of the specific AGO10-miR166/165 association. We found an increased level of miR166/165 in *ago10* mutants and the ectopic accumulated miR166/165 is redirected to AGO1, a principal regulator in various RNA silencing pathways in plants,

leading to repression of the *HD-ZIP III* transcripts and consequently the defective SAM in the mutants. However, when wild-type *AGO10* and miR166/165 target mimicry (*MIM166*) were introduced to *ago10* mutants, accumulation of both miR166/165 and their targets were restored to wild-type levels. Thus we propose that AGO10, in contrast to all other characterized AGOs, functions to antagonize miRNA while protecting the miRNA targets.

Next we explored how RISC is assembled using AGO10 as a platform. By proteomics approaches, a number of AGO10 cofactors including RISC-implanted clearance exoribonuclease1 (RICE1) were recovered. RICE1 turns out to be a 3' to 5' single strand sRNA specific exoribonuclease. Genetic and biochemical studies of *RICE1* and its paralog, *RICE2*, implicated their important role in RISC activation by clarifying miRNA* during the RISC assembly. Thus, the result provides new insights into how RISC is activated after miRNA/* duplexes are loaded into AGO proteins.

DEDICATION

I dedicate my dissertation work to my family. A special gratitude to my parents whose love and encouragement shine light into my life. I am grateful for my sister who has always been on my side and makes me never feel alone.

I also dedicate this dissertation to my husband Cong Gao for cheering me up and guiding me out of depression throughout the entire doctorate program.

ACKNOWLEDGEMENTS

First of all, I would like to thank my committee chair, Dr. Xiuren Zhang for his training, encouragement and patience during my Ph.D. period. I want to give special thanks to my committee members, Dr. Dorothy Shippen, Dr. Pingwei Li and Dr. Alan Pepper, for agreeing to be my committee and thank them for their time and support throughout the course of this research.

I would like to thank Dr. Pingwei Li, Dr. Xiuren Zhang, Dr. Tatyanan Igumenova and Dr. Craig Kaplan for allowing me to do rotations in their labs. This was an invaluable experience for me. In addition I want to extend my gratitude to Dr. Geoffrey Kapler for his critical advice and tremendous help during the course of my study.

Thanks also go to my colleagues who helped me in my research. I am grateful for my labmates and members from Dr. Shippen and Dr. Kapler's lab for sharing their opinions and ideas about my work. Finally, I want to acknowledge Dr. Chang Shu for his valuable expertise and help during my research.

NOMENCLATURE

SAM	Shoot apical meristem
RAM	Root apical meristem
DNA	Deoxyribonucleic acid
RNA	Ribonucleic acid
RNAi	RNA interference
AGO	Argonaute
sRNA	Small RNA
RISC	RNA-induced silencing complex
miRNA	MicroRNA
siRNA	Small-interfering RNA
dsRNA	Double-strand RNA
ssRNA	Single-strand RNA

TABLE OF CONTENTS

Page

Page

LIST OF FIGURES

Page

Page

Page

LIST OF TABLES

Page

CHAPTER I

INTRODUCTION AND LITERATURE REVIEW

SAM maintenance and vascular patterning in *Arabidopsis thaliana*

To successfully complete their lifetime, land plants rely on stem cells to continuously produce new organs to ensure proper development and repair of damaged tissues caused by abiotic and biotic stresses. The above-ground organs are differentiated from shoot apical meristem (SAM) while root apical meristem (RAM) gives rise to the below-ground organs.

During embryogenesis, SAM and RAM are made and they become active upon seed germination. In the dicotyledonous plant *Arabidopsis thaliana* SAM adopts a three-layer organization and stem cells are located at the tip of SAM (Reddy, 2008) (Figure 1-1). The niche of stem cells is named the central zone (CZ) and cells within this region maintain stem cell property throughout the lifecycle of the plants. A subset of stem cells divide to provide undifferentiated daughter cells to the peripheral zone (PZ) for the initiation of leaves, branches, flowers and stem. Some progeny of stem cells enter the organizing center (OC) and cells in the OC are responsible for providing cues for the stem cells in the CZ to retain their pluripotency and to prevent them from differentiation.

The two opposing fates of stem cells--to divide and generate organs for plant growth and development and to maintain the stem cell activity in SAM for new organ formation--must be precisely regulated. Failure in SAM maintenance results in growth and development abnormalities in *Arabidopsis thaliana*.

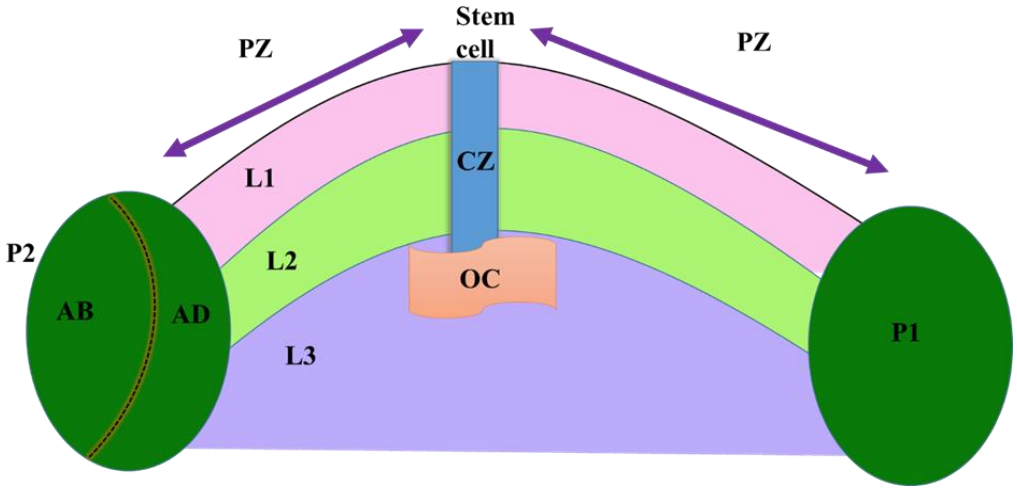

Figure 1- 1 Schematic of SAM organization.

The three clonal layers (L1, L2 and L3) are colored in pink, green, and purple, respectively. The stem-cell niche contains stem cells (the central zone; CZ), differentiating cells (the peripheral zone; PZ) and rib meristem cells (the organizing center; OC). P1 and P2 denote differentiated organ primordia. AB: abaxial side; AD: adaxial side.

Over the past two decades numerous genes affecting SAM action have been identified through genetic screening and a complex spatial-temporal gene regulatory network has been established (Barton, 2010; Xie et al., 2009; Zhang and Zhang, 2012) (Figure 1-2). *WUSCHEL (WUS)* is the central integrator for this network. *WUS* encodes a homeodomain transcription factor and is expressed in the OC (Mayer et al., 1998) and *wus* mutants lack functional SAM, suggesting that *WUS* is required for SAM

maintenance. *WUS* overexpression represses cytokinin response regulators *ARR5*, *ARR6* and *ARR7* (Leibfried et al., 2005) and this may explain how WUS specifies stem cell identity and inhibits stem cell differentiation. The *CLAVATA (CLV)* class of genes including *CLV1*, *CLV2* and *CLV3* forms a signaling pathway to repress *WUS* expression (Muller et al., 2006; Reddy and Meyerowitz, 2005) and *clv* mutants have enlarged SAM. Interestingly, *WUS* is able to enhance *CLV3* expression and this entails a negative feedback loop for *WUS* in SAM regulation (Barton, 2010; Schoof et al., 2000). *SHOOT MERISTEMLESS (STM)*, which encodes a KNOTTED1-like HOMEOBOX (KNOX) transcription factor, is expressed in CZ and PZ region and *stm* mutants also fail to maintain SAM (Barton and Poethig, 1993; Long and Barton, 1998; Long et al., 1996). *STM* has been proposed to repress the differentiation of stem cells in the SAM through repression of *ASYMMETRIC LEAVES1 (AS1)*(Byrne et al., 2002). Taken together, *WUS* and *STM* function to promote stem cell proliferation while *CLV* genes stimulate stem cell differentiation.

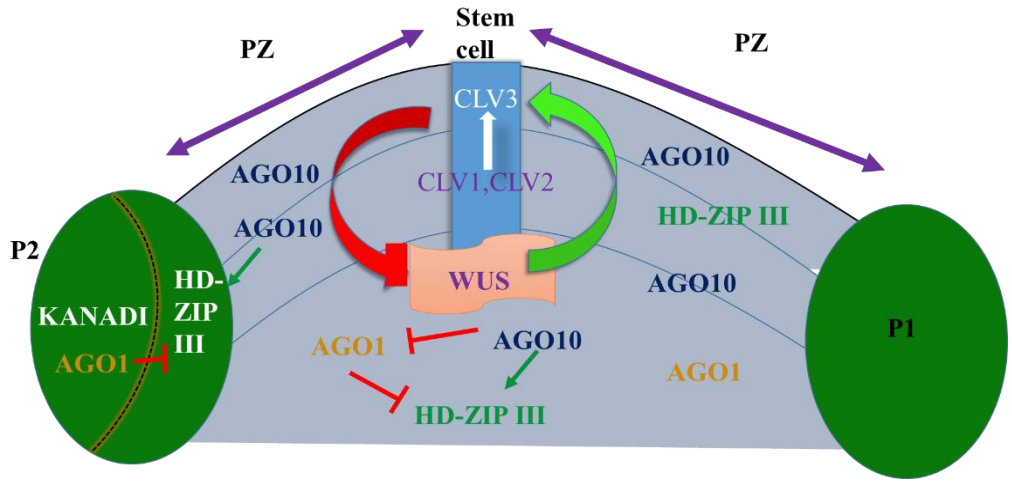

Figure 1- 2 Schematic representation of gene regulatory network in SAM maintenance. Genes are shown in their respective expression domains. *CLV* genes and *WUS* form a feedback network to restrict WUS expression in the OC. *AGO10* and *AGO1* in the SAM regulate the expression of *HD-ZIP III* genes with opposing effects. In organ primordia (P2), the *HD-ZIP III* expression region is specified in the adaxial side while *KANADI* family genes are expressed in the abaxial domain of primordia.

Besides the genes discussed above, genes expressed outside of the SAM also play important roles in SAM regulation (Barton, 2010; Xie et al., 2009). In *Arabidopsis thaliana*, five *Class III homeodomain-leucine zipper* (*HD-ZIP III*) transcription factors - *PHABULOSA (PHB), PHAVOLUTA (PHV), REVOLUTA (REV), CORONA (CNA)* and *ATHB8*- have been implicated in SAM maintenance, vascular development and leaf polarity formation (Ariel et al., 2007; Byrne, 2006; Liu et al., 2009a; McConnell et al., 2001; Prigge et al., 2005; Zhu et al., 2011). *HD-ZIP III* family members, at their N-

termini, all contain a HD-ZIP domain involved in DNA binding, a leucine zipper domain involved in protein dimerization and START domain engaged in a lipid or steroid binding (Ponting and Aravind, 1999; Sessa et al., 1998). At their C-termini a conserved MEKHLA domain is present and it is proposed to activate the HD-ZIP III DNA binding activity upon sensing developmental signals (Magnani and Barton, 2011; Mukherjee and Burglin, 2006). Among all *HD-ZIP III* members, only *REV* loss-of-function mutants show subtle phenotypes. However, *rev phb* double and *rev phb phv* triple mutants display pin-like cotyledon structures (Prigge et al., 2005), suggestive of their functional redundancy. Interestingly, *CNA* functions to repress the *WUS* expression and *cna phb phv* mutant displays enlarged SAM, a phenotype which is contrary to the *rev phb phv* phenotype (Prigge et al., 2005; Williams et al., 2005), indicating that *CNA* and *REV* might antagonize each other in SAM regulation.

Leaf and lateral organ development initiates from the leaf primordia derived from the SAM. Differentiation of daughter stem cells in the leaf primordia region is inhibited by the activities of the KNOX homeobox transcription factors and this inhibition could be released by polar auxin transport through down regulation of *KNOX* genes (Reinhardt et al., 2003; Scanlon, 2003). *Arabidopsis thaliana* have polar and dorsoventral leaves: the upper side of a leaf is called an adaxial side and the bottom side of a leaf is called an abaxial side. The adaxial domain is specified by the *HD-ZIP III* family transcription factors (Emery et al., 2003; Reinhart et al., 2013; Zhong and Ye, 2004). Gain of function mutants have adaxialized leaves while loss of function of the five genes have additive effects on the severities of radial abaxial leaves. In *Arabidopsis*

thaliana, it is well characterized that the *HD-ZIP III* genes are subjected to regulation by a group of sRNAs--miR165/166--through posttranscriptional gens silencing (Kidner and Martienssen, 2004; Liu et al., 2009a; Miyashima et al., 2011; Zhou et al., 2007a; Zhu et al., 2011). If the binding sites of the *HD-ZIP III* transcripts for sRNA are disrupted, dominant phenotypes are observed; while when miR166/165 is ectopically expressed, phenotypes corresponding to loss of function of *HD-ZIP III* genes show up (Zhong and Ye, 2004; Zhu et al., 2011). Consistent with this, *HD-ZIP III* and miR166/165 have complementary expression patterns with *HD-ZIP III* accumulation in the adaxial side and miR166/165 distribution in the abaxial side of leaves (Kidner and Martienssen, 2004). On the other hand, the abaxial identity is controlled by the *KANADI (KAN)* transcription factors and there are four members. Similarly, combined loss of function of *KAN* genes have partially or completely adaxialized leaves (Eshed et al., 2001; Eshed et al., 2004; Kerstetter et al., 2001). The *HD-ZIP III* and *KAN* family genes cooperate to control the polar development of leaf vasculature (Engstrom et al., 2004).

RNAi

RNAi (Figure 1-3) was first discovered in *Arabidopsis thaliana* in 1980-90s. By that time researchers had engineered a constitutive transgenic petunia overexpressing a chalcone synthase (CHS) in the hope of producing purple flowers. However, introduction of the transgene frequently caused repression of the endogenous homologous *CHS* and the transgenic plants show a bleached flower phenotype instead (Napoli et al., 1990). At that time, this phenomenon was called co-suppression. This and

similar observations in other organisms lead to the proposal of a concept of RNA interference (RNAi) (Fire et al., 1998).

Cumulative knowledge from various organisms and pathways has demonstrated that RNAi is a fundamental gene regulatory mechanism that is conserved in all eukaryotic organisms and is involved in diverse biological processes including stem cell development and maintenance. The key machinery that fulfills gene silencing functions is called RISC and its core components include AGOs and sRNAs (Lindbo, 2012; Mallory and Vaucheret, 2010a; Martinez de Alba et al., 2013). The conventional view is that sRNAs guide RISCs to the complementary target transcripts or gene loci and AGOs and other cofactors execute silencing either by sRNA-mediated target degradation (Chapman and Carrington, 2007; Ramachandran and Chen, 2008b; Vaucheret, 2008), translational inhibition (Brodersen et al., 2008; Chen, 2004) and chromatin remodeling (Zilberman et al., 2003). Different modes of silencing can act on the same mRNA targets; for example, it is believed that translation repression is the predominant effect at the earlier stage of the silencing and mRNA degradation occurs later (Huntzinger and Izaurralde, 2011; Krol et al., 2010). An exception has been reported that *Drosophila* AGO1 can be directly recruited to mRNA targets to repress protein translation by the RNA binding protein Smaug without the guidance of sRNAs (Pinder and Smibert, 2013). Also it has been observed that the RISC assembly can bypass the sRNA loading process and AGOs can directly bind to pre-annealed miRNA-mRNA duplexes to repress gene expression in human cells (Janas et al., 2012).

Figure 1- 3 Schematic of RNAi pathway in *Arabidopsis thaliana*.

The biogenesis of miRNAs and siRNAs takes place in the nucleus. *MIRNA* genes are typically transcribed by RNA polymerase II and the resultant *MIRNA* transcripts are pri-miRNAs. Pri-miRNAs adopt stem-loop fold backs and can be processed by DCL1-containing complex in two consecutive steps to release mature miRNA/* duplexes. Similarly, siRNA duplexes are produced by the activities of DCL2/3/4 complexes from long dsRNA precursors. Both miRNA and siRNA duplexes are methylated by the methyltransferase HEN1 at the 3' termini of both strands. Methylation prevents sRNA duplexes from trimming and tailing modifications and nucleolytic attacks. Methylated sRNA duplexes are exported into cytoplasm through the importin family protein HASTY located in the nucleus membrane. In the cytoplasm, sRNAs get loaded into AGO-containing pre-RISCs and during the loading process, the passenger strands of miRNA/* and siRNA/* are removed through an unknown mechanism and the guide strand miRNA/siRNA will be associated with AGO proteins. After sRNA loading, RISCs are now activated and can be guided to sequence homologous mRNA transcripts or gene loci to carry out gene silencing. In the cytoplasm, RISCs repress gene expression by the post-transcription gene silencing mechanism which is achieved through mRNA cleavage and translational repression. Mature RISCs can also be shuttled to the nucleus to implement transcriptional gene silencing which involves DNA and histone methylation.

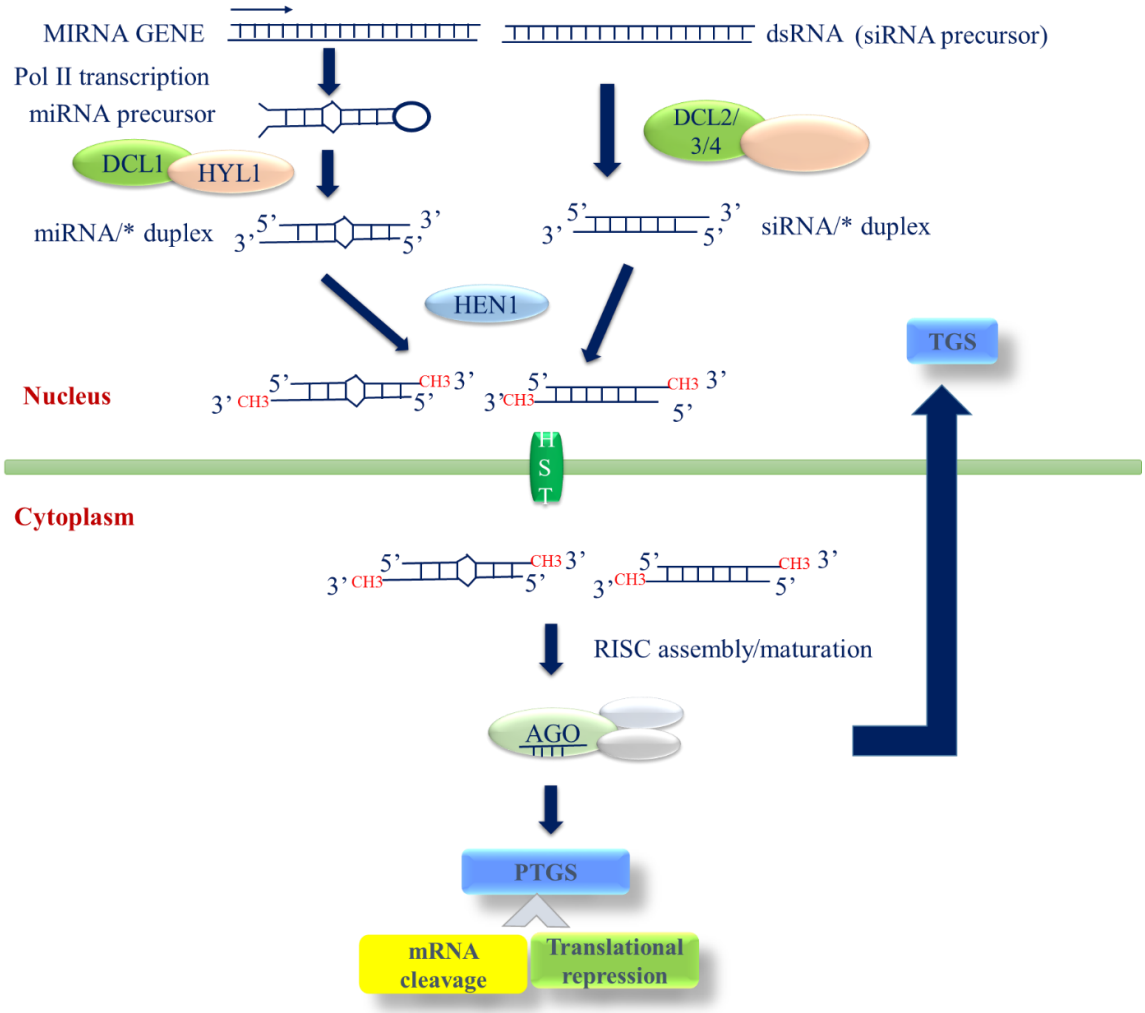
MIRNA GENE
dsRNA (siRNA precursor)
Pol II transcription
miRNA precursor
DCL1
HYL1
DCL2/
3/4
miRNA/* duplex
siRNA/* duplex
HEN1
TGS
Nucleus
H
S
T
Cytoplasm
RISC assembly/maturation
AGO
PTGS
mRNA
cleavage
Translational
repression

sRNA biogenesis

The RNAi process (Figure 1-3) starts from biogenesis of sRNAs which are approximately 21-30 nucleotides (nt) in length. sRNAs can be classified into two major classes: miRNAs and siRNAs. miRNAs normally harbor central-mismatches in the miRNA-miRNA* (miRNA/*) duplex, in contrast, siRNA-siRNA* (siRNA/*) duplexes are fully complementary. miRNA biogenesis starts with the transcription of long primary-miRNAs (pri-miRNAs), typically by RNA polymerase II. In animals, pri-miRNAs, characterized by stem-loop structures, are first processed in the nucleus by an RNase III enzyme, Drosha (Kim, 2009). The resultant ~70 nt hairpin RNA products, also known as precursor miRNAs (pre-miRNAs), will be further processed by another RNase III enzyme, Dicer, in the cytoplasm to release 21-22 bp miRNA/* duplexes. Recently it was reported that pre-miRNAs can bypass the processing step by Dicer, instead, the pre-miRNAs can be directly loaded into AGO and undergo further maturation steps (Cheloufi et al., 2010). In plants, DCL1 orchestrates the entire process including the pri-miRNAs to pre-miRNAs conversion and the pre-miRNAs to miRNA/*s release, and both processes take place in the nucleus (Dong, 2008; Kurihara, 2004; Song, 2007; Voinnet, 2009). siRNA biogenesis is more or less similar to that of miRNAs except that siRNA/*s are derived from long double-strand RNAs (dsRNAs) resulting from the transcription of inverted repeats, viral genes, or the activity of RNA-dependent RNA polymerases (RDRs) (Ahlquist, 2002; Chen, 2005; Tretter et al., 2008). sRNAs are not always processed into duplex forms. In *Drosophila* and humans, single strand functional miRNAs can also be produced from the miRNA loop regions (Okamura et al., 2013).

Numerous factors regulate the sRNA precursor transcript levels and I will focus on those identified in *Arabidopsis thaliana*. *Cis*-elements that correspond to the binding motifs of several transcription factors including LEAFY (LFY), Auxin Response Factors (ARFs) and AtMYC2SUO have been shown to be concentrated more in certain *MIRNA* gene promoters than in protein-coding gene promoters (Megraw et al., 2006; Zhou et al., 2008; Zhou et al., 2007b), raising a possibility that transcription of these *MIRNA* genes are controlled by these transcription factors. Pri-miRNAs, as other Pol II transcripts, contain a 5' 7-methylguanosine cap and a 3' polyadenylation tail (Xie et al., 2005; Zhang et al., 2005). Introns are also present in long pri-miRNA transcripts and bioinformatics studies have also identified alternative-splicing variants of pri-miRNAs (Mica et al., 2009; Song, 2007; Szarzynska et al., 2009). Conceivably, accumulation of pri-miRNAs can be modulated by the co-transcriptional cap addition, polyadenylation as well as the splicing processes. Indeed, in CAP-binding protein (CBP) CBP20 and CBP80 mutants pri-miRNAs accumulate but mature miRNA levels decrease (Gregory et al., 2008; Kim et al., 2008; Laubinger et al., 2008), possibly because of the failure of pri-miNRA processing and recruitment of pri-miRNA processing machinery through CBPs and SE interaction (Laubinger et al., 2008; Rogers and Chen, 2013b). Another line of evidence comes from the recent finding that decapping enzymes DCP1 and DCP2 also contribute to the accumulation of miRNAs (Motomura et al., 2012). In *dcp1* and *dcp2* mutants the steady state miRNAs decrease but the levels of pri-miRNAs and pri-miRNA processing factors remain unaffected. The mechanism by which DCP1 and DCP2 affect miRNA accumulation is not clear. SUO is a GW-repeat containing protein that can enhance

miRNA mediated translational repression and the levels of a subset of mature sRNAs and their corresponding precursors increased in *suo* mutants (Yang et al., 2012), indicating that SUO might be a *MIR* gene transcription repressor. Notably, a splicing factor SmD1 in *Drosophila* and humans can interact with Dicer-2, double strand sRNA precursors and AGO2 to regulate the steady state level of sRNAs (Xiong et al., 2013) .

The accurate processing of pri-miRNAs by DCL1 is strongly affected by the secondary structures of pri-miRNAs, especially by the complexity of the pri-miRNA terminal loops (Zhu et al., 2013). Generally DCL1 productively processes pri-miRNA with linear stem-loop structures to produce canonical miRNAs while pri-miRNAs with complex terminal loop structures will be processed bi-directionally by DCL1 and this leads to the production of both functional and nonfunctional mature miRNAs. DCL1 has two well characterized cofactors HYPONASTIC LEAVES1 (HYL1) and SERRATE (SE). HYL1 is a double-strand RNA binding protein and can directly associate with sRNA precursors to enhance the accuracy of DCL1 processing while SE functions as a scaffold between HYL1 and DCL1. In *hyl1* and *se* mutants, the mature miRNA levels significantly decrease and miRNA precursors accumulate (Grigg et al., 2005; Han et al., 2004; Lobbes et al., 2006; Vazquez et al., 2004). Besides DCL1, HYL1 and SE, many other factors affecting sRNA biogenesis in plants have been identified and these factors play different roles in different steps during sRNA biogenesis. SICKLE (SIC), a proline-rich protein, is indispensable for plant development and in *sic* mutant there is an increased level of pri-miRNAs and decreased level of mature miRNAs (Zhan). It remains to be elucidated about how SIC regulates pri-miRNA processing in plants. An RNA-binding protein TOUGH

(TGH) is another factor involved in miRNA accumulation and pri-miRNA processing. TGH associates with both pri- and pre-miRNAs and it can also interact with DCL1, HYL and SE (Ren et al., 2012b). Loss of the *TGH* function leads to developmental defects (Calderon-Villalobos et al., 2005) and accumulation of pri-miRNAs (Ren et al., 2012b). RECEPTOR OF ACTIVATED C KINASE 1 (RACK1) is a scaffold protein that is present in distinct complexes such as the eukaryotic 40S ribosomal subunit (Adams et al., 2011) and is identified as a SE-interacting partner in plants from yeast two-hybrid screening (Speth et al., 2013). In the *rack1* mutant, mature miRNA levels are dramatically reduced and several pri-miRNA species accumulate, suggesting that RACK1 plays an important role in pri-miRNA processing.

AGO proteins: structure, function and expression

AGO proteins are the core effectors of RISCs and the number of AGO proteins varies among different organisms (Hutvagner and Simard, 2008). One single AGO exists in *Schizosccharomyces pombe*, two AGOs are present in *Drosophila*, four AGOs are found in humans, twenty-seven AGOs exist in *Caenorhabditis elegans*, eighteen AGOs are annotated in the *Oryza sativa* genome and ten AGOs are present in *Arabidopsis thaliana*. Structural studies revealed that both eubacterial and eukaryotic AGOs share a similar domain organization structure (Schirle and MacRae, 2012; Song et al., 2004) that consists of N-terminal, PAZ, MID and PIWI domains. The N-terminal domain is the most variable region and recent studies illustrate that it plays important roles for efficient RNA silencing. The N-terminal domain facilitates the RISC assembly by promoting

sRNA duplex unwinding (Kwak and Tomari, 2012), and it can also participate in the cleaved mRNA target strand release by interrupting the duplex formed by guide sRNAs and mRNA targets. PAZ and MID domains are responsible for recognizing and anchoring the 3' and 5' end of AGO-associated sRNAs, respectively (Frank et al., 2010; Hutvagner and Simard, 2008). PIWI domains of AGOs possess an RNase-H-like fold (Nowotny et al., 2005; Parker et al., 2004; Song et al., 2004; Yuan et al., 2005), and the catalytic residues constitute the "DDH motif". Biochemical studies have confirmed that the DDH motif is responsible for AGO slicer activities (Mi et al., 2008; Qian et al., 2011). However, having the "DDH" motif in the PIWI domain doesn't ensure the slicer activity of AGOs and vice versa.

Elegant biochemical studies by domain swapping between human AGOs indicate that two sequence motifs residing in the N-terminal domain are linked to the slicer activity of AGOs (Faehnle et al., 2013; Hauptmann et al., 2013; Hur et al., 2013; Mallory and Vaucheret, 2010b; Schurmann et al., 2013). Additionally, by releasing the 3' end of guide sRNAs the PAZ domain can act as a switch to turn on the RSIC slicing activity (Wang et al., 2009). To date, the slicer activity has only been reported for AGO1 from *Schizosccharomyces pombe* (Irvine et al., 2006), AGO1 and AGO2 from *Drosophila* (Miyoshi et al., 2005; Rand et al., 2005), AGO2 from humans (Liu et al., 2004; Meister et al., 2004), AGO1, AGO2, AGO4, AGO7 and AGO10 from *Arabidopsis thaliana* (Baumberger and Baulcombe, 2005; Carbonell et al., 2012; Montgomery et al., 2008b; Qi et al., 2005a; Qi et al., 2006; Zhu et al., 2011). Notably, all 10 members of the *Arabidopsis thaliana* AGOs contain the "DDH" motif in their PIWI domains.

Structural analysis of full-length eukaryotic AGO structures (Elkayam et al., 2012a; Schirle and MacRae, 2012) reveals that eukaryotic AGO forms two globular lobe structures: one contains the N-terminal and PAZ domain while the other one contains MID and PIWI domains. The two lobes are connected by a linker region--L2. Residues in L2 are identified to form a "kink" and this is believed to be important for target recognition and cleaved product release. Additionally another conserved Glu residue in the PIWI domain is proposed to compose the slicer engine of AGO besides the previous known "DDH" motif.

Ten *AGO* genes have been identified in the *Arabidopsis thaliana* genome (Vaucheret, 2008), and *AGO8* is a pseudo gene and does not produce a functional protein (Takeda et al., 2008). Phylogenetic analysis classifies the nine *Arabdidopsis thaliana* AGO proteins into three main clades (Figure 1-4). Structural remodeling (Figure 1-5) of these AGO proteins based on the crystal structure of their human homolog AGO2 reveals that plant AGOs are distinct from each other even for AGOs that belong to the same clade, implying their functional divergence. AGO2 governs plant immunity in antiviral and antibacterial defense responses (Jaubert et al., 2011; Zhang et al., 2011). AGO4, AGO6 and AGO9 are the major AGO proteins that can associate with 24nt sRNAs and direct RNA-dependent DNA methylation to repress transposons and repetitive elements activities (Havecker et al., 2010; He et al., 2009; Matzke et al., 2009; Wang et al., 2011a; Zheng et al., 2007; Zilberman et al., 2004). AGO7 specifically binds miR390 to initiate trans-acting siRNA biogenesis (Montgomery et al., 2008a). AGO1, the founding member of plant AGO, binds a wide spectrum of known sRNAs and is the key "slicer" in post-

transcriptional gene silencing (Kidner and Martienssen, 2005; Qi et al., 2005b; Wang et al., 2011a; Yang et al., 2006a). Recent research shows that AGO1 can also work with a membrane protein AMP1 to repress translation initiation of target transcripts at the endoplasmic reticulum (Li et al., 2013). AGO10, together with its closest paralog AGO1, regulates SAM development and leaf polarity (Bohmert et al., 1998; Lynn et al., 1999; Moussian et al., 1998a). Besides their functional divergence, AGOs from *Arabidopsis thaliana* also have different spatiotemporal expression profiles based on microarray analysis (Schmid et al., 2005). Additionally, the YFP reporter constructs of *AGO1* and *AGO10* confirmed their specific expression domains in the embryo development stages. *AGO1* is expressed throughout the embryo. *AGO10* expression domain has partial overlapping with that of AGO1 but is restricted to the SAM, the adaxial side of cotyledons and vascular tissues (Tucker et al., 2008). Additionally, GUS expression analysis of the *AGO1* promoter shows that *AGO1* is expressed throughout the lifespan of the plant (Vaucheret et al., 2006), suggesting that AGO1 is indispensable for plant development.

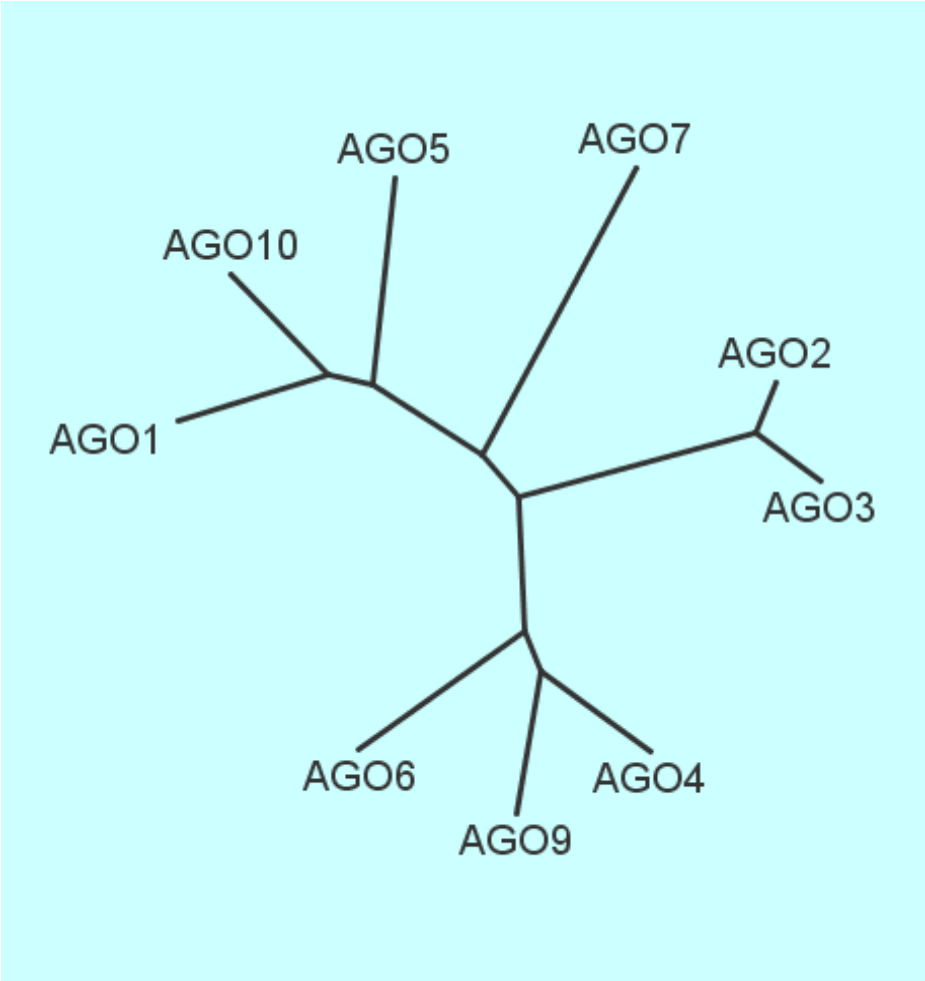

Figure 1- 4 Phylogenetic classification of *Arabidopsis thaliana* AGO proteins. Protein sequences were aligned using ClustaW (https://www.ebi.ac.uk/Tools/msa/clustalw2/). Phylogenetic tree was built with PHYLIP program.

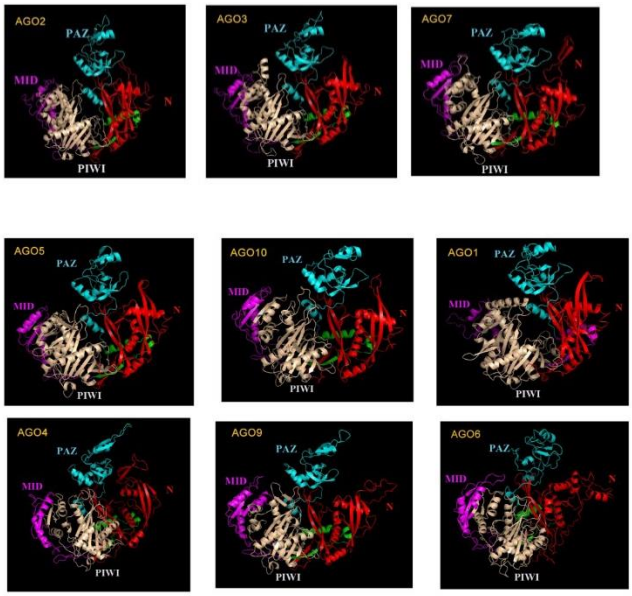

Figure 1- 5 Structural modeling of *Arabidopsis thaliana* Argonautes.

Protein modeling is generated by the SWISS-MODEL server with human AGO2 structure as a template (PDB code: 4EI1).

RISC assembly and activation

sRNAs fulfill their functions by associating with cognate AGOs. In animals, sRNA duplexes are produced in the cytoplasm while in plants sRNA duplexes are liberated from their precursors by DCLs in the nucleus. HASTY, an exportin family protein, is responsible for the sRNA duplexes nuclear export in plants (Bollman et al., 2003). Generally it is believed that the RISC assembly takes place in the cytoplasm even though some RISCs exert their functions in the nucleus to regulate gene transcription and chromatin structures (Ye et al., 2012).

The loading process of sRNAs into RISCs is ATP dependent and previously it was hypothesized that an ATP-dependent helicase unwind the sRNA duplexes first and then one strand of the duplex gets incorporated into AGO (Nykanen et al., 2001). This view has been challenged from studies in various organisms. It has been shown that in *Drosophila* Dicer-2 and R2D2 constitute the RISC loading complex to load siRNA duplexes into AGO2 (Liu et al., 2003; Pham et al., 2004; Tomari et al., 2004) and sRNAs are first loaded into AGOs in duplex forms in an ATP-dependent manner in humans as well (Kawamata et al., 2009; Yoda et al., 2010). AGO proteins are capable of directly accommodating sRNA duplexes in vitro (Hauptmann et al., 2013; Noland and Doudna, 2013); however, they have a higher binding affinity for single strand sRNAs, and the loading of sRNA duplexes into AGO generally requires the assistance from auxiliary proteins (Hauptmann et al., 2013; Lima et al., 2009; Meister et al., 2005). Among these proteins are Hsc70/Hsp90 chaperones. Hsc70/Hsp90 complex utilizes ATP to induce conformational change of AGO proteins and facilitates the loading of sRNA duplexes into

conformational open RISCs (Iki et al., 2010; Iwasaki et al., 2010; Miyoshi et al., 2010). In plants another RISC activation factor cyclophilin 40 (CYP40) associates with the sRNA duplex bound AGO1 (pre-RISC) in a HSP90 dependent manner and facilitates RISC assembly (Iki et al., 2012; Iki et al., 2010). ATP hydrolysis leads to the dissociation of HSP90 and CYP40 from pre-RISC before undergoing further maturation steps.

Once incorporated into pre-RISC, one strand of sRNA duplexes --the star strand or sRNA* will be removed and the remaining ss sRNA--the guide strand or sRNA will be stabilized within AGO proteins and guide AGO to repress its targets based on sequence complementarity (Leuschner et al., 2006; Matranga et al., 2005; Miyoshi et al., 2005; Rand et al., 2005). This activation step of RISC has been shown to be the rate-limiting step in human RISC maturation (Gu et al., 2011). This process requires the unwinding of sRNA duplexes and is ATP independent. In *Drosophila* and humans, siRNA duplexes are sorted into AGO2 containing RISC complexes (Okamura et al., 2004) where the star strand serves as the first target of RISC and is cleaved by the catalytic active AGO2. C3PO, an Mg^{2+}-dependent endoribonuclease is required for the removal of cleaved passenger strand siRNA and subsequent RISC activation (Liu et al., 2009c; Ye et al., 2011). QIP from *Neurospora crassa* is a QDE2 (an AGO in *Neurospora crassa*)-interacting 3' to 5' exoribonuclease that degrades passenger strand siRNA and leads to RISC activation. In a *qip* mutant nicked siRNA duplexes accumulate, and RNAi is compromised (Maiti et al., 2007). QIP also participates in the siRNA biogenesis pathway by functioning in conjunction with QDE2 and RNA exosome (Xue et al., 2012). In plants AGO1 catalytic activity is required for the siRNA passenger strand release and HSP90 regulates the

process of siRNA passenger strand removal from AGO1 by hydrolyzing ATP (Iki et al., 2010).) Although little is known about the miRNA loading process, a recent study suggest that removal of miRNA* strand does not entail catalytic function of AGO proteins (Carbonell et al., 2012). In plants, and other organisms, many AGOs may not necessarily function as catalytic enzymes, and the activation process of these RISCs is not clear. A slicer-independent unwinding mechanism has been proposed and according to this model several features direct the loading and unwinding processes of miRNAs. The central mismatches facilitate the loading of miRNA/* duplexes into AGOs, whereas mismatches in the guide strand positions 12-15 promote miRNA* duplex unwinding (Kawamata et al., 2009). The PAZ domain which binds the 3' end of sRNAs has been shown to be important for the slicer-independent duplex unwinding and RISC activation in humans (Gu et al., 2012). It remains to be determined about the sRNA loading process in plants.

How do AGO proteins distinguish between the two strands of sRNA/* duplexes? It is generally thought that the strand with lower 5' thermo stability will be retained as a guide strand in the RISC complex (Khvorova et al., 2003; Matranga et al., 2005; Preall and Sontheimer, 2005; Rand et al., 2005; Schwarz et al., 2003) and thermodynamic instability of sRNA/* duplexes increases the RISC maturation (Gu et al., 2011), likely due to the fact that the unwinding step is more efficient. DCL1/HYL1 in plants participate in the biased passenger strand selection (Eamens et al., 2009). In *dcl1* and *hyl1* mutants, some miRNA star strands accumulate but miRNA guide strands become undetectable (Eamens et al., 2009), suggesting that the miRNA biogenesis machinery directs the asymmetric loading of miRNAs into AGOs. Importantly, numerous studies have shown that sRNA

star strands can also be functionally incorporated into AGOs to direct gene regulation (Azuma-Mukai et al., 2008; Chiang et al., 2010; Elbashir et al., 2001a; Elbashir et al., 2001b; Ender et al., 2008; Goff et al., 2009; Nykanen et al., 2001; Okamura et al., 2008; Ruby et al., 2007; Yang et al., 2011).

How do AGO proteins select sRNAs to bind? In *Drosophila,* AGO1 mainly binds to miRNAs while AGO2 mainly associates with siRNAs. This divergence might come from the differences in the sRNA/* duplex structures and the unique association of sRNA loading complexes with each AGO (Kawamata et al., 2009; Tomari et al., 2007). Similarly, in *Caenorhabditis elegans*, siRNAs are preferentially incorporated into RDE1l and miRNAs are sorted into ALG1 (Steiner et al., 2007). In other organisms such explicit functional division has not been reported and AGOs can associate with both miRNAs and siRNAs. Nonetheless, insights regarding sRNA sorting into AGOs have been gained through biochemical and bioinformatics studies. AGO-immunoprecipitation followed by sRNA deep sequencing shows that both animal and plant AGOs have a preference toward certain nucleotides at the 5' end of sRNAs (Czech et al., 2009; Ghildiyal et al., 2008; Hu et al., 2009; Kim, 2008; Lau et al., 2001; Mi et al., 2008; Takeda et al., 2008). In *Drosophila* AGO1 prefers binding to 5' uridine (U) whereas AGO2 prefers to bind 5' cytosine (C) (Ghildiyal et al., 2010). Human AGO2 prefers binding to the miRNAs with 5' uridine (U) or 5' adenosine (A) residue (Frank et al., 2010). For plant AGOs both the length of sRNAs and the 5' end nucleotide identity account for the specific association of sRNAs with AGOS. *Arabidopsis thaliana* AGO1 prefers to bind 21nt 5'U-sRNAs, AGO2 favors 21nt sRNAs with 5' A, AGO4 prefers 24nt sRNAs with 5' A and AGO5 prefers

24nt sRNAs with 5'C (Mi et al., 2008). Structural studies of MID domains support the preference of certain AGO toward certain nucleotides (Frank et al., 2010; Zha et al., 2012). Nucleotide specificity loops are present in MID domains and the nucleotide preference could be manipulated by mutations of residues in the loops (Zha et al., 2012).

The above mentioned selection rules cannot explain all of the AGO-sRNA associations. *Arabidopsis thaliana* AGO10 specifically binds to miR166/165 to regulate SAM development (Zhu et al., 2011) and AGO7 binds to miR390 to initiate trans-acting siRNA biogenesis (Montgomery et al., 2008b). Interestingly, miR390 starts with a 5' A but only shows moderate association with AGO2. Careful examination reveals that such obliged associations between AGOs and sRNAs are determined by the special structural features of miRNA duplexes including central mismatches (Endo et al., 2013; Zhu et al., 2011). This provides evidence that sRNA loading in plants may be similar to that in animals, and sRNA duplexes are recognized and incorporated into AGOs.

sRNAs function non-cell-autonomously in plants (Baulcombe, 2004; Miyashima et al., 2013; Voinnet, 2005). The nature of the mobile signal has long been mysterious; however, recent studies demonstrate that sRNA duplexes can move intercellularly from the sites of biogenesis through plasmodesmota and phloem to the sites of action to regulate plant growth and development (Chitwood et al., 2009; Dunoyer et al., 2010; Marin-Gonzalez and Suarez-Lopez, 2012; Miyashima et al., 2011; Parent et al., 2012).

sRNA stability control

The effect of RNAi requires sequence complementarity between sRNAs and the target transcripts or loci. In this sense sRNAs are one of the most pivotal functional determinants of RISCs and the levels of sRNAs need to be precisely regulated to ensure the proper function of biological processes. Indeed, organisms possess sophisticated mechanisms to regulate every single step of the sRNA biogenesis and turn over.

Although the biogenesis pathways of sRNAs have been understood quite well, the turnover mechanisms of sRNAs await further studies. In organisms including *Arabidopsis thaliana, Drosophila,* and humans, a key process to protect sRNAs from degradation is by the 3' methylation of sRNAs by HEN1 and its homologs. In plants, HEN1 functions to stabilize the sRNA duplexes generated by DCL endonucleases through 2′-O-methy-lation at their 3′ termini (Yang et al., 2006b). In loss-of-function *hen1* mutants, the levels of miRNAs and siRNAs decrease and the unmethylated sRNAs undergo tailing and trimming processes, which lead to the instability of sRNAs (Li et al., 2005). Notably, HEN1 homologous are also present in animals, suggesting that 3' methylation is a common strategy for sRNA protection.

When sRNAs become unmethylated, 3' uridylation takes place and leads to the degradation of sRNAs (Norbury, 2010; Scott and Norbury, 2013). This post-transcriptional modification is known as the sRNA tailing and can decrease the stability of sRNAs. In plants, the poly-U tail is normally 1-7 nt in length in contrast to the 1-2 nt in animals. In plants HEN1 SUPPRESSOR1 (HESO1) is the nucleotidyltransferase that can uridylate non-methylated sRNAs and lead to their degradation (Ren et al., 2012a; Zhao et

al., 2012). It is recently reported that HESO1 can uridylate AGO1-bound non-methylated miRNA by interacting with AGO1 PAZ and PIWI domains (Ren et al., 2014). Furthermore, HESO1 is responsible for uridylation of 5' fragments of miRNA targets generated by AGO cleavage, and uridylation is a prerequisite for the degradation of 5' fragments in vivo (Ren et al., 2014). The uridyltransferase that can add uridines to the sRNA 3' ends have been found in other organisms including TUT1 and CDE1 from humans and *Caenorhabditis elegans* (Knouf et al., 2013; van Wolfswinkel et al., 2009; Wyman et al., 2011) and MUT68 from *Chlamydomonas* (Ibrahim et al., 2010). Intriguingly, high sequence complementarity between sRNAs and their targets can also lead to the trimming (sRNAs get shorter) and tailing of sRNAs and result in sRNA decay (Ameres et al., 2010).

Other than the tailing and trimming processes that repress the sRNA accumulation in vivo, exonucleolytic activities of ribonucleases can also lead to sRNA degradation. In *Caenorhabditis elegans*, XRN-2 degrades ss sRNAs in the 5'-3' direction (Chatterjee and Grosshans, 2009) and Eri-1 acts to degrade sRNA duplexes (Kennedy et al., 2004). In *Arabidopsis thaliana*, the 3'-5' exoribonuclease SDNs are responsible for turnover of ss sRNAs. Loss of function *sdn* mutants show elevated levels of miRNAs and display pleotropic developmental phenotypes (Ramachandran and Chen, 2008a).

Recent studies show that a 3' to 5' exoribonuclease named Nibbler is an important player in the sRNA regulated processes in *Drosophila*. Nibbler can edit the length of mature miRNAs as a way to modify their target specificities (Han et al., 2011; Liu et al., 2011a).

Besides the factors mentioned above, sRNA accumulation can also be regulated by AGO proteins. Generally it is thought that AGO-associated sRNAs are protected from nucleolytic attack or deleterious modifications such as trimming and tailing (Carbonell et al., 2012; Ji and Chen, 2012; Kai and Pasquinelli, 2010; Rogers and Chen, 2013a, b). For example, *Arabidopsis thaliana* AGO1 is required for the stabilization miRNAs. In *ago1* null allele mutants, levels of some miRNAs dramatically decrease (Vaucheret et al., 2004). RNA-RNA interaction represents another important layer of regulation on sRNA stabilities. In vitro synthesized miRNA antagamirs (Krutzfeldt et al., 2005), target mimicry constructs in plants (Franco-Zorrilla et al., 2007) and miRNA sponges in mammalian cells (Ebert et al., 2007) utilize the antisense strategy to produce oligonucleotides that are complementary to miRNAs in vivo. These antisense RNAs can efficiently block the function of miRNAs by preventing them from binding to target mRNAs and also they can cause the degradation of miRNAs through an unknown mechanism (Krutzfeldt et al., 2007; Krutzfeldt et al., 2005; Todesco et al., 2010). Recently a class of competing endogenous RNAs (ceRNAs) have been reported. The ceRNAs are transcripts from pesudogenes or protein-coding genes and also function as sRNA sponges in vivo by competitively binding to miRNAs, resulting in regulation of other gene transcripts which share similar miRNA binding sites (Franco-Zorrilla et al., 2007; Salmena et al., 2011; Seitz, 2009; Tay et al., 2014). Interestingly, circular RNAs, a special form of ceRNAs, have been shown to be a prevalent RNA species (Salzman et al., 2012). Circular RNAs that contain multiple miRNA binding sites can function as natural potent miRNA sponges as the circular conformation renders them more resistant

to exonucleolytic degradation. Indeed, in human and mouse a circular RNA ciRS-7 (Hansen et al., 2011) functions as a miR-7 sponge and another testis-specific circular RNA sex-determining region Y (Sry) (Capel et al., 1993) specifically down regulates miR-138 activity (Hansen et al., 2013).

Posttranscriptional and posttranslational modulations of AGOs

RNAi machineries are under exquisite control to ensure that miRNA activity and action are restricted. Cell-type and cell-stage specific transcriptional regulation on miRNA precursors and core RNAi effectors have been reported (Aboobaker et al., 2005; Levy et al., 2010; Lu et al., 2005; Su et al., 2010; Wang et al., 2013; Wienholds et al., 2005), however, less is known about the post-transcriptional regulation on RNAi pathway members. Nonetheless, posttranslational modulations on AGO proteins, the catalytic engine of RISCs, are emerging to be an important aspect of miRNA activity regulation. Posttranslational modifications of AGOs, which include hydroxylation, phosphorylation, and ubiquitination, can have profound effects on AGO stability and RNAi.

AGO expression can be regulated at a posttranscriptional level. In mouse embryonic stem cells the translation of AGO2 is correlated with miRNA abundance (Martinez and Gregory, 2013). When miRNA levels decrease such as in *Dicer* defective cells, the AGO2 protein expresses at a low level. AGO2 accumulation can be rescued by transfection of exogenous sRNAs, suggesting a manner of sRNA-dependent posttranscriptional regulation. The low level of AGO2 accumulation is a result of the instability of unloaded AGO2. In line with this, preventing RISC assembly by inhibition

of Hsp70/Hsp90 also leads to decreased AGO2 expression. Similarly the poleroviral P0 suppressor which prevents RISC assembly in *Arabidopsis thaliana* can also cause AGO1 degradation (Csorba et al., 2010). Another line of evidence comes from the fact that miR20a-loaded human AGO2 is resistant to proteolytic digestion compared to unloaded AGO2 (Elkayam et al., 2012b). Taken together, these findings suggest that miRNA association might stabilize AGOs by inducing conformational changes. Indeed, such allosteric regulation by sRNAs has been reported for AGOs from various organisms (Djuranovic et al., 2010). Lyposome is suggested to play a role in the degradation of unloaded AGO2. Findings from Hela cells show that autophagy causes degradation of AGO2 (Gibbings et al., 2012), and this supports the role of the lyposome in down regulating free AGO protein levels. However, revisit this experiment seemed not to support this model (Smibert et al., 2013). *Arabidopsis thaliana* AGO4 stability relies on the canonical siRNA biogenesis factors including NRPD1, RDR2 and DCL3, and the data suggests that siRNA association could affect AGO4 stability (Li et al., 2006).

Hydroxylation is one of the first reported posttranslational modifications of AGOs. Type I collagen prolyl-4-hydroxylase (C-P4H (I)) has been shown to physically interact with human AGO2 and specifically hydroxylates Pro 700. Hydroxylation of human AGO2 has been shown to increase its stability (Qi et al., 2008). The knocking down of C-P4H (I) by artificial sRNAs reduces the stability of AGO2 and causes compromised RNAi.

Phosphorylation represents the most extensively studied category of AGO modification. Epidermal growth factor receptor (EGFR) specifically phosphorylates Tyr 393 in human AGO2 under hypoxia stress conditions (Shen et al., 2013). The maturation

of miRNAs, specifically those tumor-suppressor-like miRNAs, is impeded under hypoxia stress presumably because of the reduced interaction between Dicer and phosphorylated AGO2. mRNA processing bodies (P-bodies) are discrete cytoplasmic speckles where prevalent posttranscriptional regulation of cytoplasmic mRNAs occurs (Anderson and Kedersha, 2006; Eulalio et al., 2007a). In P-bodies, mRNAs undergo deadenylation, sometimes followed by decapping (Parker and Song, 2004; Wilusz and Wilusz, 2004) and then get degraded by the exonucleolytic activity of exosomes (Houseley et al., 2006) or by the 5' to 3' XRN1 exonuclease (Parker and Song, 2004; Wilusz and Wilusz, 2004). RNAi can take place in P-bodies (Liu et al., 2005b), and it has been suggested that RNAi is the cause of P-body formation (Eulalio et al., 2007b). In animals it has been well documented that an AGO-interacting RISC component GW182 localizes in P-bodies and mediates translational repression of mRNAs by miRNAs (Behm-Ansmant et al., 2006; Eulalio et al., 2008; Eystathioy et al., 2003; Huntzinger et al., 2013; Liu et al., 2005a; Zekri et al., 2013). Ser 387 phosphorylation through the p38 MAPK pathway (Zeng et al., 2008) and Pro 700 hydroxylation both can enhance the P-body localization of human AGO2 (Heo and Kim, 2009).

Ubiquitination comprises another class of AGO modification. An F-box protein FBW2 in *Arabidopsis thaliana* negatively regulates the AGO1 protein level but not the mRNA level through the 26S-proteosome machinery (Earley et al., 2010). *FBW2* Loss of function mutants increase AGO1 accumulation while *FBW2* overexpression transgenic plants phenocopy *ago1* mutants, and the AGO1 protein level decreases in these plants. Ubiquitination regulation of mouse AGO2 has also been reported and the let-7 target *lin-*

41 gene encodes an E3 ligase to target AGO2 for degradation in stem cells (Rybak et al., 2009). The above-mentioned viral suppressor P0 is also an F-box protein and it has been demonstrated that P0 targets AGO1 for degradation to suppress gene silencing in transgenic *Arabidopsis thaliana* (Bortolamiol et al., 2007).

AGO and sRNA homeostasis

Although accumulation of AGOs and sRNAs are finely tuned by diversified genes and pathways, the steady state levels of these two pivotal factors in RNA silencing rely on each other's abundance--this is also known as homeostasis. As discussed above, stability of human AGO2 and *Arabidopsis* AGO1 can be regulated by miRNA availability (Csorba et al., 2010; Martinez and Gregory, 2013). Studies in *Drosophila* link AGO1 accumulation to miRNA abundance; in contrast *Drosophila* AGO2 expression is not affected by defective siRNA biogenesis (Smibert et al., 2013). Conversely, sRNA homeostasis can be affected by AGO protein expression. First of all, AGO proteins have been found to directly participate in the maturation of sRNAs (Cheloufi et al., 2010; O'Carroll et al., 2007; Shen et al., 2013; Xue et al., 2012). Second, sRNA homeostasis depends on AGO expression. The pronounced unbalanced accumulation of guide and passenger strands of sRNAs in vivo suggests that loading into RISC complexes protects sRNA guide strands. Indeed, in *Arabidopsis thaliana*, it seems that vast majority of sRNAs are present in AGO complexes (Wang et al., 2011b). Overexpression of any of the four human Argonaute proteins leads to an increase in mature, ectopically expressed miRNA (Diederichs and Haber, 2007). Similarly, in the *Arabidopsis thaliana ago1* mutant, level of most sRNA

diminishes; while overexpression of AGO1 leads to an increased level of certain sRNAs (Vaucheret et al., 2006; Vaucheret et al., 2004).

One classical example of AGO and sRNA homeostatic regulation is the *Arabidopsis thaliana* AGO1 and miR168 regulatory loop. *AGO1* transcript bears a miR168 target site and when the AGO1 protein level is high, miR168 will be efficiently incorporated into AGO1 to posttranscriptional repress *AGO1* expression; on the other hand, when the AGO1 level decreases, miR168 is destabilized (Vaucheret et al., 2006; Vaucheret et al., 2004). This feedback loop enables the homeostatic expression of both AGO1 and miR168 and it is critical for plant development. Interruption of this regulation by mutating the miR168 recognition site in *AGO1* transcripts leads to over accumulation of AGO1 protein and developmental defects. Interestingly, the high level of AGO1 protein causes defective RNA silencing where miRNA accumulation decreases but miRNA targets increase (Vaucheret et al., 2004). Recently it was found that AGO1-derived siRNAs also participate in AGO1 homeostatic control in coordination with miR168 (Mallory and Vaucheret, 2009).

Several new findings argue against the concept that sRNAs get stabilized through AGO protection. First, AGO proteins are proven to be the limiting factor for gene silencing in human cells (Khan et al., 2009; Sood et al., 2006), *Arabidopsis thaliana* (Martinez de Alba et al., 2011) and *Xenopus laevis* (Lund et al., 2011). Second, it has been clearly demonstrated that in human cells the majority of mature miRNAs actually exist in free forms, and these unbound miRNAs are stable in the naked miRNA-mRNA duplexes (Janas et al., 2012).

RISC recycling and turnover

RISC is a multi-turnover enzyme complex which achieves the broad control of gene expressions. The efficient recycling of RISC components requires dissociation of target mRNA transcripts and also AGO-associated sRNAs. Studies have shown that releasing of cleaved strands is the rate-limiting step during the RISC recycling (Ameres et al., 2007; Haley and Zamore, 2004; Rivas et al., 2005). Efforts have been made to illustrate the regulation of the RSIC recycling.

The N-terminal domain of AGOs is proposed to function as a duplex wedge by restricting base pairing between sRNAs and complementary oligonucleotides (Wang et al., 2009). During RISC maturation the N-terminal domain can help to dissociate guide and passenger (cleaved and non-cleaved) strands of sRNAs (Kwak and Tomari, 2012); after AGO slicing, the N-terminal domain facilitates RISC recycling by aiding target release and allows the accommodation of subsequent targets (Parker, 2010; Wang et al., 2009). In addition, autoantigen La can facilitate human AGO2-containing RISC recycling by assisting the cleaved target mRNA release (Liu et al., 2011b).

Proteins that regulate RISC assembly have potential roles in the RISC recycling. For example, it is found that ATP can alleviate the rate-limiting stage of RISC recycling (Haley and Zamore, 2004) and this raises a possibility that RISC chaperone proteins including Hsp90 might participate in the target release step by hydrolyzing ATP.

In order to regulate targets with diverse sequences, different sRNAs are needed to guide RISCs for precise recognition. In this sense, sRNAs need to be released out from AGOs to allow other sRNA being loaded. The mechanism controlling sRNA unloading

awaits further investigation. Nonetheless, it has been shown that sRNAs compete for AGO binding in vivo (Martinez de Alba et al., 2011; Martinez and Gregory, 2013), and a mathematical model has been made to predict the effect of sRNA competition on RISC formation and recycling (Klironomos and Berg, 2013). Notably, in vitro biochemical studies reveal that highly-complementary mRNA targets can lead to sRNA release from AGO (De et al., 2013).

In *Arabidopsis thaliana* it is found that catalytic defective forms of AGO1, AGO7 and AGO10 can stabilize miRNA-mRNA target complexes compared to wild type AGOs (Carbonell et al., 2012), indicating that RISC recycling requires AGO catalytic activity.

Little is known about how and where RISC disappearance occurs. Two studies concurrently found that multivesicular bodies (MVBs) are where miRISC turnover takes place (Gibbings et al., 2009; Lee et al., 2009; Siomi and Siomi, 2009). MVBs are endosomal compartments that form between early endosomes and lysosomes. GW bodies, different from P-bodies, are caused by the aggregation of GW182 and colocalize with MVBs. Moreover, AGO2, GW182 and sRNAs are found to be enriched in MVBs. Preventing MVBs formation causes diminished formation of GW-bodies and defective miRNA silencing; whereas preventing MVBs from maturating into lysosomes enhance sRNA-mediated gene silencing and GW-body accumulation. Further it is shown that MVBs facilitates RISC recycling by promoting sRNA loading. Collectively, MVBs is proposed to be the foci where the dynamics between active RISC assembly and turnover are modulated.

Dissertation overview

My general research interest is to investigate the functional mechanism of *Arabidopsis thaliana* AGO10 in gene silencing, specifically, I aimed to clarify how AGO10 regulates SAM development and what makes AGO10 a functional unique protein. This dissertation is composed of three main parts. In the first part (Chapter II) I present the discovery that AGO10 regulates SAM development by sequestering miR166/165 and positively regulating HD-ZIP III transcription factors expression. In the second part (Chapter III) I examine which domain(s) render AGO10 functional uniqueness. In the third part (Chapter IV and V) I switch gears and explore the function of an AGO10-interacting protein in gene silencing.

Chapter II presents the mechanic study of AGO10 in SAM regulation. I show that AGO10 specifically interacts with a group of miRNAs–miR166/165; and this obligated interaction is achieved by the recognition of the miR166/* duplex structure by AGO10. Further, I show that AGO10 functions as a miR166/165 decoy in vivo and AGO10 is a positive regulator of miR166/165 target *HD-ZIP III* genes which are required for SAM development. Loss of *AGO10* leads to increased miR166/165 accumulation and defective SAM phenotypes. This is the first report that an AGO protein functions to antagonize miRNA activity while protecting the miRNA target genes from being silenced.

In Chapter III, domain swapping was employed to study the functional uniqueness of AGO10. AGO1 is the closest homolog of AGO10 in *Arabidopsis thaliana* and AGO1 is also capable of binding miR166/165. However, AGO1 cannot replace the

AGO10 function in SAM regulation and vice versa. By swapping individual and combined domains between AGO1 and AGO10, I show that when the N-terminal domain of AGO1 is replaced by that of AGO10 the chimeric AGO1 can rescue the SAM defective phenotypes observed in AGO10 mutants. On the other hand, replacing the individual domains of AGO10 with the corresponding parts of AGO1 compromises the AGO10 function except for the PAZ domain. These findings reveal that the N-terminal domain of AGO10 is the key domain responsible for its unique function and the PAZ domain of AGO10 is changeable with the AGO1 PAZ domain.

In Chapter IV, a proteomics approach is undertaken to identify the interacting partners of AGO10 in planta. Among the numerous factors identified I focus on a protein named RICE1. Biochemical studies of RICE1 reveal that RICE1 is a sRNA specific 3' to 5' exoribonuclease. Structural studies show that RICE1 has a conserved tertiary structure of the DEDD family exonucleases. The structural analysis together with site-directed mutagenesis confirmed the key catalytic residue of RICE1. Preliminary data of the in vivo functional study of RICE1 and its homolog RICE2 which has 68% sequence similarity with RICE1 will also be included. Preliminary data suggest that RICE1 and RICE2 most likely act as a RISC activator by degrading the star strands of sRNAs in *Arabidopsis thaliana*.

CHAPTER II

Arabidopsis ARGONAUTE10 SPECFICALLY SEQUESTERS MIR166/165 TO REGULATE SHOOT APICAL MERISTEM DEVELOPMENT *

Summary

The shoot apical meristem (SAM) comprises a group of undifferentiated cells that divide to maintain the plant meristem and also give rise to all shoot organs. SAM fate is specified by class III HOMEODOMAIN-LEUCINE ZIPPER (HD-ZIP III) transcription factors, which are targets of miR166/165. In *Arabidopsis*, AGO10 is a critical regulator of SAM maintenance, and here we demonstrate that AGO10 specifically interacts with miR166/165. The association is determined by a distinct structure of the miR166/165 duplex. Deficient loading of miR166 into AGO10 results in a defective SAM. Notably, the miRNA-binding ability of AGO10, but not its catalytic activity, is required for SAM development, and AGO10 has a higher binding affinity for miR166 than does AGO1, a principal contributor to miRNA-mediated silencing. We propose that AGO10 functions as a decoy for miR166/165 to maintain the SAM, preventing their incorporation into AGO1 complexes and the subsequent repression of *HD-ZIP III* gene expression.

***** Reproduced with permission from "Arabidopsis Argonaute10 Specifically Sequesters miR166/165 to Regulate Shoot Apical Meristem Development" by H. Zhu, F. Hu, R. Wang, X. Zhou, S-H. Sze, L.W. Liou, A. Barefoot, M. Dickman, X. Zhang. 2011. *Cell.* 145, 242–256.

Introduction

Arabidopsis SAM contains several organized layers of stem cells located at the shoot tip. The SAM is maintained in a pluripotent state in its central region, and it also provides cells to the peripheral region to form differentiated organs. Among the factors that regulate whether or not cells in the SAM differentiate are class III *HD-ZIP* family genes, which include *PHABULOSA (PHB), PHAVOLUTA (PHV), REVOLUTA (REV),* and *ATHB-8* and *-15* (Barton, 2010) . The *HD-ZIP III* genes are regulated by miR166/165 in *Arabidopsis* (Mallory et al., 2004).

AGO10 (originally identified as *PNH* or *ZLL*) plays a critical role in multiple developmental processes, such as the maintenance of undifferentiated stem cells in the SAM (Lynn et al., 1999; Moussian et al., 1998b) and the establishment of leaf polarity (Liu et al., 2009a). In the *Arabidopsis* ecotype Ler, *ago10* mutant seedlings (pnh/zll) display differentiated cells or complete organs in place of the SAM (denoted as the pinhead phenotype), whereas these phenotypes are rarely seen in Col-0 background (Mallory et al., 2009). Recent studies indicate that AGO10 modulates these developmental processes by genetically repressing miR166/165, two related miRNAs that differ in sequence by only a single nucleotide (Liu et al., 2009a). Both miRNAs target the same *HD-ZIP III* family genes to regulate plant development (Jung and Park, 2007; Zhou et al., 2007a).

Although the genetic functions of AGO10 have been described, the molecular mechanism by which it regulates SAM development remains unknown. Here, using an unbiased biochemical approach, we show that AGO10 specifically binds to miR166/165.

We further show that deficient loading of miR166/165 into AGO10 resulted in the pinhead phenotype. The defective SAM in an *ago10* mutant was rescued by simply sequestering miR166/165 in the expression niche of AGO10, but not AGO1. Notably, the binding capability of AGO10 to miR166/165, but not its catalytic activity, is both necessary and sufficient for the proper SAM development. Moreover, AGO10 has a higher affinity for miR166 than does AGO1, leading to the preferential loading of miR166 into AGO10. We propose that AGO10 controls SAM development by specifically sequestering miR166/165 and preventing their loading into AGO1, allowing miR166/165 activity to be antagonized, and therefore the *HD-ZIP III* genes to be upregulated.

Materials and methods

Plant materials and growth conditions

Homozygous *ago10-3* and/or *ago10*$^{pnh-2}$ mutants were transformed with the native promoter-driven *AGO10* cDNA containing dual epitopes fused to its N terminus (*P*$_{AGO10}$ *-8His-Flag (HF)-AGO10*) by the floral dip transformation method (Clough and Bent, 1998).This dual-tagged AGO10 was detected in 10-day-old T2 transgenic seedlings by western blot analysis. The pinhead phenotype was rescued in the T2 progeny of the *P*$_{AGO10}$ *-HF-AGO10* transgenic plants (n > 30), indicating that the dual-tagged AGO10 is as functionally active as wild-type AGO10. These stable transgenic lines are physiologically relevant and will be useful for further studies.

Similarly, *ago10*$^{pnh-2}$ mutants were transformed with P_{AGO10} *-HF-AGO10 (DDH),* a series of target mimicry constructs, or other constructs by the floral dip transformation method.

Seeds from infiltrated plants were selected on standard MS medium containing the appropriate selective agents: 10 mg/l glufosinate ammonium (Sigma) and/or 25 mg/l hygromycin (Sigma) together with 100 mg/l cefotaxime (Sigma). Homozygous progeny of T2 transgenic plants were identified by the lack of segregation in the presence of selective agents on MS plates.

Plants were grown in LP5 Metromix (SunGro, Canada) in a walk-in growth chamber at 22 ℃ with relative humidity of 50% under long-day conditions (16 hours light/8 hours dark) unless otherwise noted. Light illumination (110 mmol photons/m^2s) was provided by a Spec-tralux T5 high-output lamp (Hydro warehouse).

Material preparation for coimmunoprecipitation experiment

For transient experiments, 4-week-old *N. bentha* leaves were infiltrated with *A. tumefaciens* ABI harboring a variety of binary plasmids. The ODs of *A. tumefaciens* cultures were normally diluted to 0.4 in most experiments except the competition immunoprecipitation experiment where the OD of the 35S-miR166a culture was diluted to 0.1. *N. bentha* leaves were collected two days after agroinfiltration. For *Arabidopsis* plants, inflorescences were collected from 6-week-old adult plants. In most cases, 7-day-old seedlings were used.

Coimmunoprecipitation experiments

Total protein was extracted in the IP buffer containing 50 mM Tris-HCl, pH 7.5, 300 mM NaCl, 4 mM $MgCl_2$, 5 mM DTT, 0.1% Triton-100, and the complete protease inhibitor cocktail (Roche). Cleared protein extracts were immunoprecipitated with agarose-conjugated monoclonal antibodies against Flag or Myc or HA (Sigma). For the immunoprecipitation of YFP-AGO10 or endogenous AGO1, protein extracts were mixed with a monoclonal anti-YFP (Invitrogen) or a polyclonal anti-AGO 1 antibody together with Protein A beads and incubated for 2 hours. Beads were washed four times with the same buffer before recovery of sRNAs and analyses of sRNA and western blots.

RNA blot and western blot analyses

Total RNA was extracted using Trizol reagent from Agrobacterium-transfected N. bentha leaves or Arabidopsis tissues, including 7-(or 10)-day-old seedlings and inflorescences, depending on the desired assays. RNA blot hybridizations of low-molecular-weight RNAs (sRNA blot) were performed as described (Zhang et al., 2006). Each lane contained sRNAs, which were recovered from isolated AGO complexes prepared from 0.4 g tissues. For input, 5 μg of total RNA was used in most cases, except in transient experiments where only 1~2 μg RNA was used. Blots were hybridized with ^{32}P-radiolabeled oligonucleotide probes complementary to the sRNAs of interest. In some experiments, the same blots were stripped and re-probed with ^{32}P-labeled oligos complementary to the indicated miRNAs. U6 served as loading controls. RNA blots

were detected after exposure to a phosphor plate and quantified using the Quantity One Version 4.6.9 according to the manufacturer's instructions (Bio-Rad).

Western blot analyses were performed as previously described (Zhang et al., 2006). Western blots were developed with ECL^{+}, detected with ChemiDoc XRS+ and quantified using the ImageLab Software (Bio-Rad).

Results

Identification of AGO10-associated sRNAs

To investigate the biological function of AGO10, we purified AGO10-containing RISCs from flowers of transgenic plants expressing *P_{AGO10}-8His-Flag-AGO10* in the *ago10-3* background using a two-step affinity purification strategy (Figure 2-1A). Briefly, the total cellular extracts were first incubated with Ni-NTA resins, and elutes from the Ni-NTA column were further immune-purified with agarose conjugated anti-Flag beads. sRNAs were recovered from AGO10 immunoprecipitates. We sequenced AGO10-bound sRNAs using Illumina technology. More than 3.5 million genome-matched reads were obtained. Astonishingly, 90% of the AGO10-bound sRNAs were indeed miR166/165 (Figure 2-1B).

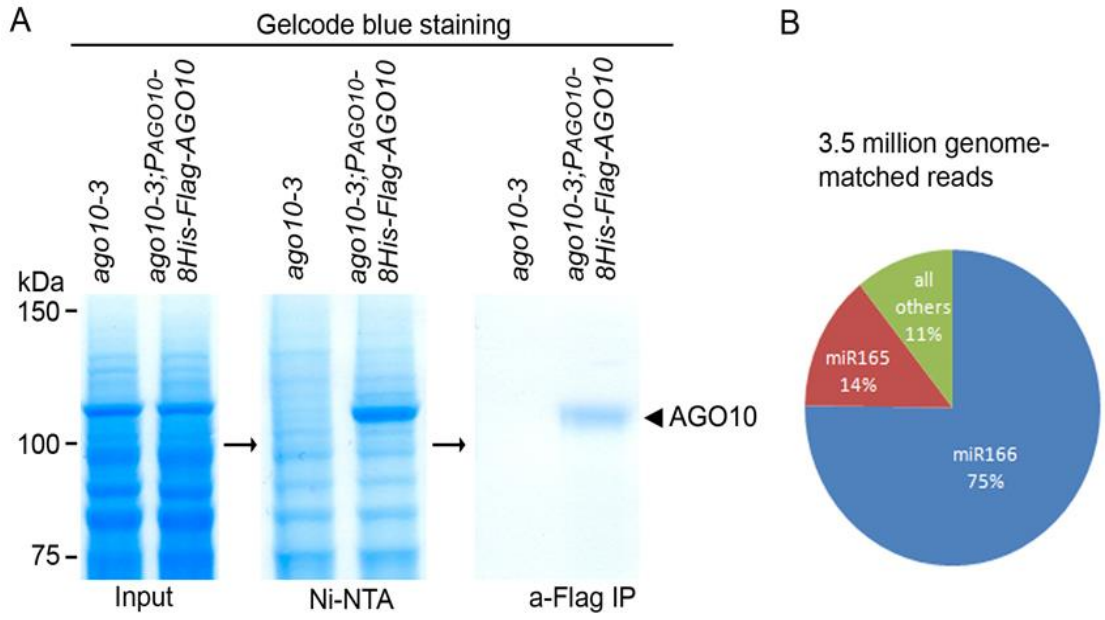

Figure 2- 1 AGO10 predominantly recruited miR166/165.

(A) Two-step purification of AGO10-containing RISCs. Samples from each purification step were resolved by SDS-PAGE and stained with Gelcode blue to monitor AGO10 purity (left panels).

(B) Approximately 90% of AGO10-bound sRNAs were miR166/165.

We confirmed that there is a specific interaction between AGO10 and miR166/165 *in planta* by a series of competitive immunoprecipitation (IP) assays in *Arabidopsis* and *Nicotiana. Benthamiana (N.bentha)* expression systems. We next co-expressed different *35S-Flag-4Myc-AGO* constructs with precursors of miR166a, -168a, and -390b in *N. bentha* (Figure 2-2A). We immunoaffinity-purified AGO1, -2, -3, and -10 complexes and assayed their binding to particular miRNAs. Figure 2-2A shows that

AGO10 indeed only recruited miR166 but not miR168 or -390, whereas other AGOs did not demonstrate this preference. To more precisely control the spatiotemporal co-expression of the tested miRNAs in the transient system, we constructed clusters of miRNA precursors, represented by two contiguous miRNA precursors in the same vectors driven by the 35S promoter (i.e., 35S-miR166a-miR168a or 35S-miR168a-miR166a) (Figure 2-2B). Both miR166 and miR168 were efficiently processed regardless of the order in which the precursors were placed (Figure 2-2C). When coexpressed with the AGO genes, only miR166, but not miR168, was sorted into AGO10. Our co-IP competition experiments clearly indicated that there is a specific interaction between AGO10 and miR166/165 in planta.

AGO10/miR166 interaction is determined by the internal structure of miR166/166 duplex*

Next we set out to explore the molecular mechanism underlying the predominant association of AGO10-miR166/165. The initial hypothesis was that miR166/165 might possess some unique sequences that are recognized by AGO10. However, we excluded this possibility by a series of experiments including nucleotide swapping between miR166 and its star strand (data not shown). Then we tested whether the duplex regions of miR166 contribute to the specific preference of AGO10 for miR166 because miR166 and its star strands contain distinct stem-loop structure. This hypothesis was tested by introducing two forms of miR166a duplexes into pre-miR390b precursors in place of miR390/390* duplexes. One duplex contained the authentic miR166/166* duplex-

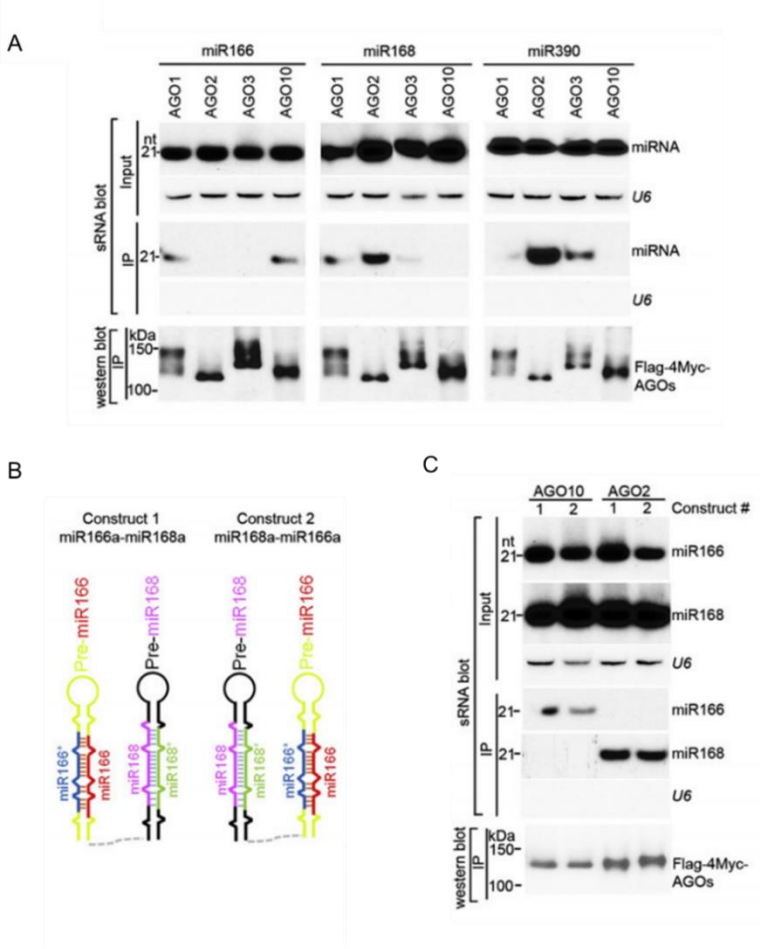

Figure 2- 2 AGO10 predominantly recruits miR166.

(A) The specific AGO10 - miR166 interaction was confirmed in *N. bentha*. sRNA blots were conducted with total RNA and sRNAs recovered from immunoprecipitated AGO complexes (IP). Western blot analyses were done with the crude extract and aliquots of the IP products using an anti-Myc antibody.

(B) Schematic of clustered miRNA precursors.

(C) AGO10 specifically recruits miR166 regardless of the position of miR166 precursor in the clustered precursor constructs.

mispairing structure (miR166/166*^{390}), and the other contained 390b-like duplex-mispairing structure (miR166/390*-like^{390}) (Figure 2-3A). We found that the ability of miR166 derived from miR166/390*-like^{390} to co-IP with AGO10 was abolished, whereas miR166 processed from miR166/166*^{390} maintained a strong association with AGO10 (Figure 2-3B). In contrast, the differential binding abilities of miR166 from different stem-loop contexts were not obvious with AGO1 (data not shown). These results indicated that the stem-loop structures of miR166/166* were sufficient to direct its predominant association with AGO10.

Deficient loading of miR166/165 leads to defective SAM development

In light of our finding that AGO10 specifically recruits miR166/165, we predicted that AGO10 controls stem cell maintenance through miR166/165. We reasoned that introducing into plants an excess of ‘‘dominant-negative’’ miR166 that could not be sorted into AGO10 might allow us to determine whether *ago10* phenotypes arise from an inability to load miR166 into AGO10. We tested this hypothesis by generating transgenic plants that constitutively express miR166/390*-like^{390}, which should be selectively loaded onto AGO1, but not AGO10, in the wild type Col-0 background. Transgenic plants overexpressing miR166a, and miR166/166*^{390} were also generated as controls. Consistent with our prediction, transformants overexpressing miR166/390*-like^{390} showed a significantly higher frequency of the *ago10* phenotype than other miR166 transformants (Figure 2-4A). Analyses of sRNA and northern blots showed that these phenotypes

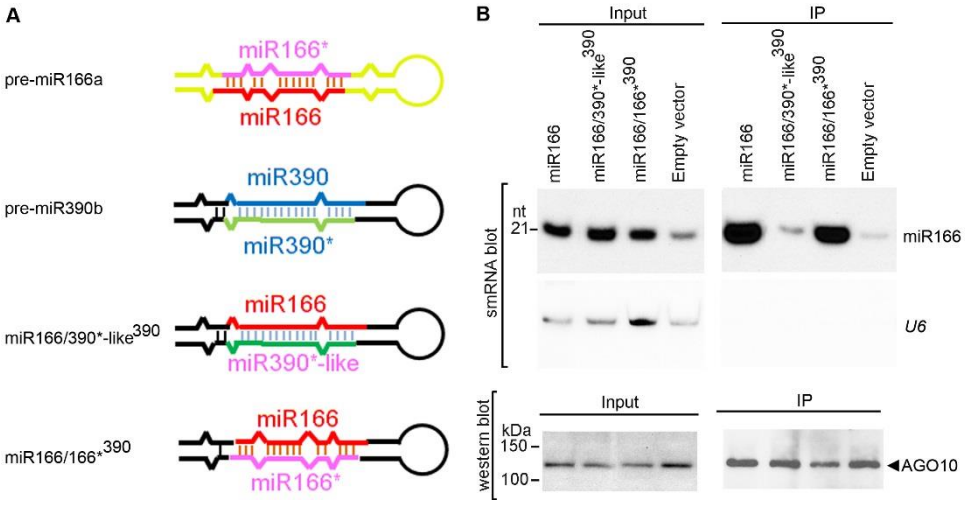

Figure 2- 3 Swapping assays of miRNA/* duplexes and their precursors.

(A) Predicted foldbacks of miR166a and 390b native and chimeric precursors. miR166 and 390 and their * strands are shown in different colors. Note: different budges exist in the precursors.

(B) Change of the miR166/166* duplex structure dramatically decreased the loading of miR166 to AGO10. The miR166a and chimeric precursors were co-expressed with AGO10 in *N. bentha*. miR166 from total RNA (Input) and AGO10 complex (IP) were detected by RNA blot. AGO10 IP was measured by western blot.

correlated with miR166 over accumulation and subsequent downregulation of its target genes.

To investigate whether deficient loading of miR166 accounted for the higher frequency of the ago10 phenotype in miR166/390*-like 390 transformants than in other miR166 transformants, we created double transgenic plants expressing β-estradiol-inducible pER8 -miR166a , -miR166/390*-like 390 ,or -miR166/166* 390 in *ago10*$^{pnh-2}$*;*P_{AGO10}*-HF-AGO10* and *ago1-27;*P_{AGO1}*-HF-AGO1* backgrounds (Zuo et al., 2000). Co-IP experiments showed that when expression of the precursors was induced, miR166 was efficiently processed from miR166/390*-like 390, and its association with AGO10, but not with AGO1, was significantly reduced. In contrast, miR166 generated from miR166a and miR166/166* 390 did not show this discrimination (Figure 2-4B and C). These results indicated that inefficient AGO10-miR166 assembly led to an imbalance in the distribution of miR166/165 between AGO10 and AGO1 and a corresponding defect in the shoot apex (Figure 2-4D).

Figure 2- 4 Deficient loading of miR166 into AGO10 causes pinhead phenotypes in the Col-0 background.

(A) Shared morphological phenotypes of 35S-miR166a, -miR166/166* 390, and -miR166/390*-like 390 plants. Photographs were taken of 10-day-old seedlings. Two representative lines are shown for each construct.

(B and C) Deficient loading of miR166 from the mi 166/390*-like390 precursor into AGO10 (B) but not AGO1 (C) in *Arabidopsis*. Analyses of sRNA blot and western blot (using an anti-Flag antibody) were conducted as in Figure 2-2A. The exposure times for AGO10 and AGO1 protein blots were 30 and 5 s, respectively. The relative mean ratio of miR166/AGO10 (or AGO1) was normalized to that obtained with *XVE*-miR166 where the ratio was arbitrarily assigned a value of 1 with ±SD from three experiments (bottom panels in B and C).

(D) Correlation of the imbalanced loading of miR166/165 into AGO1/AGO10 with pinhead phenotype.

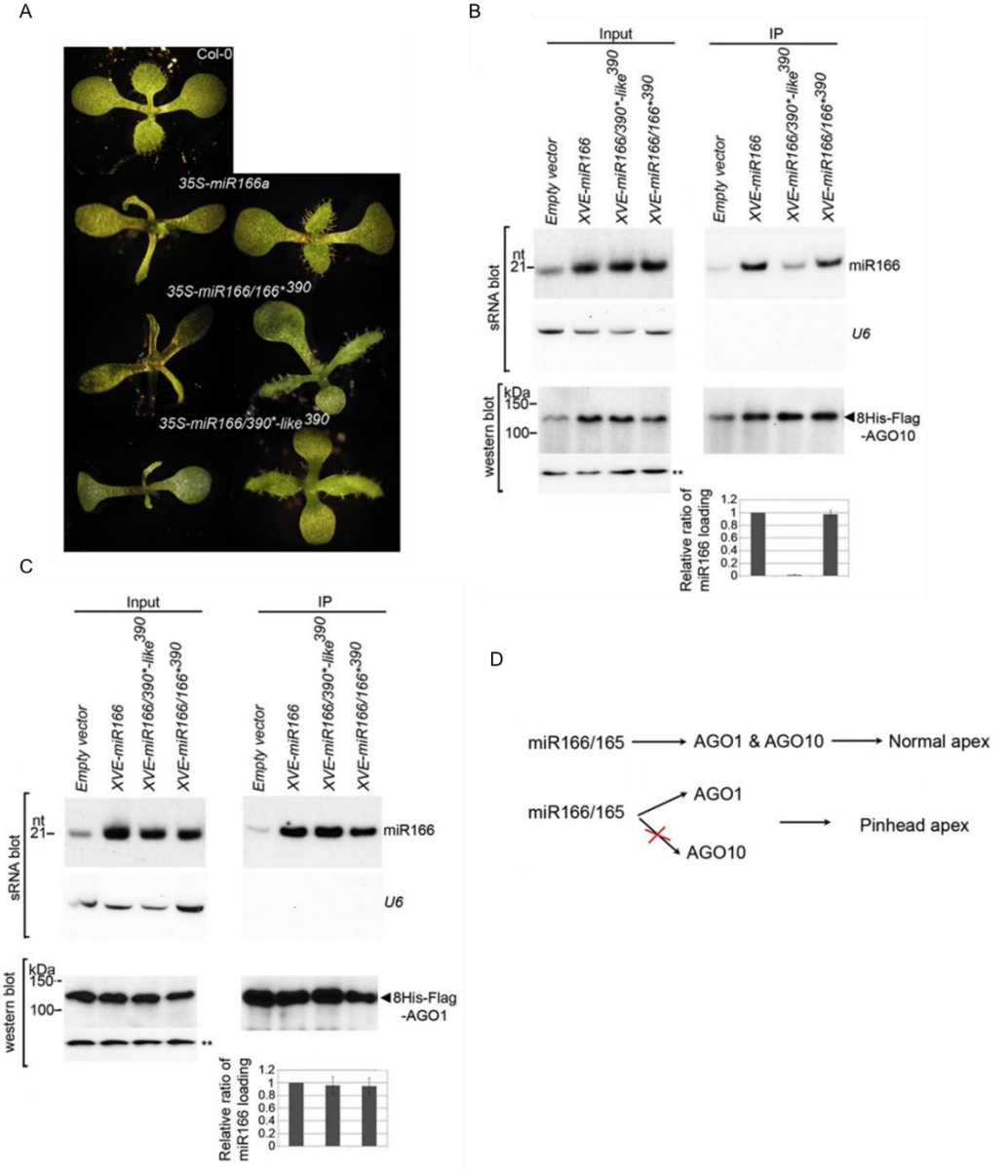
A
Col-0
35S-miR166a
35S-miR166/166*390
35S-miR166/390*-like390
B
Input
IP
Empty vector
XVE-miR166
XVE-miR166/390*-like390
XVE-miR166/166*390
sRNA blot
nt
21–
miR166
U6
western blot
kDa
150–
100–
8His-Flag
-AGO10
Relative ratio of miR166 loading
1.2
1
0.8
0.6
0.4
0.2
0
C
Input
IP
Empty vector
XVE-miR166
XVE-miR166/390*-like390
XVE-miR166/166*390
sRNA blot
nt
21–
miR166
U6
western blot
kDa
150–
100–
8His-Flag
-AGO1
Relative ratio of miR166 loading
1.2
1
0.8
0.6
0.4
0.2
0
D
miR166/165
AGO1 & AGO10
Normal apex
miR166/165
AGO1
AGO10
Pinhead apex

Sequestering elevated miR166/165 from the expression region of AGO10 rescues the ago10 phenotype

In *ago10* mutants, miR166/165 levels are abnormally increased and they accumulate ectopically in the developing meristem (Liu et al., 2009b). By examining the levels of miR166 and selected miRNAs in AGO1 complexes isolated from wild-type Ler, two *ago10* alleles, and complemented transgenic lines, we found that the ectopically accumulated miR166/165 in *ago10* mutants is re-directed to AGO1, a master repressor of miRNA targets. sRNA blot analysis showed that the relative amount of miR166/miR159 associated with AGO1 was much higher in *ago10* mutants than that in the wild-type Ler and the complemented *ago10* $^{pnh-2}$*;* P_{AGO10} *-HF-AGO10* plants (Figure 2-5 A and B). These results indicated that loss-of-function mutations of AGO10 caused a significant increase in the loading of miR166 into AGO1.

In the *ago10* mutant, the increased binding of miR166 by AGO1 might result in the down regulation of *HD-ZIP III* transcripts in the AGO10 expression domain and further lead to the terminal differentiation of the SAM. According to this model, we reasoned that *ago10* mutants might be rescued by hijacking the extra miR166/165 or inhibiting miR166/165 activity in the AGO10 expression domain. When target mimicry construct (Figure 2-6A) P_{AGO10} *-MIM166/165* was introduced into the *ago10* mutants to sequester miR166/165 from the expression niche of *AGO10*, the *ago10* mutants were rescued. Consistent with our expectation, when transformed into the *ago10* $^{pnh-2}$ mutant, the target mimicry construct largely rescued the shoot apex defects in the *ago10* $^{pnh-2}$ mutant (Figure 2-6B).

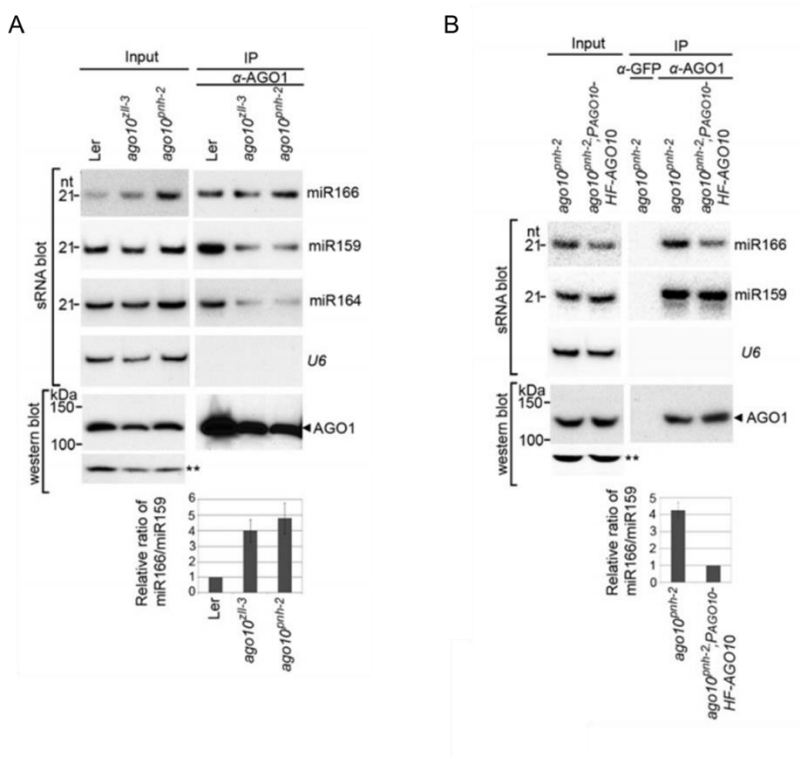

Figure 2- 5 *ago10* mutation resulted in a significant increase in miR166 binding by AGO1 in *Arabidopsis*.

(A and B) sRNA blot analyses were conducted with total RNA (input) and sRNA recovered from the AGO1 complexes (IP). Western blot assays were performed using an anti-AGO1 antibody. A cross-reacting band (**) served as a loading control. The relative signal ratio of miR166 to miR159 in AGO1 complexes was normalized to that obtained from the wild-type Ler or the *P* $_{AGO10}$*-HF-AGO10* complemented lines where the ratio was arbitrarily assigned a value of 1 with ± SD from three experiments (bottom panels in A and B).

Along with the complementation of the phenotypes, the steady-state levels of miR166/165 and their targets in the transgenic lines expressing target mimicry were restored compared to those in the wild-type plants (Figure 2-6C). As a result, *HD-ZIP III* transcripts were up regulated compared to those in *ago10* $^{pnh\text{-}2}$ plants (Figure 2-6D). These results indicate that the increased binding of miR166 by AGO1 results in the down-regulation of *HD-ZIP III* transcripts in the *AGO10* expression niche and further leads to the defective SAM in the *ago10* mutants.

AGO10 rescues the ago10 $^{pnh\text{-}2}$ *mutant by sequestering miR166/165 from AGO1*

AGO10 contains the catalytic Asp-Asp-His (DDH) motif in its PIWI domain. To test its catalytic potential directly, we incubated immunoaffinity-purified AGO10 with a part of a *PHV* transcript containing a sequence complementary to miR166/165. The *PHV* mRNA was sliced by AGO10 protein, but not by AGO10 mutants with substitutions of essential catalytic residues (D709A, D793A, or H935A; referred to hereafter as DDH mutants) despite comparable miR166/165-binding capacities (Figure 2-7A and B).

Given that simple sequestration or decoy of miR166/165 in the *AGO10* expression domain rescued *ago10* mutants, we reasoned that AGO10 DDH mutants might also complement *ago10* mutants because they retain miR166/165-binding capacity and can form an unproductive RISC (Figure 2-7B). To this end, we examined the T3 progeny of the transformants harboring wild-type *AGO10* and each DDH mutant expressed from the *AGO10* promoter or the constitutive 35S promoter in the *ago10* $^{pnh\text{-}2}$ background.

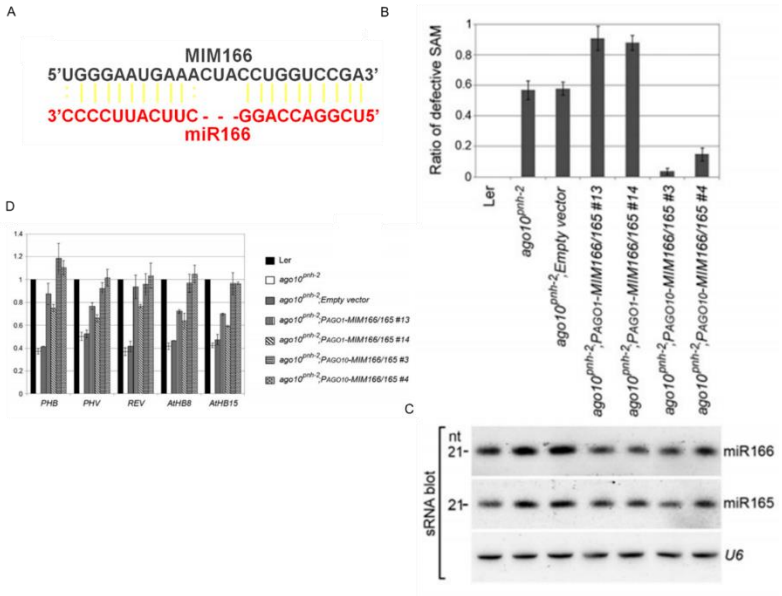

Figure 2- 6 Sequestering elevated miR166/165 from the expression region of *AGO10*, but not *AGO1*, by target mimicry rescues the *ago10*$^{pnh-2}$ phenotype.

(A) Schematic of target mimicry construct for miR166 (MIM166).

(B) Defective SAM was rescued in *ago10*$^{pnh-2}$ plants by mi R166/165 target mimicry expressed from the promoters of *AGO10*, but not *AGO1*. The ratios of defective SAM are shown as mean ± SD from three replicates (n > 200/each replicate).

(C and D) Levels of miR166/165 and their target transcripts were measured by RNA blot assays (C) and real-time RT-PCR (D). The relative level of *HD-ZIP III* transcripts was normalized to that in Ler plants where the amount was arbitrarily assigned a value of 1 with ± SD from four experiments in (D).

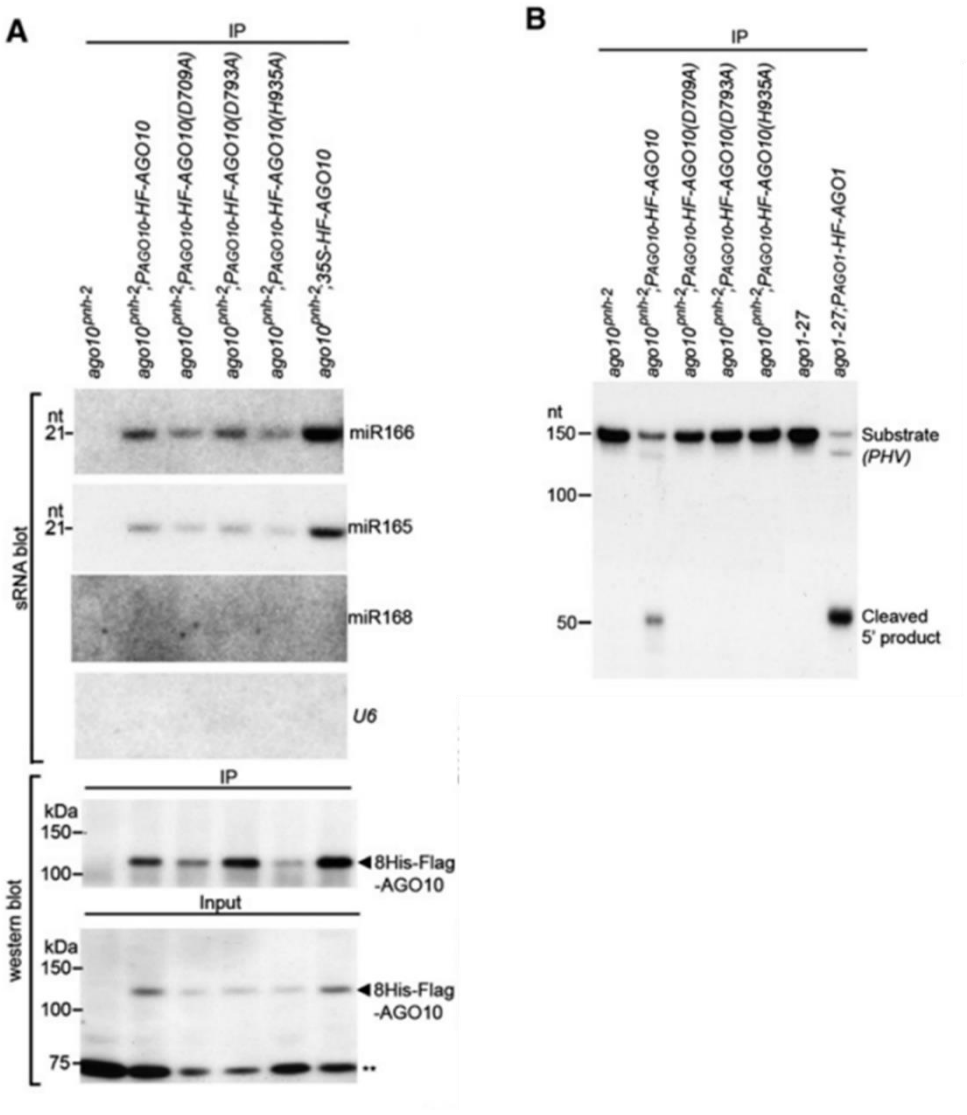

Figure 2- 7 Functional characterization of AGO10 DDH mutants.

(A) AGO10 DDH mutants maintained miR166/165-binding capacity. Assays of sRNA blot and western blot (using anti-Flag antibody) were conducted as in Figure 2-1A.

(B) RISC reconstitution assays of AGO10 and AGO10 DDH mutants. AGO1 was included as a positive control.

Intriguingly, more than 95.7% of all T3 transformants (20 lines; n > 200 plants/line) expressing AGO10 from both the native *AGO10* and the 35S promoters, or AGO10 DDH mutants from the *AGO10* promoter, displayed a normal shoot apex, whereas those with the empty vector did not (Figure 2-8A). Moreover, miR166 accumulation was decreased in these complemented lines relative to levels in *ago10* $^{pnh-2}$ mutants (Figure 2-8B). These results indicated that the slicer activity of AGO10 is unnecessary to rescue the pinhead phenotype.

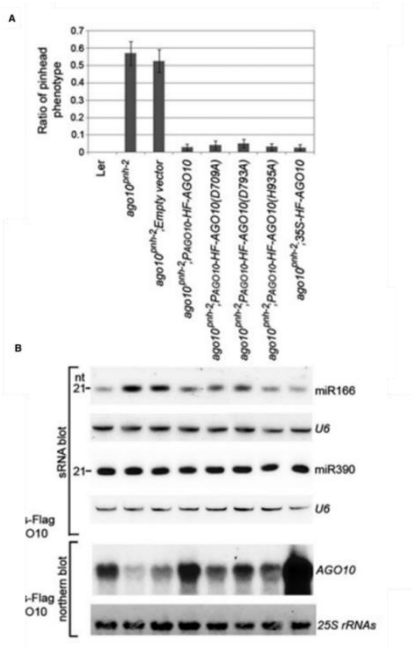

Figure 2- 8 AGO10 DDH mutants function as catalytic active AGO10 in *ago10*$^{pnh-2}$. (A) Noncatalytic AGO10 rescued the *ago10*$^{pnh-2}$mutant as efficiently as catalytic AGO10. The pinhead ratios are shown as mean ± SD from 16 lines (n > 200/line). (B) Levels of miR166/165 and *AGO10* were measured by analyses of sRNA and northern blots.

AGO10 acts as a miR166/165 decoy

Given the strikingly similar molecular and phenotypic characteristics of *ago10* $^{pnh\text{-}2}$; P_{AGO10} *-MIM166/165* and *ago10* $^{pnh\text{-}2}$; P_{AGO10} *-HF-AGO10 (DDH)* plants, we propose that the main regulatory function of AGO10 in SAM maintenance is to sequester miR166/165 and to antagonize their activity. Under this model, we expect that AGO10 should have a higher affinity for miR166 than AGO1. To test this hypothesis, we first investigated the relative binding affinity of AGO1 and AGO10 to miR166 in *N. bentha*. When coexpressed with AGO1 or AGO10 genes, overaccumulated miR166 was readily loaded into either of the AGO complexes (Figure 2-9A). However, when coexpressed with both AGO1 and AGO10, more miR166 was recruited into AGO10 than AGO1 despite a lower amount of AGO10 protein compared to that of AGO1. Imaging quantification analysis showed that the relative signal ratio of miR166/AGO10 was significantly higher than that of miR166/AGO1, indicating that miR166 was preferentially loaded into AGO10 over AGO1 when both were present (Figure 2-9B).

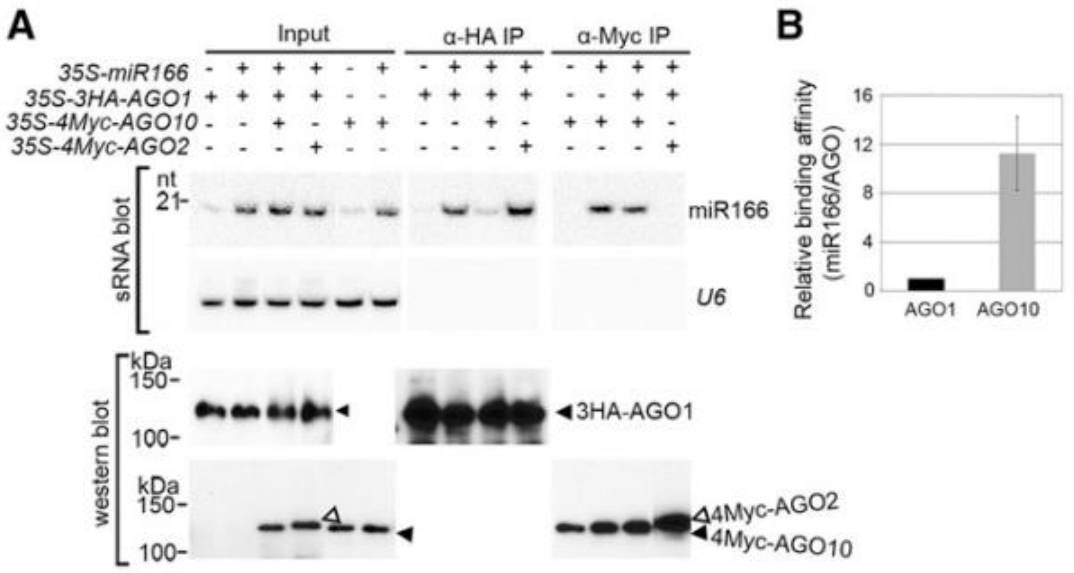

Figure 2- 9 AGO10 has a higher binding affinity for miR166 than AGO1 does.

(A and B) Relative binding affinity of AGO10 and AGO1 to miR166 was examined by competitive immunoprecipitation assays in a transient expression system. 35S-miR166a and different *AGO* genes were coexpressed in *N. bentha*. AGO1, AGO2, or AG O10 complexes were immunoprecipitated with an anti-HA or anti-Myc antibody, respectively (A). The relative mean signal of miR166/AGO10 in the treatment (35S- miR166, 3HA-AGO 1 and 4Myc-AGO10) was normalized to that of miR166/AGO1 where the ratio was arbitrarily assigned a value of 1 with the ± SD from three experiments (B).

We further examined levels of miR166 in AGO1 and AGO10 complexes isolated from complemented transgenic plants expressing *P $_{AGO10}$-HF-AGO10* or -*AGO10 (H935A)* and *35S-HF-AGO10*. Because the accumulation of dual-tagged AGO10 was about 40-fold less than that of endogenous AGO1 in *ago10 $^{pnh-2}$; P $_{AGO10}$-HF-AGO10* plant (Figure 2-10A and B), the absolute amount of miR166 in AGO10 was slightly less than that in AGO1 complexes (Figure 2-10C). However, the relative level of miR166 recovered from immunoprecipitated AGO10 was 4- to 6-fold higher than the amount recovered from AGO1 (Figure 2-10C and D). More strikingly, more than 80% of miR166, but not control miRNAs, was redirected from AGO1 to AGO10 upon expression of *35S-HF-AGO10* relative to the distribution in the plants expressing *P_{AGO10}-HF-AGO10*, despite only a twofold increase in the levels of dual-tagged AGO10 (Figure 2-10C and D). Together, these results indicate that AGO10 binds to miR166 with a higher affinity than does AGO1 and thus possesses the capability to function as a decoy for miR166 in plants.

Figure 2- 10 AGO10 rescues the *ago10*$^{pnh-2}$ mutant by sequestering miR166/165 from AGO1.

(A and B) Expression levels of *AGO1* and *AGO10* transcripts and proteins in *Arabidopsis*. Northern blot analyses were performed using total RNA prepared from 7-day-old complemented *ago10*$^{pnh-2}$*; P*$_{AGO10}$*-HF-AGO10* seedlings using probes specific to *AGO1* and *AGO10* transcripts, respectively. The blots were exposed to the same phosphor plate for 2 or 4 hours before signal detection. 25S *rRNA* served as a loading control. The relative signal of *AGO10* was normalized to that obtained with *AGO1* where the ratio was arbitrarily assigned a value of 1 with the ± SD derived from at least four experiments. Western blot assays were performed with total crude protein extract using an anti-Flag antibody. Actin served as a loading control. For accurate quantification, a series of dilutions were prepared from input of the AGO1 protein. The relative signal ratio of AGO10 was normalized to that obtained with AGO1 in crude extract where the ratio was arbitrarily assigned a value of 1 with the ± SD from four experiments. The results from two biological replicates are shown for both northern and western blots.

(C) AGO10 sequestered miR166 from AGO1.

(D) The relative binding of miR166 by dual-tagged AGO10 was normalized to that of miR166/AGO1 isolated from *ago10*$^{pnh-2}$*; P*$_{AGO10}$*-HF-AGO10* plants where the ratio was arbitrarily assigned a value of 1 with ± SD from three experiments.

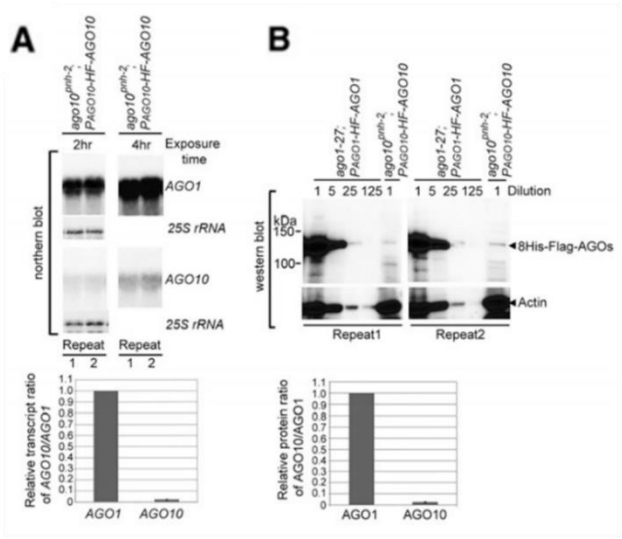
A
B
2hr
4hr
Exposure time
AGO1
25S rRNA
AGO10
25S rRNA
northern blot
Repeat
Repeat
Relative transcript ratio of AGO10/AGO1
AGO1
AGO10
Dilution
kDa
150
100
8His-Flag-AGOs
Actin
western blot
Repeat1
Repeat2
Relative protein ratio of AGO10/AGO1

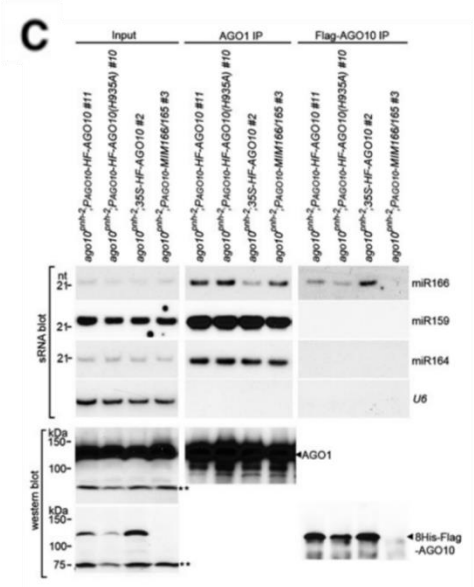
C
Input
AGO1 IP
Flag-AGO10 IP
miR166
miR159
miR164
U6
sRNA blot
AGO1
8His-Flag-AGO10
western blot

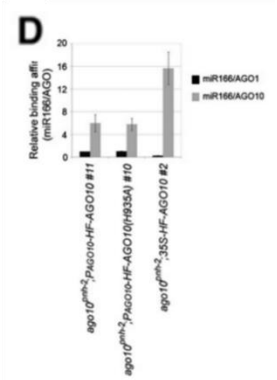
D
Relative binding affi (miR166/AGO)
miR166/AGO1
miR166/AGO10

AGO1 and AGO10 are functionally distinct in SAM regulation

Because *AGO1* and *AGO10* are the closest genetic paralogs and are believed to have functional redundancy, we used promoter swapping to directly test whether *AGO1* could replace *AGO10* and vice versa. We transformed P_{AGO10} *-HF-AGO1* into $ago10^{pnh\text{-}2}$. Surprisingly, about half of the primary transformants harboring P_{AGO10} *-HF-AGO1* showed phenotypes suggestive of *AGO1* cosuppression and the *ago10* phenotype. An additional 10% of the transgenic plants exhibited a pinhead phenotype (Figure 2-11A). These results indicate that *AGO1* cannot substitute for *AGO10* in SAM maintenance. On the other hand, P_{AGO1} *-HF-AGO10* was unable to rescue the morphological defects in *ago1-27* hypomorphs (Figure 2-11B) and also caused upward curled leaves. Taken together, these data suggest that *AGO10* and *AGO1* have functionally distinct roles and are unable to complement each other, with the additional implication that these functions may result from intrinsic differences in sRNA binding preferences.

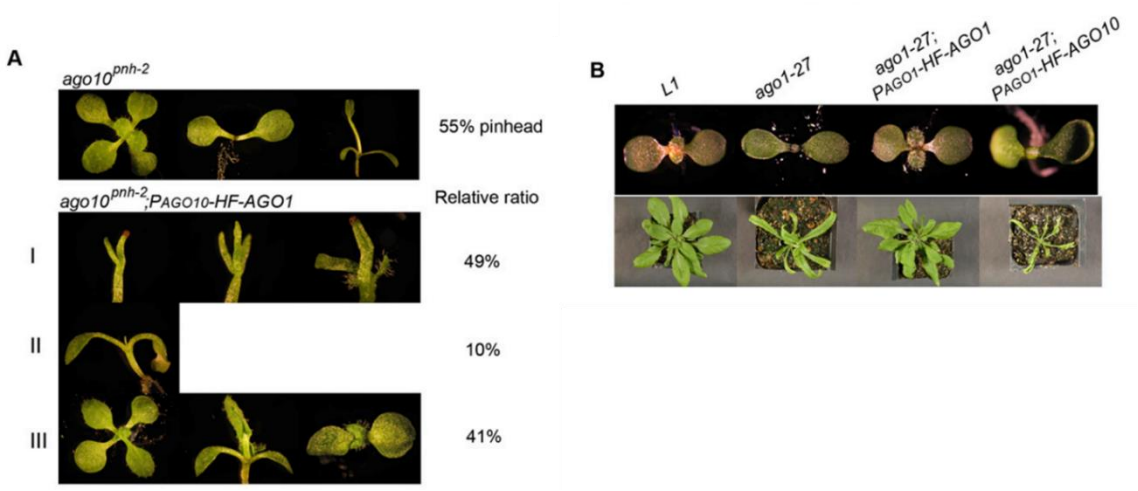

Figure 2- 11 *AGO10* and *AGO1* could not substitute for each other with respect to SAM maintenance and leaf morphology.

(A) *AGO1* expressed from the *AGO10* promoter could not complement the *ago10*$^{pnh-2}$ mutant. Approximately 55% of *ago10*$^{pnh-2}$ plants (n > 200) show a pinhead phenotype (empty apex or terminal organs). Diverse phenotypes of *ago10*$^{pnh-2}$; *P* $_{AGO10}$*-HF-AGO1* transformants (n = 133, bot tom panels). (I) Phenotypes suggestive of *AGO1* cosuppression and the *ago-10* phenotype (49%); (II) SAM replaced by a pin-like organ (10%); (III) plants with normal SAM (41%). Photographs were taken of 10-day-old seedlings.

(B) *AGO10* expressed from the *AGO1* promoter could not rescue *ago1-27* morphology. Photographs were taken of cotyledons (top panels) and 4-week-old adult plants (bottom panels).

Discussion

By identifying sRNAs of AGO10-containing RISCs, we discovered that AGO10 predominantly associates with miR166/165to regulate SAM development. The AGO10-miR166/165 interaction is a unique case in which an AGO protein specifically binds to a particular group of miRNAs to execute its biological function.

How does AGO10 specifically select miR166/165 among hundreds of miRNAs and an overwhelming number of siRNAs? All miR166/165 family members have adopted distinct structures in their miRNA/* regions that are absent among the rest of the *Arabidopsis* miRNAs. We found that this distinct structure accounts for the specific affinity of AGO10 for miR166/165. We have further mapped the critical positions (miR166 12U/*8U and its adjacent nucleotides) that are responsible for the specific sorting of miR166/165 to AGO10. Intriguingly, miR166/165 12U/*8U is the only mismatch conserved among the entire miR166/165 family (data not shown). How can the unique mispairing and adjacent residues in miR166/165 be sensed? One possibility is that there is a factor that recognizes this particular region of miR166/165 and funnels this group of miRNAs into AGO10. However, we favor the idea that specific recognition could be conferred by AGO10 itself. It has been proposed that sRNA duplexes are unwound before loading into an AGO so that only the guide strand, which contains the less stably paired 5' end, is incorporated into the AGO (Tomari et al., 2004). However, in *Drosophila*, siRNA duplexes are indeed loaded into RISCs so that the guide strand of the siRNA duplexes directs Argonaute-catalyzed cleavage of the passenger strand (Matranga et al., 2005). Moreover, there is increasing evidence that AGOs participate

directly in miRNA biogenesis and maturation (Cheloufi et al., 2010; Cifuentes et al., 2010; Diederichs and Haber, 2007). Although the RISC loading process has not yet been investigated in *Arabidopsis*, a previous study with suppressor 2b from *Cucumber Mosaic Virus* strongly suggests that miRNA/* duplexes might be loaded into an AGO by a passenger-strand cleavage-assisted mechanism (Zhang et al., 2006). If so, the distinct structure of the miR166/165 duplex may be recognized and further selected by AGO10.

The mechanism by which the miRNA/* structure determines its routing, which we have uncovered here in plants, is reminiscent of mechanisms that have been reported in *Drosophila* and *C. elegans* (Forstemann et al., 2007; Steiner et al., 2007; Tomari et al., 2007). In *Drosophila*, perfectly complementary duplexes are channeled into AGO2 as siRNAs. In contrast, the presence of mismatches in miRNA duplexes promotes their incorporation into AGO1 (Forstemann et al., 2007). Nevertheless, there is a fundamental difference between the AGO10-miR166/165 association in plants and the sRNA-sorting mechanisms described in animals. In *Arabidopsis*, most miRNA duplexes harbor mismatches, whereas they were not enriched in AGO10, indicating specific mismatch recognition by AGO10. However, in animal systems, structures of sRNA duplexes play a general instructive role in their sorting to various AGOs.

Because the primary function of AGO proteins is to repress target genes, one would imagine that AGO10 specifically recruits miR166/165 to down regulate the *HD-ZIP III* transcripts. In fact, AGO10 possesses catalytic activity and can slice *PHV* transcripts in RISC reconstitution assays. This activity notwithstanding, AGO10 is a positive regulator of HD-ZIP III genes in vivo because transcript levels of all *HD-ZIP III*

genes were decreased in the *ago10* mutant relative to wild-type Ler plants. Consistent with this notion is the previous observation that AGO10 and *HD-ZIP III* transcripts colocalize (Kidner and Martienssen, 2004). One explanation for this positive regulation might be that AGO10 increases the accumulation of *HD-ZIP III* transcripts by genetically repressing miR166/165 expression (Liu et al., 2009a).

We favor a notion that AGO10 positively regulates *HD-ZIP III* family genes by acting as a specific decoy for miR166/165 (Figure 2-12A). Several lines of evidence support this model: (1) In *ago10* mutants, ectopically accumulated miR166/165 are redirected into AGO1, causing a reduction of *HD-ZIP III* transcripts in the *AGO10* domain during SAM development and corresponding shoot apex defects (Figure 2-12B). (2) Simple sequestration of miR166/165 in the expression niche of *AGO10* by target mimicry or noncatalytic AGO10 DDH can up regulate the expression of *HD-ZIP III* family genes and rescue the *ago10* phenotype (Figure 2-12C and D). (3) Deficient incorporation of miR166 into AGO10 and the resulting imbalanced distribution of miR166/165 between AGO10 and AGO1 lead to a defective SAM. Interestingly, *ago10* mutants display significant phenotypic differences in Ler and Col-0 backgrounds. In our study, making miR166 more accessible to AGO1 than to AGO10 by producing them in a different way leads to a similar phenotype in both ecotypes. This result suggests that there may be a factor in Col-0 that normally prevents miR165/166 incorporation into AGO1 in the *AGO10* domain in *ago10* mutants. (4) AGO10 exhibits a stronger binding affinity for miR166 than does AGO1 and thus possesses ability as a decoy for these miRNAs. Therefore, we propose that the biological role of AGO10 is to compete with

AGO1 by sequestering miR166/165, preventing them from being loaded into AGO1 and subsequently targeting *HD-ZIP III* genes.

Given that AGO10 retains catalytic activity, how is its slicing activity avoided while acting as a decoy for miR166/165 in plants? Several nonexclusive models may apply. First, we envision that there may be some unidentified AGO10-interacting partners that inhibit the slicing function of AGO10. A recent report has shown that leucine-rich repeat kinase 2 (LRRK2) associates with *Drosophila* and human AGOs and represses their activities (Gehrke et al., 2010). The *Arabidopsis* genome encodes numerous LRRK proteins, some of which might interfere with the AGO10 function. Alternatively, AGO10 may sequester miR166/165 away from the developing meristem into a particular niche in planta to prevent the ectopic accumulation of these sRNAs in the SAM. Consistent with this view is the finding that AGO10 is specifically required in the vasculature below the SAM (Tucker et al., 2008). Considering the cell-autonomous accumulation of AGO proteins and non-cell-autonomous functions of miRNAs, AGO10 may sequester miR166/165 in the vasculature and prevent their movement into the meristem above (Chitwood and Timmermans, 2010). Third, AGO10 slicing activity may be less efficient than that of AGO1 in vivo, resulting in a net reduction of miR166/165 potency when sequestered into AGO10. Finally, AGO10 may trigger miR166/165 turnover in addition to its sequestration, lowering the effective miR166/165 population.

In addition to SAM maintenance, AGO10 also plays a critical role in organ polarity and vascular development. Although we have not examined these developmental processes in our study, it is likely that AGO10 regulates these biological

Figure 2- 12 AGO10 maintains the SAM by specifically decoying miR166/165 to upregulate *HD-ZIP III* family genes.

Panels A–D illustrate the different destinations of miR166/165 to AGO1 or -10 and corresponding fates of the SAM in wild-type plants (A), *ago10* mutants (B), and complemented transgenic lines expressing target mimicry (C) and catalytic-inactive forms of AGO10 (D), respectively. SAM (red crescent) is specified by the *HD-ZIP III* transcription factors (brown rectangle) located within the *AGO10* expression niche. *AGO10* expression (light green) is limited to the provasculature and the adaxial side of the cotyledons. *AGO1* is expressed ubiquitously in the whole embryo (gray), partially overlapping the *AGO10* expression domain. AGO10 is a positive regulator of *HD-ZIP III* family genes (red arrow), whereas AGO1 is a negative regulator (white T). The terminated SAM is indicated by a red stop sign. miR166/165 and MIM166/165 are shown as yellow and white bars.

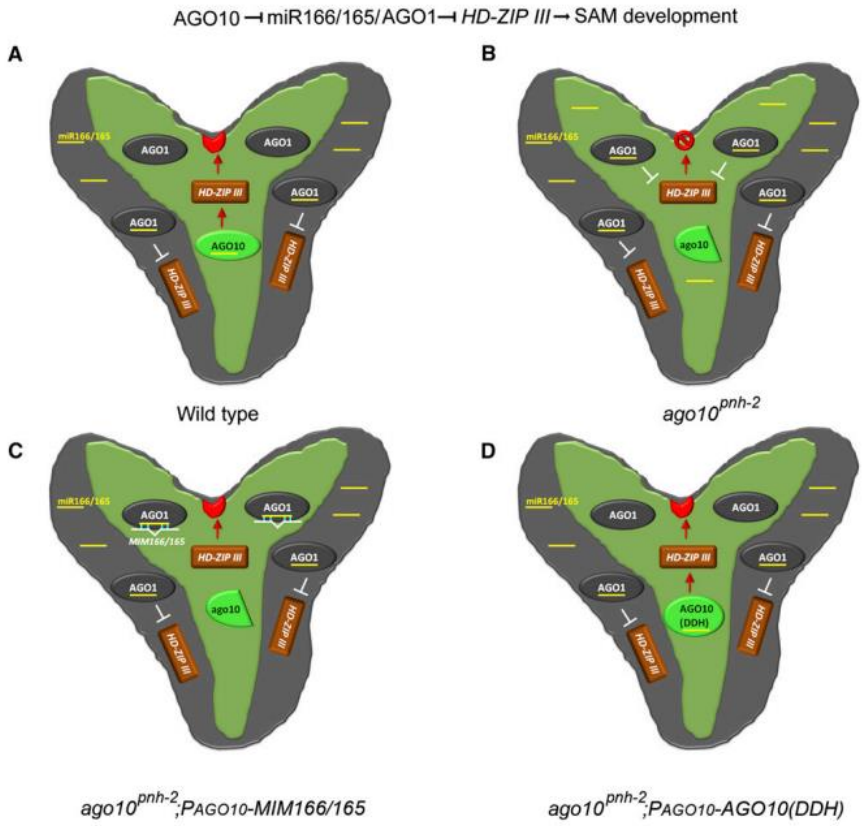
AGO10 ⊣ miR166/165/AGO1 ⊣ HD-ZIP III → SAM development
A
B
C
D
miR166/165
AGO1
HD-ZIP III
AGO10
ago10
MIM166/165
AGO10 (DDH)
Wild type
ago10pnh-2
ago10pnh-2;PAGO10-MIM166/165
ago10pnh-2;PAGO10-AGO10(DDH)

events through its association with miR166/165. Of course, we have no reason to exclude the possibility that AGO10 might bind to other sRNAs to regulate their targets. Our sequencing results revealed that AGO10 does recruit a spectrum of miRNAs and numerous ta-siRNAs, although their relative ratios are very low. A previous study with *Arabidopsis* AGO4 suggests that a single AGO protein may function as a catalytic engine of RNA cleavage while it can also execute slicing-independent regulation of sRNA targets (Qi et al., 2006). Given that AGO10 does possess slicer activity, it will be intriguing to investigate whether or not this activity is required for regulation of sRNA targets other than *HD-ZIP III* family genes.

Can the role of AGO10 in SAM maintenance be performed by other AGOs? Here, we showed that AGO1 could not replace AGO10 with regard to SAM maintenance and vice versa, in terms of leaf morphology. This functional diversification between AGO1 and AGO10 is apparently determined by differential binding capacities for different spectrums of miRNAs. Intriguingly, AGO1 and AGO10 have 86% similarity and 78% identity in their PAZ/PIWI domains but less than 20% similarity in their N-terminal regions; yet their miRNA-binding preferences are distinct. Recently, an elegant study showed that only the PAZ domain, which is thought to bind to the 3' end of sRNA, is interchangeable between both proteins, whereas the MID-PIWI and N-terminal domains appear to contribute to their functional specificity (Mallory et al., 2009). Further dissection of the AGO10 and AGO1 protein structures will advance our insight into the mechanisms underlying the differential miRNA-binding preferences of these AGOs.

CHAPTER III

DELINEATE CRITICAL DOMAINS OF AGO10 INVOLVED IN SPECIFIC MIR166/165 ASSOCIATION AND SAM REGULATION

Summary

AGO proteins recruit sRNAs to regulate their sequence-complementary targets. *Arabidopsis* encodes nine functional AGO proteins, among which, AGO1 and AGO10 are two closest paralogs to each other. Both proteins are capable of binding to miR166/165; however, AGO1 cannot replace AGO10 with regard to SAM development and maintenance and vice versa. Moreover, AGO10 possesses higher binding affinity for miR166/165 than AGO1 does. AGO10-miR166/165 interaction and the decoy activity of AGO10 are crucial for SAM maintenance. By conducting a series of domain-swapping experiments, I here report that the chimeric protein $AGO1^{AGO10NT}$ is able to rescue the *zll3-2* phenotype while $AGO10^{AGO1NT}$ fails to do so. This result suggests that N-terminal domain of AGO10 confers its unique function in meristem development.

Introduction

One outstanding question from our research described in Chapter III is how AGO10 specifically recognizes the relevant structural features of duplexes of miR166/166 and their star strands, hereafter, refer to miR166/*). I hypothesized that the AGO10 protein contained certain unique domains or docking pockets for recognizing and binding to miR166/*. Structural analysis of a eubacterial AGO/guide/target ternary complex unveils that the PIWI and N-terminal domains comprise a channel to

accommodate a lengthening of up to 14-bp guide-target duplexes (Wang et al., 2009b). Interaction interfaces between human AGO2 and miRNAs mainly involve positions from nucleotides 8 to 13 of miRNAs (Hafner, 2010). Consistently, the equivalent positions of miR166/* duplexes are critical for their predominant association with AGO10 (Zhu et al., 2011). Therefore, AGO10 most likely contains specific regions to interact with the critical nucleotides of miR166/*. AGO proteins harbor the 3' and 5' ends of sRNAs through PAZ and MID domains, respectively. However, little is known about how AGOs recognize duplex structures of sRNAs and the role of N-terminal domain in AGO-sRNA association remains to be investigated.

The goal of my study is to delineate critical domains in AGO10 involved in its specific miR165/166 association. Because of low sequence homology of Arabidopsis AGOs compared to the ones from eubacteria and other higher organisms and difficulty in crystallization of full-length *Arabidopsis thaliana* AGOs from higher organisms, I employ biochemical and genetic approaches to study interaction of AGO10-miR166/165. I found that N-terminal domain is a determining factor for uniqueness of AGO10 function in SAM maintenance.

Materials and methods

DNA Construction

Constructs were generated using the Gateway cloning system (Invitrogen). Destination vectors (DC) pBA-P_{AGO1}-Flag-4Myc-DC and pBA-P_{AGO10}-Flag-4Myc-DC were generated by modifying the pBA-35S-Flag-4Myc-DC vector. Restriction sites were

introduced into *AGO1*, *AGO4* and *AGO10* cDNAs by point-directed mutagenesis. cDNAs were cloned into pENTR/D vectors, confirmed by sequencing and transferred to the appropriate DC vectors by recombination using the LR Clonase (Invitrogen).

Plant materials and growth condition

Binary vectors expressing P_{AGO10}- *Flag-4Myc (FM)*-chimeric or control proteins were transformed into *zll3-2* background by the floral dip transformation method (Clough and Bent, 1998). Similarly, P_{AGO1} *-Flag-4Myc (FM)*-chimeric or wild-type genes were transformed into hypomorphic mutant *ago1-27* by the same method (Clough and Bent, 1998).

Transformants were selected on a standard MS medium containing the appropriate selective agents: 10 mg/l glufosinate ammonium (Sigma) with 100 mg/l cefotaxime (Sigma).

Plants were grown in LP5 Metromix (SunGro, Canada) in a walk-in growth chamber at 22 °C with relative humidity of 50% under long-day conditions (16 hours light/8 hours dark) unless otherwise noted. Light illumination (110 mmol photons/m^2s) was provided by a Spec-tralux T5 high-output lamp (Hydro warehouse).

Material preparation for western and coimmunoprecipitation

4-week-old *N. bentha* leaves were infiltrated with A. tumefaciens ABI harboring a variety of binary plasmids. The ODs of A. tumefaciens cultures were diluted to 0.4 in all experiments. *N. bentha* leaves were collected two days after agroinfiltration.

RNA blot and western blot analyses

Total RNA was extracted using Trizol reagent from Agrobacterium-transfected *N. bentha leaves*. RNA blot hybridizations of low-molecular-weight RNAs (sRNA blot) were performed as described (Zhang et al., 2006). Each lane contained sRNAs, which were recovered from isolated AGO complexes prepared from 0.4 g tissues. For input, 5 μg of total RNA was used in most cases, except in transient experiments where only 1~2 μg RNA was used. Blots were hybridized with ^{32}P-radiolabeled oligonucleotide probes complementary to the sRNAs of interest. In some experiments, the same blots were stripped and re-probed with ^{32}P-labeled oligos complementary to the indicated miRNAs. U6 served as loading controls. RNA blots were detected after exposure to a phosphor plate and quantified using the Quantity One Version 4.6.9 according to the manufacturer's instructions (Bio-Rad).

Western blot analyses were performed as previously described (Zhang et al., 2006). Western blots were developed with ECL^{+}, detected with ChemiDoc XRS+ and quantified using the ImageLab Software (Bio-Rad).

Coimmunoprecipitation experiments

Total protein was extracted in the IP buffer containing 50 mM Tris-HCl, pH 7.5, 300 mM NaCl, 4 mM MgCl 2 , 5 mM DTT, 0.1% Triton-100, and the complete protease inhibitor cocktail (Roche). Cleared protein extracts were immunoprecipitated with agarose-conjugated mono clonal antibodies against Myc (Sigma). Beads were washed

four times with the same buffer before recovery of sRNAs and analyses of sRNA and western blots.

Results

Domain swapping between AGO10 and AGO1/AGO4

To gain insight into the functions of individual domains of AGO10 I performed domain domain-swapping experiments to make a series of constructs that produce chimeric proteins among AGO1, AGO4 and AGO10. AGO1 and AGO10 have 86% similarity and 78% identity in their PAZ/PIWI domains but less than 20% similarity in their N-terminal regions; yet their miRNA-binding preferences are distinct (Zhu et al., 2011). AGO4 is selected for the domain-swapping experiment because it has only 41% similarity with AGO10 in their PAZ and MID domains and does not bind to miR166/165 (Qi et al., 2006).

By using the DNA shuffling method 16 chimeric constructs were generated (Figure 3-1).

Chimeric construct #		Chimeric construct #	
1	*AGO1*^{AGO10PAZ}	13	*AGO1*$^{AGO10\ (NT+PAZ)}$
2	*AGO1*^{AGO10MID}	14	*AGO10*$^{AGO1\ (NT+PAZ)}$
3	*AGO1*^{AGO10PIWI}	15	*AGO10*$^{AGO4\ (NT+PAZ)}$
4	*AGO10*^{AGO1PAZ}	16	*AGO10*$^{AGO4\ (MID+PIWI)}$
5	*AGO10*^{AGO1MID}		
6	*AGO10*^{AGO1PIWI}		
7	AGO10^{AGO4PAZ}		
8	*AGO10*^{AGO4MID}		
9	*AGO10*^{AGO4PIWI}		
10	*AGO1*^{AGO10NT}		
11	*AGO10*^{AGO1NT}		
12	*AGO10*^{AGO4NT}		

Figure 3- 1 Experimental design of domain swapping. Total 16 constructs are generated and numbered.

The mutated and chimeric *AGO* genes were first introduced into pBA-6Myc-DC vectors and tested in *N. bentha* transient system (Figure 3-2). Surprisingly, most of the chimeric proteins were expressed as truncated forms; and the truncations were not correlated to certain domain(s). These truncations likely resulted from disrupted folding and consequently lower protein stabilities account for the AGO variants and chimeric forms.

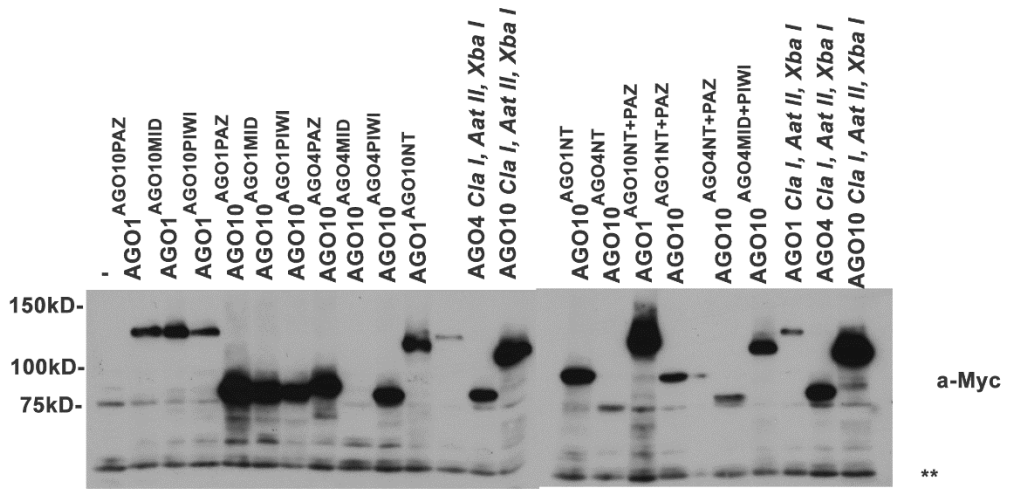

Figure 3- 2 Expression of mutated and chimeric *Arabidopsis thaliana* AGO proteins in *N. bentha*.

Proteins were extracted directly with 2X SDS buffer from leaves two days post agro-infiltration. Western blots were carried out with anti-Myc antibody.

The sRNA binding capabilities of chimeric proteins were also checked in the transient assay by co-expressing these 6-Myc tagged wild-type and mutated AGO proteins with miR166/165. sRNA bot analysis of sRNAs recovered from immunoprecipitates showed that only full length but not truncated chimeric proteins associated with miR166/165 (Figure 3-3). Also some truncated proteins cannot be effectively immuno-affinity purified suggesting that they might not be stable.

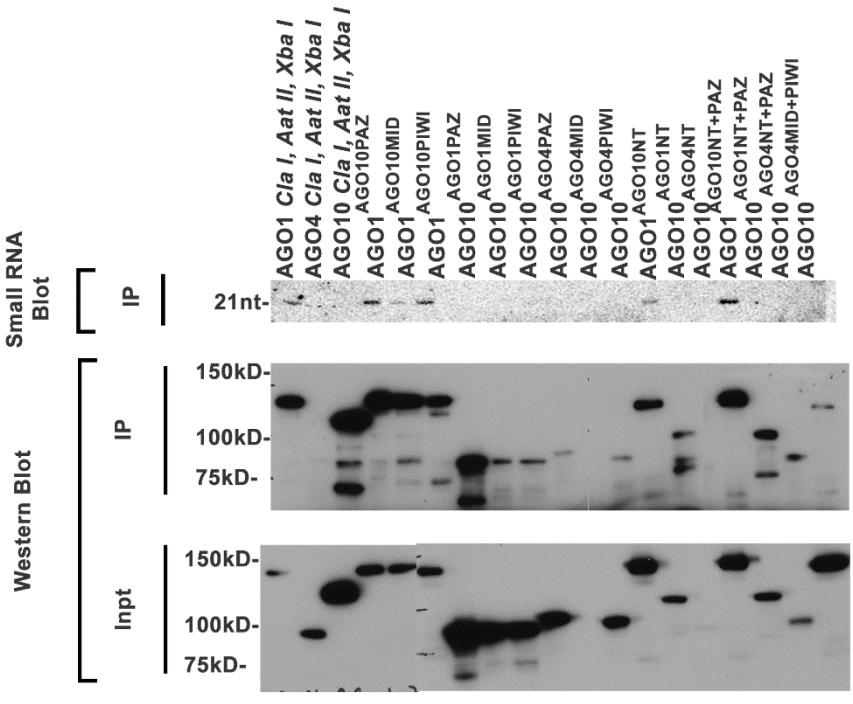

Figure 3- 3 Full-length chimeric proteins binds to miR166.

Chimeric AGO proteins and pri-miR166f were coexpressed in *N. bentha* leaves. Total protein extracts were immunoprecipitated with anti-Myc antibody (Sigma) and AGO-bound sRNAs were recovered and probed using ^{32}P-labelled complementary oligomers. Western blot were done using anti-Myc antibody.

Phenotypic characterization of transgenic plants

To identify protein domains of AGO1 and AGO10 critical for their specific functions, domain-swapped constructs expressed under the *AGO10* and *AGO1* promoters were introduced into *zll3-2* and *ago1-27* mutant backgrounds, respectively. SAM phenotypes of T2 transgenic seedlings were examined. While P_{AGO10} – *Flag-4Myc-*

AGO10 Cla I, Aat II, Xba I complemented the SAM defect of *zll3-2* mutants, (Figure 3-4A), P_{AGO10}*-Flag-4Myc-AGO1 Cla I, Aat II, Xba I* failed to do so (Figure 3-4B).

A

AGO10 ClaI, AatII, XbaI			
Line #	Pinhead	Normal	Pnh ratio
1	0	22	0

B

AGO1 ClaI, AatII, XbaI			
Line #	Pinhead	Normal	Pnh ratio
1	34	4	0.894737
2	23	7	0.766667
3	21	4	0.84

Figure 3- 4 *AGO10* but not *AGO1* recues *zll3-2* phenotype.

(A) *AGO10 ClaI, AatII, XbaI* expressed under *AGO10* native promoter successfully complemented SAM defects of *zll3-2*. SAM phenotypes were examined with 7-day old seedlings.

(B) *AGO1 ClaI, AatII, XbaI* expressed under *AGO10* promoter did not complement *zll3-2* phenotype. SAM phenotypes were examined with 7-day old seedlings.

Strikingly, the pinhead ratios in *zll3-2; P_{AGO10}-Flag-4Myc-AGO1^{AGO10NT}* transformants (T2) dramatically decreased (Figure 3-5A and B). In contrast, no complementation was observed for the reciprocally swapped construct *P_{AGO10}-Flag-4Myc-AGO10^{AGO1NT}* (data not shown). This result indicates that the N-terminal domain of AGO10 is a determining factor for its specific interaction with miR166/165.

A

AGO1^{AGO10NT}			
Line #	Pinhead	Normal	Pnh Ratio
1	7	38	0.155555556
2	12	25	0.324324324
3	15	24	0.384615385
5	0	61	0
6	24	53	0.311688312
7	28	45	0.383561644
8	8	18	0.307692308
9	18	53	0.253521127
10	8	45	0.150943396
11	15	28	0.348837209
12	12	88	0.12
13	6	102	0.055555556
14	63	22	0.741176471
15	9	57	0.136363636
16	5	8	0.384615385
17	23	46	0.333333333
18	8	36	0.181818182
19	16	64	0.2
21	50	26	0.657894737

B

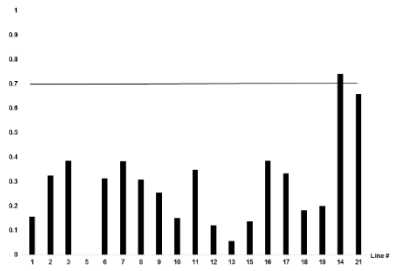

Figure 3- 5 *AGO1^{AGO10NT}* rescues *zll3-2* mutant phenotype.

(A) *AGO1^{AGO10NT}* expressed under *AGO10* native promoter successfully complements *zll3-2* SAM defects. SAM phenotypes were examined with 7-day old seedlings.

(B) A bar graph showing the complementation efficiency of individual lines.

Discussion

By expressing chimeric genes *AGO1*^{AGO10} or *AGO10*^{AGO1} under *AGO10* promoter in *zll3-2* background we discovered that the AGO1^{AGO10NT} chimera protein was able to rescue the SAM defects in *zll3-2* mutant. This finding uncovers an unappreciated function of the N-terminal domain of AGO10. To this point, I have only examined the phenotypic rescue effects of chimeric constructs in *zll3-2* mutant, and it will be important to also study the effects of these chimeras in the *ago1-27* mutant. One possibility for the lack of complementarities is that some constructs only expressed truncated forms of proteins and this might be caused by the direct swapping of cDNAs rather than genomic sequences of *AGO* genes as shown in the work of Mallory and his colleagues. In order to circumvent this problem, I designed primers to introduce unique restriction sites into *AGO1* and *AGO10* genomic sequences (Table 3-1).

Recently, an elegant study showed that only the PAZ domain, which is thought to bind to the 3' end of sRNA, is exchangeable between both proteins, whereas the MID-PIWI and N-terminal domains appear to contribute to their functional specificity (Mallory et al., 2009). In line with these findings, here I show that the N-terminal domain of AGO10 plays a decisive role in its functional specificity. Although the underlying mechanism remains elusive, I favor a hypothesis that the N-terminal domain might interact with some unknown factors and lead to the unique function mode of AGO10 and AGO1^{AGO10NT}. Future collaborative effort to this end will certainly yield interesting results.

Table 3- 1 Primers used to clone *AGO1*^{AGO10} and *AGO10*^{AGO1} chimeric genes.

Gene	Region	Primer	Restriction
AGO1	N terminal	CACCGCGGCCGCACAGGAATCATCATGGTGAG	NotI
		CCGCTCGAGTAGACGTCCCATGAGTTAAACATTCAAG	AatII/XhoI
AGO1	PAZ	TTGGACGTCTTGTGCTGCAATTTTGTCTG	AatII
		CCGCTCGAGTAGCTAGCATAAACAATTGAGTTTTCAA	NheI/XhoI
AGO1	MID	CTAGCTAGCTGCTAACATTATACAATATTTTC	NheI
		CCGCTCGAGTACCCGGGGGGTAGACAATGAAACATCCG	XmaI/XhoI
AGO1	PIWI	CCCCCCGGGGGGCTTCTGCTTAGGAACACAC	XmaI
		CCGCTCGAGTAGGCCGGCCTCAACTCAGCAGTAGAACAT	FseI/XhoI
AGO1	3' UTR	CAGGCCGGCCTTCACCCTCTATCTATCTTTATGAC	FseI
		CCGCTCGAGTATGTGGTCGACAATACAAACA	XhoI
AGO10	N terminal	CACCGCGGCCGCCAACAAAAAATGCCGATTAG	NotI
		CCGCTCGAGTAGACGTCTTGGGCTGACTTATAAAATA	AatII/XhoI
AGO10	PAZ	CCCCCCGGGGGGACAGGAATCATCATGGTGAG	AatII
		CCGCTCGAGTAGACGTCCCATGAGTTAAACATTCAAG	NheI/XhoI
AGO10	MID	CTAGCTAGCTTAGAAGTGAGGATTAATCTTG	NheI
		CCGCTCGAGTACCCGGGCAAAAGGGTTAAGTTTATG	XmaI/XhoI
AGO10	PIWI	CCCCCCGGGGGGCCTTCTTTAGTAATGG	XmaI
		CCGCTCGAGTAGGCCGGCCTGGATTTTTAGCAGTAGAAC	FseI/XhoI
AGO10	3 ŬTR	GGCCGGCCAACATTCCTTAATCAGTTTT	FseI
		CTCGAGGTGCGGTATACTGCAGGTTAATA	XhoI

CHAPTER IV

FUNCTIONAL AND BIOCHEMICAL INSIGHTS OF RISC-IMPLANTED CLEARING EXORIBONUCLEASES (RICES) IN *Arabidopsis thaliana*

Summary

miRNA and its complementary strand (*) are products from Dicer or Dicer-like enzymes. miRNA is incorporated into from RNA-induced Silencing Complex (RISC) to guide Argonaute (AGO) protein to repress expression of target genes, whereas miRNA* is clarified in RISC. However, how miRNA* is removed from RISC remains poorly understood. Here, I identified and experimentally confirmed a novel cofactor of Arabidopsis AGO10, named as RICE1 (RISC Implanted Clearing Exoribonuclease 1). In vitro biochemical assays demonstrated that RICE1 and its closest paralogs, RICE2, were 3'- 5' exoribonucleases specifically degrading single strand small RNAs. I found that miRNA accumulation was inversely correlated with the level of RICEs in vivo. We further solved the crystal structure of RICE1 at 2.9 Å and identified critical residues required for its catalytic activity. Overexpression of the catalytic-inactive RICEs recapitulated molecular phenotypes of *rice1 rice2* double mutants generated from artificial miRNAs. Moreover, active function of RICEs entails tis dimerization structures in vitro and in vivo. Together, I propose that RICEs act to clear miRNA* to activate RISCs before execution of their regulatory roles. Thus, this study provides new mechanistic insight into the underlying assembly and activation of RISC in Arabidopsis and beyond.

Introduction

RNA silencing is a fundamental gene regulatory mechanism in diverse biological processes in all eukaryotic organisms (Hannon, 2002; Meister and Tuschl, 2004; Mello and Conte, 2004; Tomari and Zamore, 2005). The key machinery that fulfills RNA silencing is called RISC and its core components include AGOs and sRNAs (Lindbo, 2012; Mallory and Vaucheret, 2010; Martinez de Alba et al., 2013). sRNAs can be classified into two major classes: miRNAs and siRNAs. In animal systems, miRNAs derive from primary miRNA transcripts (pri-miRNAs) that contain imperfectly-folded hairpin structures. The pri-miRNAs are canonically processed first by Drosha and its dsRNA-binding cofactors and subsequently by Dicer, or Dicer-like enzymes into duplexes of miRNA and its complementary strand (miRNA*). In *Arabidopsis thaliana*, the entire miRNA biogenesis process is orchestrated by DCL1/HYL1/SERRATE complexes in nuclei (Dong, 2008; Kurihara, 2004; Song, 2007; Voinnet, 2009). In contrast, siRNAs largely derive from processing of dsRNAs by Dicer, or DCLs into siRNA duplexes (guide and passenger strands, equivalent to miRNA/*).

Much remains to be understood about the loading process of miRNA/* into RISCs, the loading and processing of siRNA duplex into AGO proteins are relatively well documented. AGO proteins are capable of directly accommodating siRNA duplexes in vitro (Hauptmann et al., 2013; Noland and Doudna, 2013). In *Drosophila* Dicer-2 and R2D2 constitute the RISC loading complex to load siRNA duplexes into AGO2 in an ATP dependent manner (Liu et al., 2003; Pham et al., 2004; Tomari et al., 2004). Similar processes have been reported in human (Kawamata et al., 2009; Yoda et

al., 2010). In these organisms, once siRNA duplexes are sorted into AGO2 containing RISC complexes (Okamura et al., 2004) the star strand serves as the first target of RISC and is cleaved by the catalytic active AGO2. The nicked passenger strand of siRNA is degraded to liberate the guide-strand siRNA inside AGO proteins. In human, the degradation of nicked siRNA passenger strand is conducted through C3PO, an Mg^{2+}-dependent endoribonuclease (Liu et al., 2009b; Ye et al., 2011). In another organism, *Neurospora crassa*, *a* 3' to 5' exoribonuclease, QIP (QDE2-interacting protein) from *Neurospora crassa* is responsible for degrading the nicked passenger strand of siRNA. In a *qip* mutant nicked siRNA duplexes accumulate, and RNA silencing is compromised (Maiti et al., 2007). In *Arabidopsis thaliana*, recent elegant study demonstrates that siRNA/* duplexes enter pre-RISC in duplex form just like in other organisms and this process is facilitated by ATP hydrolysis through the Hsc70/Hsp90 chaperone complex. Energy generated by ATP hydrolysis induces conformational change of AGO proteins and promotes the loading of siRNA duplexes into conformational open RISCs (Iki et al., 2010; Iwasaki et al., 2010; Miyoshi et al., 2010). In plants another RISC activation factor cyclophilin 40 (CYP40) associates with the siRNA duplex bound AGO1 pre-RISC in a HSP90 dependent manner and facilitates RISC assembly (Iki et al., 2012; Iki et al., 2010). ATP hydrolysis leads to the dissociation of HSP90 and CYP40 from pre-RISC and pre-RISC will undergo further maturation steps. AGO1 catalytic activity is required for the siRNA star strand release and HSP90 regulates the process of siRNA star strand removal from AGO1 by hydrolyzing ATP (Iki et al., 2010).

Little is known about the miRNA loading process. AGOs cannot cleave miRNA* due to extensive mismatches in the miRNA/* duplexes. Moreover, catalytic-inactive AGO can recruit miRNA as efficiently as catalytic-active AGO protein, thus it has been proposed a slicer-independent unwinding mechanism. Under this model several features direct the loading and unwinding processes of miRNA/* dulplexes. The central mismatches facilitate the loading of miRNA duplexes into AGOs, whereas mismatches in the guide strand positions 12-15 promote miRNA/* duplex unwinding (Kawamata et al., 2009). The PAZ domain of AGO proteins have been shown to be important for the slicer-independent duplex unwinding and RISC activation (Gu et al., 2012).

We previously discovered that *Arabidopsis thaliana* AGO10 specifically sequesters a group of miRNAs, miR165/166 to antagonize their silencing activity. In an extended study, we wanted to study how AGO10 function is modulated by its cofactor. Here I reported a novel AGO10-bound partner, RICE1. RICE1 functions as a 3' to 5' exoribonuclease specifically degrading small RNA specific. Importantly, RICE1 not only interacts with AGO10, but also AGO1, suggesting its general role in RISC complexes. I found that overexpression of RICEs increased miRNA levels, whereas downregulation of *RICE1 RICE2* through artificial miRNA technology decreased miRNA accumulation. We further solved the crystal structures of RICE1 and pinpointed the critical residues required for its catalytic activity and dimerization. Importantly, introduction of these structure-interrupted RICE1 into plants compromised RNA silencing in vivo. Given that AGO1 and AGO10 predominantly function through miRNA pathway to regulate gene expression, I proposed that RICE1and its paralogs,

RICE2, function as a RISC activator through degrading miRNA*. Thus, this study provides new insight into the poorly understood the loading of miRNA/* and the maturation of RISCs that are predominantly occupied by miRNAs.

Materials and methods

AGO10 complex isolation

Arabidopsis thaliana suspension MM1 cell lines *expressing Flag-4Myc-AGO10* under the control of Cauliflower Mosaic Virus 35S promoter was generated following the standard transformation procedure (Forreiter, 1997**) (**Menges, 2002)**.** Transgenic MM1 cells were collected and ground in liquid nitrogen and AGO10 protein complexes were extracted using four volumes of extraction buffer (20 mM Tris- HCl, pH 7.5, 150 mM NaCl, 2 mM $MgCl_2$, 1 mM DTT, 1 mM EDTA, 10 μM MG132, and EDTA-free protease inhibitor cocktail (Roche)). After removal of insoluble materials by centrifugation twice at 16,000 g for 10 minutes at 4 ℃, extracts were incubated with anti-Flag magnetic beads (Sigma) for two hours at 4 ℃. The beads were washed five times with the extraction buffer (5 min/each time) before elution with 1.2 ml of elution buffer (extraction buffer containing 100 μg/ml 3XFlag peptide). The elutes were then incubated with anti-Myc M2-agarose beads (Sigma) for 2 hours. The beads were washed three times with the extraction buffer, and the dual-tagged AGO complexes were eluted by incubation with 400 μl of basic buffer (0.5 mM EDTA and 30 mM NH_4OH) for 20 minutes at room temperature. The eluted immunoprecipitates were frozen in liquid N_2

and vacuum dried before being resolved in 4-20% gradient SDS-PAGE and proteomic sequencing analysis.

DNA construction

Most of constructs were generated through a gateway system. Full-length cDNAs of *RICE1* and *RICE2* were cloned into pENTR vectors using pairs of primers (RICE1 For: 5’ - CACCATGGCCTCATTCGATGGGC -3’; RICE1 Rev: 5'-GAGCTCTCACTGCTGCAATTGATCG -3'; RICE2 For: 5’ - CACCATGGCCTCCTTTGATGGGCC – 3’, and RICE2 Rev: 5’ – TCACTCATCGGACAATTGATCCC -3’). The genes were further transferred into gateway compatible binary vectors including pBA-35S-DC-3HA and pBA-35S-3HA-DC.

pET28-SUMO-RICE1 was cloned as follows: full-length cDNA of *RICE1* was cloned by a polymerase chain reaction (PCR) using primers (RICE1 Forward: 5'-GGTGGATCCATGGCCTCATTCGATGGGC -3', and RICE1 Reverse: 5'-GAGCTCTCACTGCTGCAATTGATCG -3'). The resultant PCR products were double digested with *BamHI* and *SacI* and ligated into *BamHI* /*SacI*-treated pET28a-SUMO (Lu et al., 2010) to produce pET28-SUMO-RICE1. The construct was then confirmed by sequencing.

Site-directed mutagenesis

For catalytic active sites analysis, numerous point mutations were introduced into RICE1 by using PCR with pET28a-SUMO-RICE1 as a template with primers listed in Table 4-1. In parallel, several mutations were created for potential dimerization assays using primers summarized in Table 4-2.

Table 4- 1 Primers used to generate RICE1 catalytic mutants.

Mutation	Primer sequences
D52A	Forward: 5'- CCATTGTCTTTGCTGTGTATTG -3'
	Reverse: 5'- CAATACACAGCAAAGACAATGG -3'
Y54S	Forward: 5'- GTCTTTGATGTGTCTTGGGATG -3'
	Reverse: 5'- CATCCCAAGACACATCAAAGAC -3'
D114A	Forward: 5'- GATTCAAGAAGCCCTCGCTTTGC -3'
	Reverse: 5'- GCAAAGCGAGGGCTTCTTGAATC -3'
E187A	Forward: 5'- CTGCCATTGCAGGTTGGC -3'
	Reverse: 5'- GCCAACCTGCAATGGCAG -3'

Table 4- 2 Primers used to generate RICE1 dimerization mutants.

Mutation	Primer sequences
R47E	Forward: 5'- GGAATGGAAACGAGTCCATTG -3'
	Reverse: 5'- CAATGGACTCGTTTCCATTCC -3'
R127E	Forward: 5'- GTATTGTGATCGAAAGCTCGTTG -3'
	Reverse: 5'- CAACGAGCTTTCGATCACAATAC -3'
K102E	Forward: 5'- CTTTGCTTCCGAATTTGTCAC -3'
	Reverse: 5'- GTGACAAATTCGGAAGCAAAG -3'
K119E	Forward: 5'- GCTTTGCTTGAAGAAAACCACG -3'
	Reverse: 5'- CGTGGTTTTCTTCAAGCAAAGC -3'

Protein expression and purification

For the overexpression of recombinant native RICE1 and various mutants in E. coli system, competent BL21 (DE3) cells were transformed with plasmid DNA carrying the gene of interest. Cells were grown at 37 ℃ in LB medium in the presence of antibiotics (100 μg/ml kanamycin) to an OD_{600} of 0.6-0.8. Protein expression was induced by the addition of Isopropyl-β-D-1-thiogalactopyranoside (IPTG) to a final concentration of 0.5 mM. After further growth overnight at 16 ℃, cells were harvested by centrifugation at 4 ℃, 6000 rpm for 10 min.

For purification, cell pellets were re-suspended in lysis buffer (150 mM NaCl, and 20 mM Tris-HCl pH 7.5) and disrupted by sonication at 60% amplitude for 5 to 10 min, using a Sonic Dismembrator (Model 500, Fisher Scientific). Cell lysate was then centrifuged down at 4 ℃, 8000 rpm for 15 minutes. Supernatant was further centrifuged at 4 ℃, 16000 rpm for 30 minutes to completely remove the cell

debris. The 6×His-SUMO-tagged fusion proteins were first purified by Ni-NTA resin. After the loading of soluble extracts, the resin was washed with 1st washing buffer (500 mM NaCl, 20 mM Tris-HCl pH 7.5, and 25 mM imidazole) and 2nd washing (500 mM NaCl, 20 mM Tris-HCl pH 7.5, and 00 mM imidazole) buffer to remove nonspecific proteins, prior to elution with elution buffer (150 mM NaCl, 20 mM Tris-HCl pH 7.5, and 250 mM imidazole).

For enzymatic assay purposes, proteins were further purified by gel filtration chromatography on a Superdex75 (1.6 × 60) column (GE Healthcare) eluted with the running buffer (150 mM NaCl, and 20 mM Tris-HCl pH 7.5). The purity of the proteins was analyzed by sodium dodecyl sulfate (SDS) polyacrylamide gel electrophoresis (PAGE) on a 15% gel, which was stained with Coomassie Brilliant blue R-250.

RICE1 enzymatic assay

Each 20 µl reaction contains 0.5 µM of enzyme and 5nM of substrate to make sure that there is at least 50 times molar excess of enzyme over substrate and reactions were incubated at 37℃ in reaction buffer containing 20 mM HEPES, pH 7.0, 50 mM KCl, 5 mM $MgCl_2$, 1/10 V/V RNase inhibitor superaseIn (Ambion) and 1 mM DTT.

The RNA substrates (Table 4-3) used here was commercially synthesized by IDT and 5' and labeled with γ-AT^{32}P by T4 PNK following CIP treatment. RNAs were 3' labeled with α-^{32}pC^{32}p by T4 RNA ligase followed by CIP treatment. After the reaction, RNA was extracted with a standard phenol-chloroform extraction method. The resulting RNA fragments were separated by 20% denaturing polyacrylamide gels.

Table 4- 3 Sequences of RNA used in this study.

9 nt ssRNA	5’ pppGGACUGUUG 3’
12nt ssRNA	5’ pppUCUGGCUCGAGG 3’
19nt ssRNA	5’ GUACGCGGGUUUAAACGAU 3’
21nt ssRNA	miR166: 5’ pppUCGGACCAGGCUUCAUUCCCC 3’
	miR166*: 5’ pppGGACUGUUGUCUGGCUCGAGG 3’
24nt ssRNA	5’ CGUACGCGGAAUAGU UUAAACUGU 3’

Transgenic plant generation

Ler/Col-0 and *pnh-2* mutants were transformed with a series of constructs expressing wild-type *RICE1 and variants* cDNA, *as well as* artificial miRNA constructs driven by *35S, AGO10* or *AGO1* promoters by the floral dip transformation method (Clough and Bent, 1998).

Seeds from infiltrated plants were selected on standard MS medium containing the appropriate selective agents: 10 mg/l glufosinate ammonium (Sigma) together with 100 mg/l cefotaxime (Sigma).

Plants were grown in LP5 Metromix (SunGro, Canada) in a walk-in growth chamber at 22 ℃ with relative humidity of 50% under long-day conditions (16 hr light/8 hr dark) unless otherwise noted. Light illumination (110 mmol photons/m^2s) was provided by a Spec-tralux T5 high-output lamp (Hydro warehouse).

Coimmunoprecipitation experiments

For transient experiments, 4-week-old *N. bentha* leaves were infiltrated with *A. tumefaciens* ABI harboring variety of binary plasmids. The ODs of *A. tumefaciens* cultures were diluted to 0.4. *N. bentha* leaves were collected two days after agroinfiltration. For *Arabidopsis thaliana* plants, 7-day-old seedlings were collected from MS plates.

Total protein was extracted in the IP buffer containing 50 mM Tris-HCl, pH 7.5, 300 mM NaCl, 4 mM MgCl 2 , 5 mM DTT, 0.1% Triton-100, and the complete protease inhibitor cocktail (Roche). Cleared protein extracts were immunoprecipitated with agarose-conjugated mono clonal antibodies against Flag or Myc (Sigma).

RNA blot and western blot analyses

Total RNA was extracted using Trizol reagent from Agrobacterium -transfected *N. bentha* leaves or *Arabidopsis thaliana* tissues, including 7-(or 10)-day-old seedlings and inflorescences, depending on the desired assays. RNA blot hybridizations of low-molecular-weight RNAs (sRNA blot) were performed as described (Zhang et al., 2006). Each lane contained sRNAs, which were recovered from isolated AGO complexes prepared from 0.4 g tissues. For input, 5 μg of total RNA was used in most cases, except in transient experiments where only 1~2 μg RNA was used. Blots were hybridized with ^{32}P-radiolabeled oligonucleotide probes complementary to the sRNAs of interest. In some experiments, the same blots were stripped and re-probed with ^{32}P-labeled oligos complementary to the indicated miRNAs. U6 served as loading controls. RNA blots

were detected after exposure to a phosphor plate and quantified using the Quantity One Version 4.6.9 according to the manufacturer's instructions (Bio-Rad).

Western blot analyses were performed as previously described (Zhang et al., 2006). Western blots were developed with ECL^{+}, detected with ChemiDoc XRS+ and quantified using the ImageLab Software (Bio-Rad).

Small RNA enrichment

sRNA enrichment was performed with 5% PEG 8000 and 500 mM NaCl according to previous literature (Catalanotto et al., 2000; Maiti et al., 2007).

Results

Isolation of AGO10 protein complex from Arabidopsis thaliana

To identify AGO10 cofactors, I generated stable *Arabidopsis thaliana* transgenic cell lines expressing *35S-Flag-4Myc-AGO10.* I used the suspension cell culture because it mimics plant stem cells where AGO10 is specifically expressed. After obtaining and confirming the positive transgenic cell lines (Figure 4-1A and B), I purified AGO10 complex though two-step immunoprecipitation processes with anti-Flag first and then anti-Myc conjugated agarose beads. The isolated AGO10 protein complexes were resolved on SDS-PAGE gradient gels (4-20%). Distinct bands that were absent from the control IP with non-transgenic suspension cells were cut out for mass spectrometric analysis (Figure 4-1C).

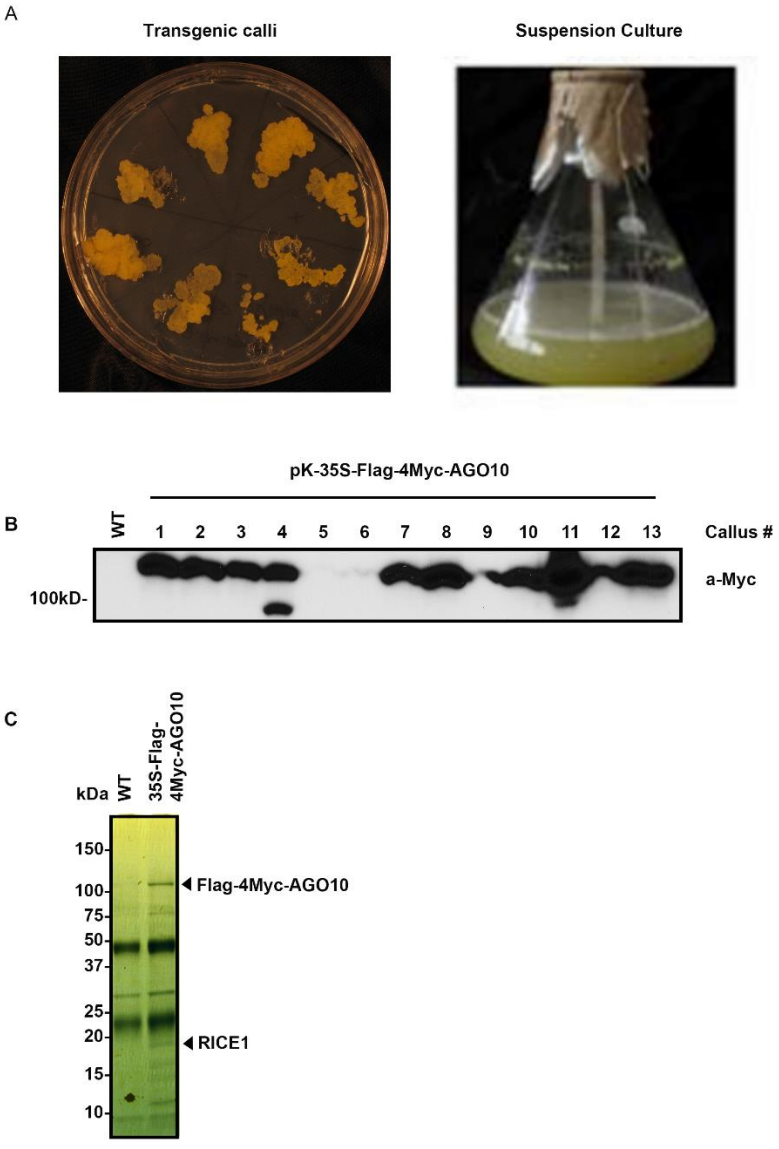

Figure 4- 1 Isolation of AGO10-containing protein complex.

(A) Transgenic cell lines selected on Kan^{+} MS plates and cell suspension culture.

(B) Screening of transgenic cell lines by western blot with anti-Myc antibody.

(C) Gel-code blue staining of SDS-PAGE after two-step immunoprecipitation.

Through the mass spectrometric sequencing, we identified numerous cofactors including HSP90 and cyclophilin 40 which are already known to be required for RISC assembly (Iki et al., 2012; Iki et al., 2010) among others. The protein that I focus on is annotated as a 23-kDa polynucleotidyl transferase from the TAIR website, and we renamed it as RICE1 (RISC-Implanted Clearing Exoribonuclease1) (Figure 4-2A). RICE1 contains a conserved domain characteristic of the DnaQ_like_exonuclease superfamily (Figure 4-2B). This superfamily proteins are a structurally conserved group of 3'-5' exonucleases, which act on the 3' termini of DNA or RNA to degrade the substrates.

RICE1 has a close paralog that has 67% sequence identity in *Arabidopsis thaliana* and we named it RICE2. (Figure 4-2C). Both RICE1 and RICE2 are hypothetical 3'-5'exonucleases and their functions have not been characterized.

Experimental confirmation of AGO10 and RICE1 interaction

To examine whether RICE1 is a *bona fide* partner of AGO10, we performed three independent assays. First, we carried out a split luciferase complementation assay (LCI) (Gehl et al., 2011) (Figure 4-3A). For LCI experiments, *NLuc* and *CLuc*, which are N- and C-terminal parts of an integral luciferase, were fused to different tested genes and transfected to a leaf. When the split NLuc and CLuc are brought together through direct interaction of the tested proteins, active catalytic activity is restored. In our LCI assays, we observed that AGO10 indeed showed LUC complementation with *Cucumber mosaic virus*-encoded 2b protein (CMV2b) (Zhang et al., 2006) and RICE1 (Figure 4-3A), but not with other combinations, indicating the direct interaction of AGO10 with

A

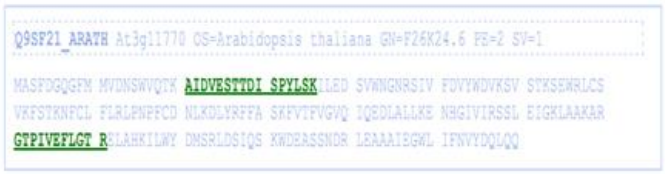

Position	MH+	Sequence (click to highlight)
141-151	1190.3849	GTPIVEFLGTR
21-36	1739.9171	AIDVESTTDISPYLSK

B

C

```
1    MASFDGQGFMMVDNSWVQIKAIDVESTTDISPYLSKILEDSVWNGNRSIVFDVYWDVKSV   60  RICE1
1    MASFDGPKFKMTDGSYVQTKTIDVGSSTDISPYLSLIREDSILNGNRAVIFDVYWDVGFP   60  RICE2
     ******  * *.* *:****:*** *:******** * ***: ****:::*******

61   -----STKSEWRLCSVKFSIKNFCLFLRLPNPFCDNLKDLYRFFASKFVIFVGVQIQEDL  115  RICE1
61   ETETKTKTSGWSLSSVKLSIRNLCLFLRLPKPFHDNLKDLYRFFASKFVIFVGVQIEEDL  120  RICE2
          :..* * *.***:**:*:*******:** **********************:***

116  ALLKENHGIVIRSSLEIGKLAAKARGTPIVEFLGTRELAHKILWYDMSRLDSIQSKWDEA  175  RICE1
121  DLLRENHGLVIRNAINVGKLAAEARGTLVLEFLGTRELAHRVLWSDLGQLDSIEAKWEKA  180  RICE2
      **:****:***.::::*****:**** ::**********::** *:.:****::**::*

176  SSNDRLEAAAIEGWLIFNVYDQLQQ-  200  RICE1
181  GPEEQLEAAAIEGWLIVNVWDQLSDE  206  RICE2
     . :::***********.**:***.::
```

Figure 4- 2 Bioinformatic analysis of RICE1.

(A) Peptide details from mass spectrometric sequencing. Underlined peptides are recovered from the sequencing data and they cover 13% of the full length RICE1.

(B) RICE1 contains a conserved domain of DnaQ superfamily.

(C) Sequence alignment between RICE1 and RICE2.

the indicated proteins. Next, using confocal microscopy, we observed that AGO10 co-localized with the aforementioned proteins in the nucleus and the cytoplasm, suggesting that they may function in both subcellular compartments

Finally, we performed a co-immunoprecipitation (co-IP) experiment. To this end, I transiently expressed RICE1-HA3 with either Flag-AGO10 or a control protein, Serrate (Lobbes et al., 2006) by agro-infiltration. I conducted an IP with anti-flag antibody and detect co-immunoprecipitates with anti-HA antibody (Figure 4-3C). RICE1 was indeed pull-down by AGO10, but not by the control Serrate protein. Collectively, these experiments demonstrated that RICE1 is a novel AGO10-interacting protein in plants. Interestingly, RICE1 also interacts with AGO1, suggesting its conserved role in RISC complexes (data not shown). Moreover, further in vitro pull-down assays by my collaborator Dr. Zhonghui Zhang, showed that RICE1 interacts with the MID domain of AGOs in which 3'end of miRNA* is located (data not shown).

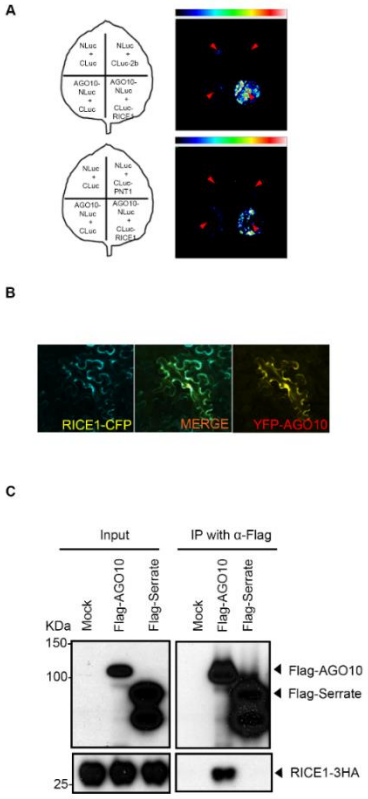

Figure 4- 3 Experimental confirmation of AGO10-RICE1 interaction.

(A) Split luciferase assay. AGO10-CMV2b (citation) interaction serves as a positive control.

(B) Confocal microscopy to show AGO10 and RICE1 localization.

(C) Co-IP of AGO10 and RICE1. Serrate protein is the negative control for AGO10 in this experiment.

RICE1 acts as a 3' to 5' single strand RNA specific exonuclease

Several members from the DnaQ exoribonuclease (DEDD) family are involved in the metabolism of RNA or DNA. For example, SDN proteins in *Arabidopsis thaliana* have been well characterized as a class of sRNA specific 3'-5' exonucleases (Ramachandran and Chen, 2008). Human WRN exonuclease is another member of this family. Mutations in mammalian WRN lead to premature aging and the cancer-related disorder Werner syndrome. WRN has been shown to function on a variety of structured DNA substrates, including bubbles, stem-loops, forks and Holliday junctions, as well as on RNA-DNA duplexes (Perry et al., 2006).

To characterize the biochemical function of RICE1, we prepared RICE1 proteins from *E. coli* through Ni-NTA affinity purification followed by gel filtration (Figure 4-4A). The majority of the purified enzyme eluted from a peak corresponding to a molecular weight of 50kD during gel filtration. Because the theoretical molecular weight of RICE1 dimer is approximately (~46kD), this result suggested that RICE1 most likely forms a dimer in solution.

Next, we examined whether the purified RICE1 has RNase activity. In vitro enzymatic assays were carried out similarly to that described for its human homolog WRN (Perry et al., 2006). Our result shows that RICE1, in contrast to a control protein, Sting (Yi et al., 2013) that underwent the same purification process, degraded 5' labeled ss sRNAs into shorter ladders, indicating that PNT1 acted as a potent RNase (Figure 4-4B).

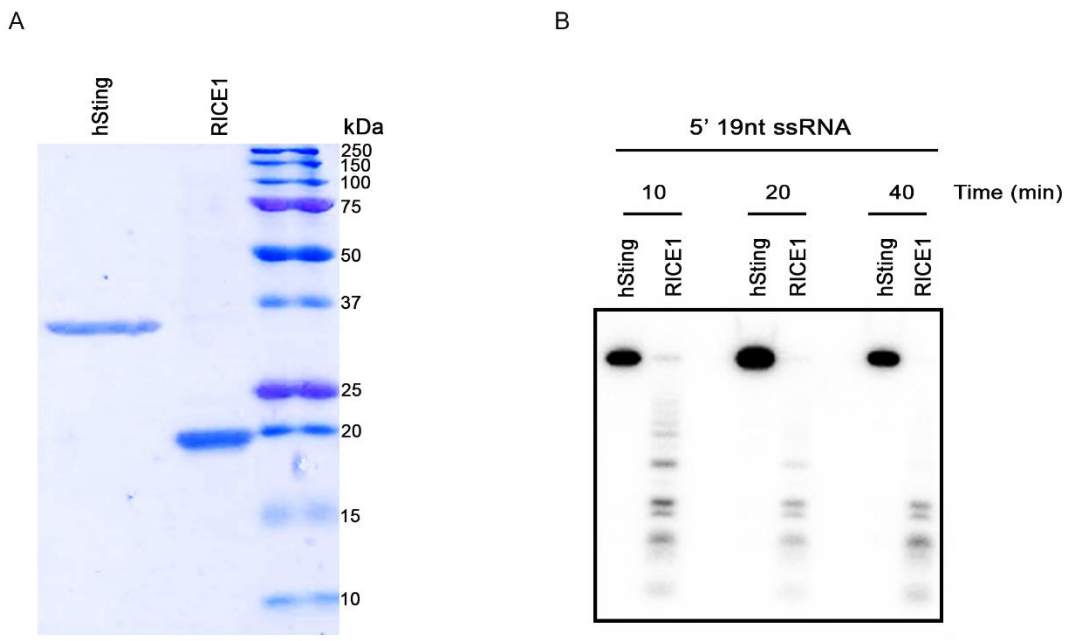

Figure 4- 4 RICE1 possesses RNase activity.

(A) Coomassie stained SDS gel of purified hSting (negative control) and RICE1 proteins used in the assay.

(B) Degradation of 5' 19nt ssRNA by RICE1 at different time points.

To distinguish whether RICE1 is a 5' to 3' or 3' to 5' ribonuclease, we repeated the RNA degradation experiments with substrates labeled on different ends. When a 5' labeled substrate was used for the assay, various truncated fragments were observed; whereas only a single cleavage product corresponding to one nucleotide when a 3' labeled ssRNA substrate was applied. These results confirmed that RICE1 is a 3'-5' ribonuclease and cleaves nucleotides off the RNA substrates progressively from the 3'

terminus (Figure 4-5A). To further differentiate whether RICE1 is an exo- or endo-ribonuclease, a 5' labeled 21nt single strand RNA was circularized by T4 RNA ligase. While the circularized ssRNA was effectively degraded by RNaseA, it was resistant to RICE1 degradation, suggesting that RICE1 is indeed an exoribonuclease (Figure 4-5B). To investigate whether RICE1 has any substrate preference, we tested different forms of RNA or DNA substrates. Cleavage assays demonstrated that RICE1 had a clear preference towards the ssRNA substrate over the ssDNA substrate (Figure 4-5C). Next we tested RICE1 on dsRNA substrates. To make the dsRNA substrate, miR166 was 5' labeled and annealed to the cold miR166*. Figure 4-5D showed that RICE1 readily degraded the 5' labeled miR166 but not the miR166/* duplex. Upon the loading of siRNA duplexes, the star strand is nicked by catalytic active AGO proteins and subsequently is cleared via nucleases such as C3PO and QIP in organisms like human and *Neurospora* (Leuschner et al., 2006; Liu et al., 2009b; Maiti et al., 2007; Preall and Sontheimer, 2005). Whether there is such a process in *Arabidopsis thaliana* is not yet known. To determine whether RICE1 can remove the nicked passenger strand from sRNA duplexes, a 5' ^{32}P labeled 12nt RNA fragment and cold 9nt RNA fragment that are fully complementary to miR166 were annealed to cold miR166a (Figure 4-6A and B) to generate a nicked sRNA duplex. Similarly, an analogous nicked duplex was prepared by annealing 5' ^{32}Plabeled 9nt RNA fragment with cold 12nt fragment and miR166a (Figure 4-6A and B). While RICE1 cleaved the 5' labeled 9nt and 12nt ssRNAs effectively, the 9nt and 12nt RNA fragments in the duplex forms are resistant to RICE1

degradation (Figure 4-6C). Thus, RICE1, unlike previously characterized C3PO and QIP, did not degrade unreleased nicked ssRNAs.

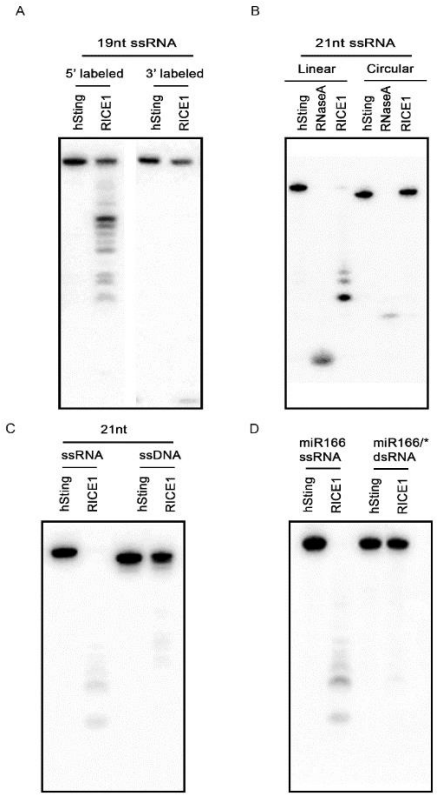

Figure 4- 5 RICE1 is a single strand RNA 3’ to 5’ exonuclease.

(A) RICE1 degrades RNA from 3’ to 5’ direction.

(B) RICE1 is an exonuclease.

(C) RICE1 degrades RNA but not DNA substrate.

(D) RICE1 degrades ssRNA but not dsRNA substrate.

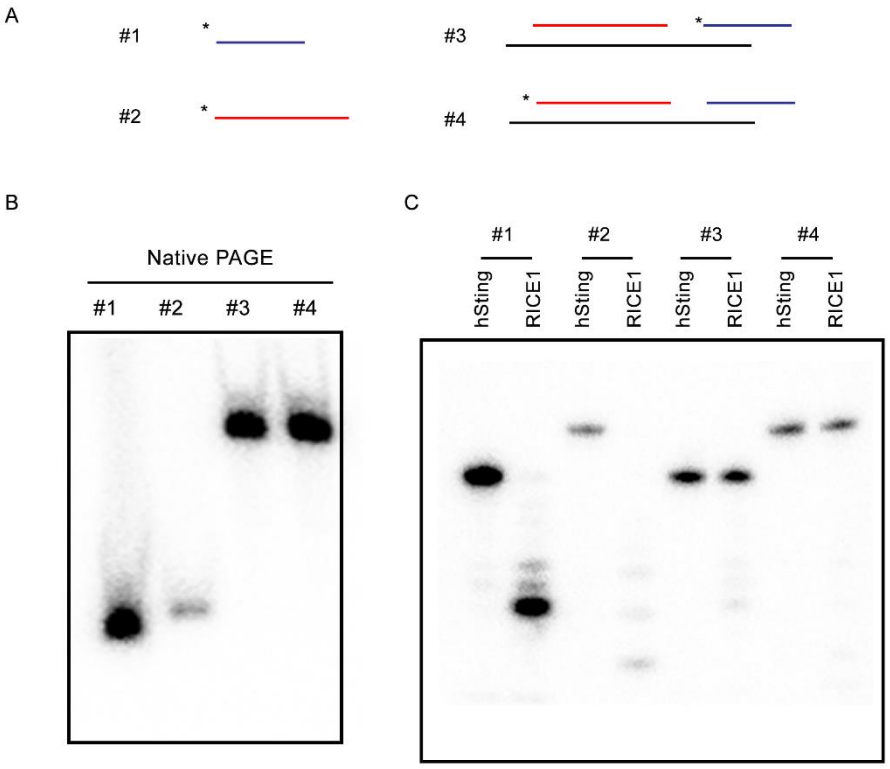

Figure 4- 6 RICE1 does not degrade nicked passenger strands.

(A) Schematics of RNA substrates. 5' labeled 32P is indicated by asterisks.

(B) Native PAGE to confirm the formation of nicked duplexes.

(C) RICE1 degrades ssRNAs but not nicked duplexes.

Finally we tested the length requirement of RNA substrates for RICE1. ssRNAs, with lengths ranging from 9to 150nt, were 5' ^{32}P labeled and subjected to RICE1 treatment. We observed that ssRNAs with lengths less than 40nt were all degraded by RICE1 while the RNAs that were 50nt long or beyond were less vulnerable to the exonucleolytic activity of RICE1 (Figure 4-7).

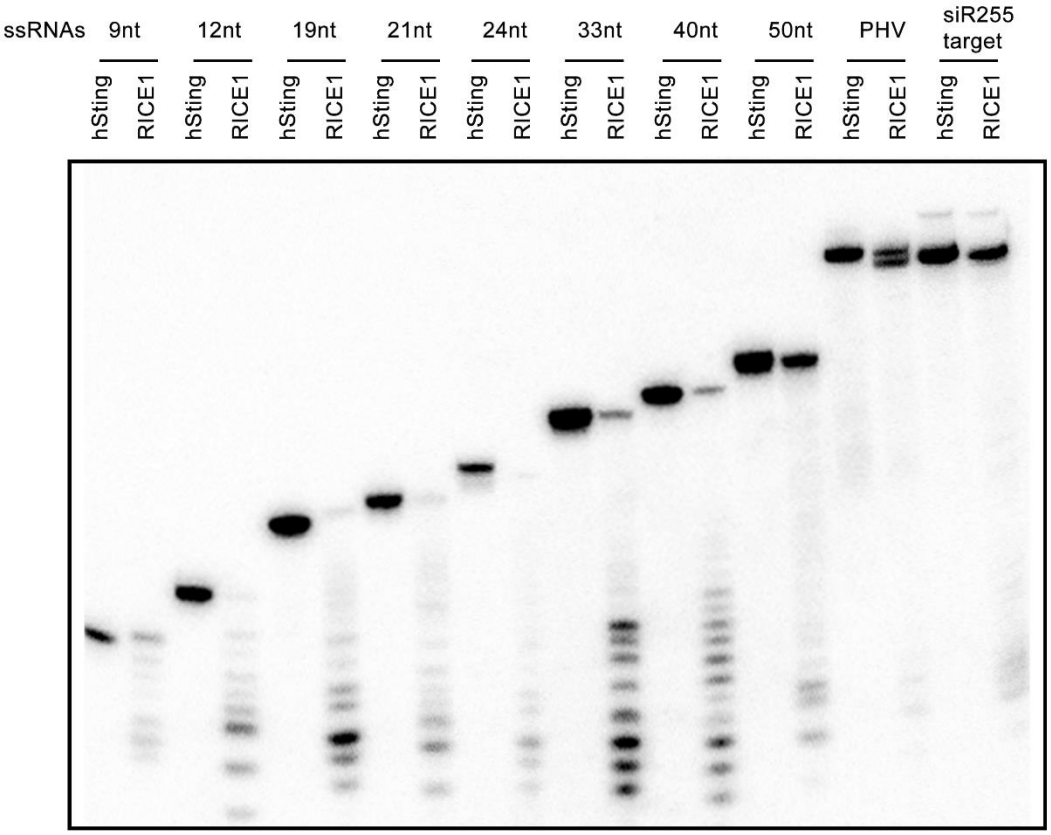

Figure 4- 7 RICE1 effectively degrades ssRNAs less than 50nt in length.

Taken together, in vitro enzymatic tests showed that RICE1 is a 3'-5' exoribonuclease specifically targeting ss sRNAs and this activity appears to be sequence-independent. Because endogenous miRNA/* duplexes are methylated at their 3' ends by HEN1 proteins for stabilization (Ji and Chen, 2012; Yang et al., 2006), we next asked whether RICE1 was able to cleave the methylated sRNA or not. To this end, we performed the RICE1 enzymatic assay with total RNAs isolated from *Arabidopsis thaliana*. After the 2 hours incubation, RNAs were extracted following the same procedure as described above, separated with 15% urea-page gel, and then sRNA blot was performed with probes specifically targeting miR166/165 and U6, respectively (Figure 4-8). We found that that RICE1 degraded miR166/165 completely but not the U6 RNA, indicating that the 2'-O-methyl group at the 3' termini of miRNA do not block RICE1 nuclease activity.

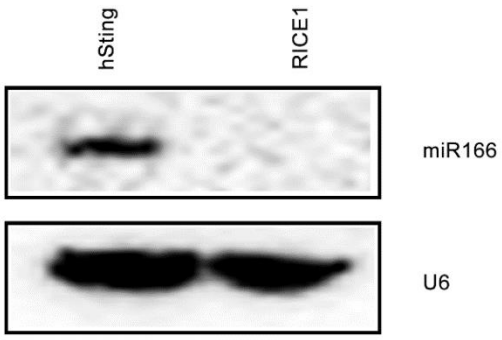

Figure 4- 8 RICE1 degrades miRNA166 from total RNA extract.

RICEs positively regulate miRNA accumulation

Given that RICE1 is housed in RISCs and a ss sRNA specific 3' to 5' exonuclease, what are the substrates of RICE1 in plants? There are two possible mutually non-excusive scenarios (Figure 4-9): RICE1 might degrade AGO-bound miRNAs. If so, the resultant sRNA-free RISCs are not stable and might undergo decay pathway. Alternatively, RICE1 might clear miRNA* strand in the loading process of miRNA/* to AGO proteins, facilitating the incorporation of miRNA strand into AGO protein and correspondingly activate and stabilize RISCs.

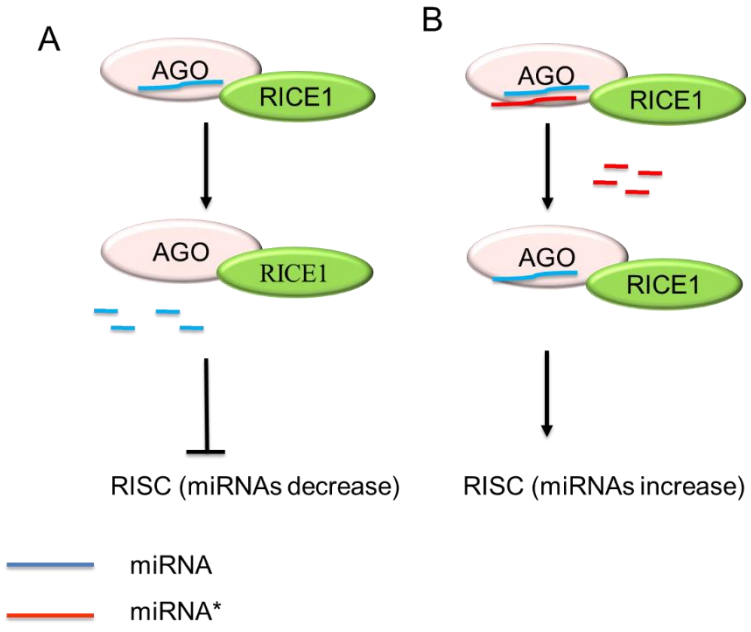

Figure 4- 9 Hypotheses for RICE1 in vivo function.

(A) RICE1 degrades miRNA strands and represses RISC activity;

(B) RICE1 activates RISC by degrading miRNA* during miRNA loading process.

To distinguish the two possibilities, we examined the miRNA accumulation in transgenic plants with altered levels of *RICE1* and *RICE2 in vivo*. First, we created transgenic plants constitutively expressing *RICE1-3HA* or *35S-RICE2-3HA. RNA blot analysis showed that* overexpression of either RICE1 or RICE2 increased the levels of all tested miRNAs compared to the control plants transformed with empty vectors or sibling plants in which no ectopic expression of RICE1-3HA or RICE2-3HA detected (Figure 4-10). Moreover, the increment in the miRNA abundance positively correlated with the expression of *RICE1* or *RICE2* transgenes (Figure 4-10). Next we generated transgenic plants expressing artificial miRNA constructs specifically targeting RICE1 (*amiR-RICE1*) or both RICE1 and RICE2 (*amiR-RICEs*). Analyses of RNA and protein blots indicated that levels of endogenous *RICE1* and *RICE2* decreased approximately ~80-90% compared to wild-type plants (In collaboration with Zhonghui Zhang; data now shown). Notably, miR165/166 accumulation in these artificial transgenic plans consistently decreased relative to the control plants (Figure 4-11). Taken together, all these in vivo data indicates that RICEs are positive regulators for miRNA accumulation, likely through clearing miRNA* and promoting miRNA incorporation into RISC.

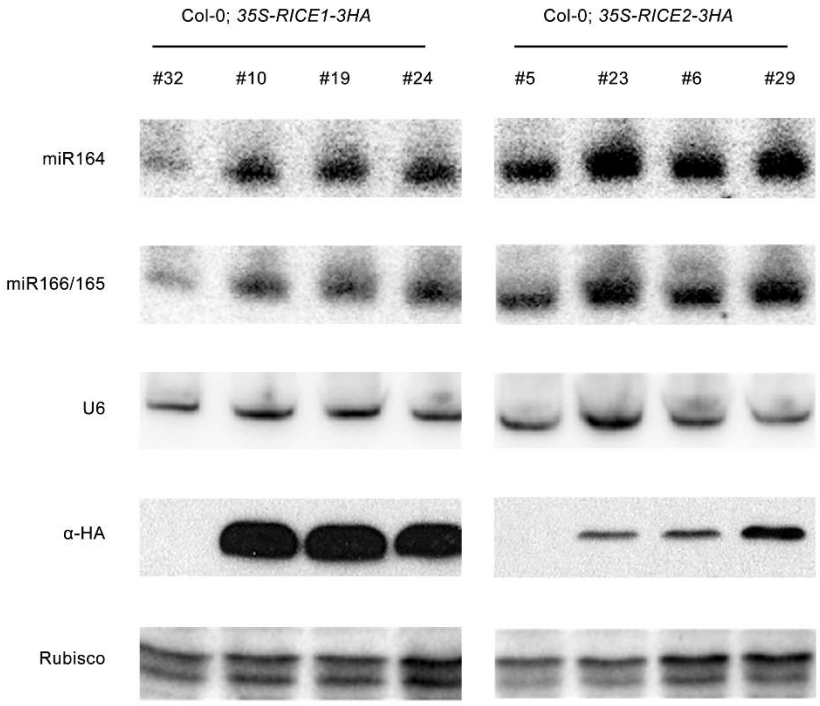

Figure 4- 10 sRNAs accumulation increase in Col-0; 35S-RICE1-3HA and Col-0; 35S-RICE2-3HA transgenic lines.

sRNA blots were performed with ^{32}P labeled probes targeting miR164 and miR166/165. Same membrane was used for probing different miRNAs after stripping. U6 snoRNA serves as a loading control. Western blot was performed with α-HA antibody. Coomassie blut staining of rubisco serves as a loading control.

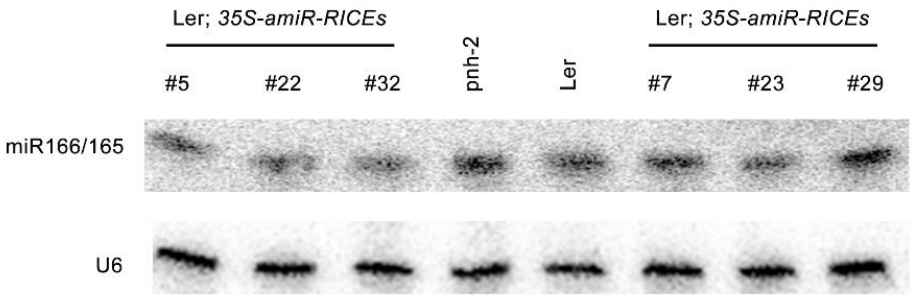

Figure 4- 11 miR166/165 accumulation increased in Ler; *35S-amiR-RICEs* and Ler; *35S-amiR-RICE1* transgenic lines.

RNA blot analysis was done with ^{32}P-labelled probes specifically targeting miR165/166. U6 snoRNA serves as a loading control.

Structure determination of RICE1

To further understand the catalytic mechanism of RICE1, we carried out structural studies of RICE1 protein. Crystallization and structure analysis were performed by Min-Woo Sung from Dr. Pingwei Li lab (Table 4-4).

Table 4- 4 Data collection and refinement statistics of RICE1.

Data collection	
Wavelength (Å)	1.54
Resolution range (Å)	50.00-2.70 (2.80-2.70)
Space group	$I4_122$
Unit cell parameters (Å)	a=b=193.26, c=214.40
Total No. of reflections	299700
No. of unique reflections	55410
Multiplicity	5.4 (4.7)
Completeness (%)	99.5 (99.4)
Mean I/δ (I)	10.2 (2.1)
R_{merge}[†] (%)	6.2 (60.6)
Refinement	
R_{work}/R_{free}[‡] (%)	20.3/23.0
Bond lengths (Å)	0.027
Bond angles (°)	2.279

The monomeric structure of RICE1 is consisted of 7 β sheets and 9 α helices (Figure 4-12A and B). RICE1 structure shared high similarities with those of its closest paralog in *Arabidopsis*, RICE2 and its human homolog WRN (Perry et al., 2006), with r.m.s. deviation values of 1.8Å and 2.7Å, respectively. The hexametric ring of RICE1 forms through hydrogen bonds and electrostatic interactions at dimer interfaces (Figure 4-12C and D).

Active site and dimer-interface analysis of RICE1

The DnaQ-like exonuclease superfamily members have four conserved acidic residues in their catalytic sites, this exonuclease family is also called the DEDD superfamily. The structural analysis predicted that RICE1contains three acidic residues at the catalytic site. To test this hypothesis, we performed site-directed mutagenesis of these residues (RICE1 D52A, RICE1 Y54S, RICE1 D114A and RICE1 E187A). For RICE1 D52A and RICE1 Y54S, the gel filtration profile was identical to that of wild type protein - the main peak corresponding to the dimer size of RICE1 (data not shown). We prepared the mutated protein with high quality and repeated the exoribonuclease assays (Figure 4-13). The D52A and Y54S point mutations almost completely abolished the exonuclease activity of RICE1 (Figure 4-13), indicating that Asp 52 and Tyr 54 are the critical residues that is indispensable for RICE1 exonuclease activity.

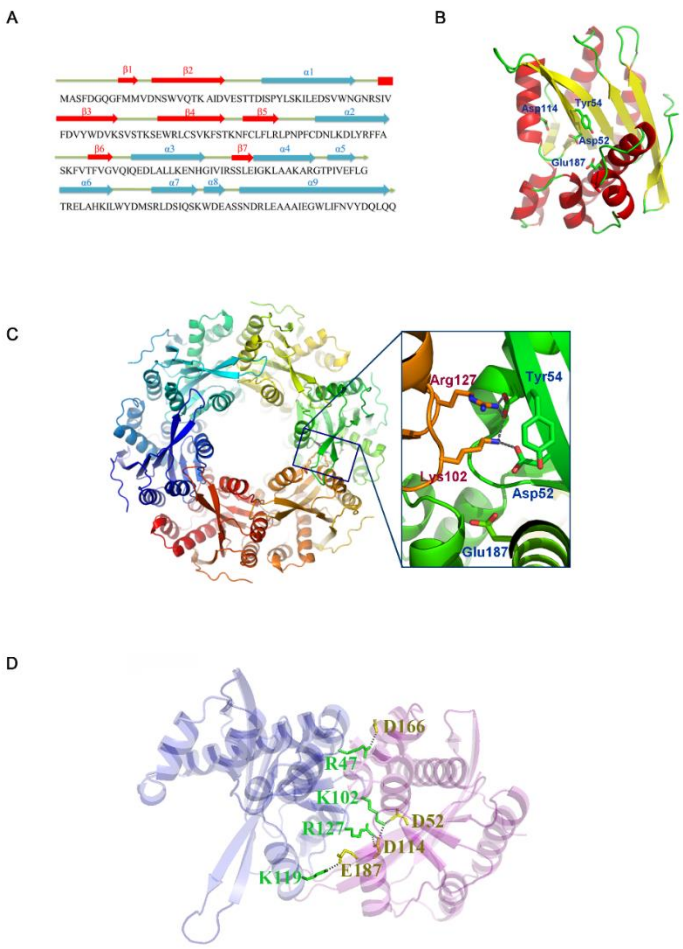

Figure 4- 12 Structure determination of RICE1.

(A) RICE1 primary- and secondary-structure alignment.

(B) RICE1 monomer is consisted of seven beta sheets and nine alpha helixes. Residues that correspond to DEDD motif are shown as stick.

(C) Hexametric ring of RICE1 and electrostatic interactions in the interface.

(D) Detailed analysis of dimer interface.

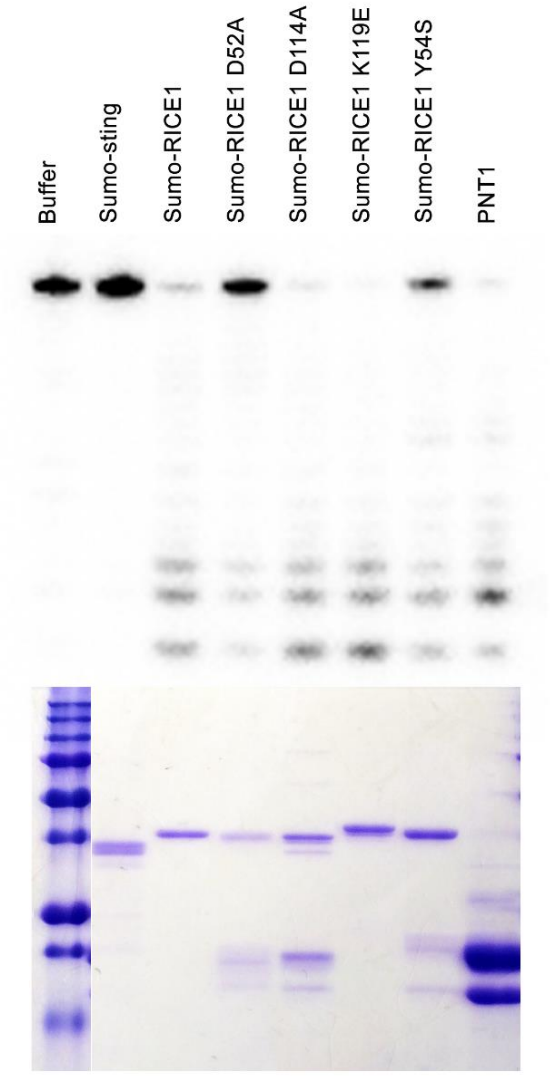

Figure 4- 13 D52A and Y54S point mutations reduce RICE1 RNase activity.

Upper panel: enzymatic assays on 5’ labeled 21nt ssRNA with purified proteins.

Bottom panel: coomassie stained SDS gel of purified hSting, RICE1 and RICE1 D52A proteins used in the assay.

The electro static interaction analysis predicts that eight groups of residues are involved in the dimer formation of RICE1 (Table 4-2). To test this prediction, we created four pairs of mutations of R47E, K102E, R127E and K119E by changing the positively charged residues to Glu. Gel-filtration assays showed that PNT1 R47E displayed a distinct chromatograph profile compared with WT PNT1 with the main peak shifted to a position corresponding to a monomer size (data not shown). However, K119E mutant protein can still form dimer during gel filtration purification (data not shown). These results indicated that Arg 47 but not Lys 119 is essential for dimer formation. Importantly, the enzymatic activity of PNT1 R47E, but not PNT1 K119E, is compromised (Figure 4-13), indicating that dimer formation is required for the nuclease activity of PNT1. The effects of other two point mutations on PNT1 dimer formation awaits to be tested.

Table 4- 5 Interactions between two chains of RICE1.

*: residues selected for mutagenesis for dimer formation analysis.

Residues in B molecule	Residues in C molecule	Distance (Å)	Atoms involved
Asp90	Ser61	2.8	O---O
Gly123	Trp66	2.9	O---NE1
Arg127 *	Asp114	3.3	NH2---OD2
Ser35	Asp173	3.1	OG---OD2
Lys102 *	Asp52	3.1	NZ---OD1
His122	Ser64	2.8	O---OG
Lys119 *	Glu113	3.1	NZ---OE2
Arg47 *	Asp166	2.7	NH2---OE1

Catalytic-inactive RICE1 caused developmental defects and decreased miRNA accumulation

Given that RICE1 is a novel AGO-bound exoribonuclease and that RICE1 promotes miRNA accumulation, RICE1 might function as a RISC activator by degrading miRNA* and facilitating miRNA incorporation into AGO protein. To further examine whether the catalytic activity is critical for this process, we generated transgenic

plants constitutively expressing catalytically-dead RICE1 variants and examined their biological consequence.

D52A is a conserved residue essential for catalytic activity, whereas Tyr54 is our newly identified non-canonical residue that is also critical for enzymatic function of RICE1. Although RICE1 D52A and Y54S mutations abolished the catalytic activity, they did not interfere with the RICE1-AGO10 interaction in the tobacco transient assay (data not shown). I screened numerous transgenic plants expressing *35S-3HA -RICE1 (D52A)* and *35S-3HA-RICE1 (Y54S)* by western blot analysis (Figure 4-14A and Figure 4-15A). Astoundingly, overexpression of *35S-HA3-RICE1 D52A and 35S-HA3-RICE1 Y54S* caused pleiotropic developmental defects including the leaf morphology change (Figure 4-14B and Figure 4-15B) and fertility defects (Figure 4-14C). In a sharp contrast with *35S-RICE1-3HA* plants, overaccmulation of these catalytic-inactive forms of RICE1 D52A and RICE1 Y54S significantly decreased the levels of all tested sRNAs compared to Ler wild type as analyzed by RNA blots (Figure 4-16 and Figure 4-17) or qRT-PCR (Varkonyi-Gasic et al., 2007) (data not shown).

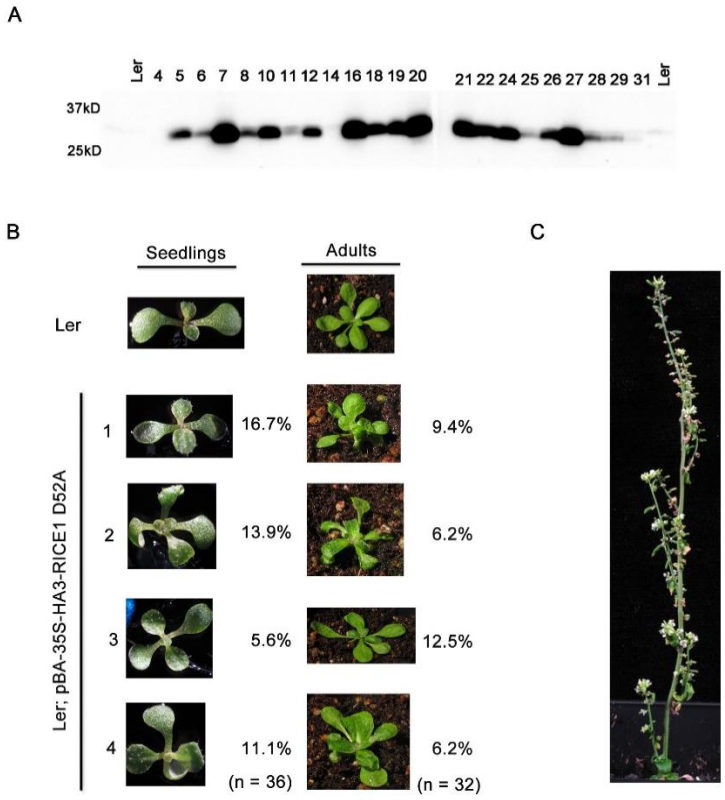

Figure 4- 14 Ectopic expression of RICE1 D52A mutant protein in wild-type Ler plants causes pleiotropic developmental defects.

(A) Western blot with anti-HA antibody to screen positive transgenic lines. 7-day old seedling samples were collected and ground with liquid nitrogen. Total proteins were extracted by 2XSDS buffer.

(B) Developmental abnormalities observed in T2 transformants. Pictures were taken with both 7-day old seedlings and 3-week old plants grown in soil.

(C) Adult mutant shows reduced fertility.

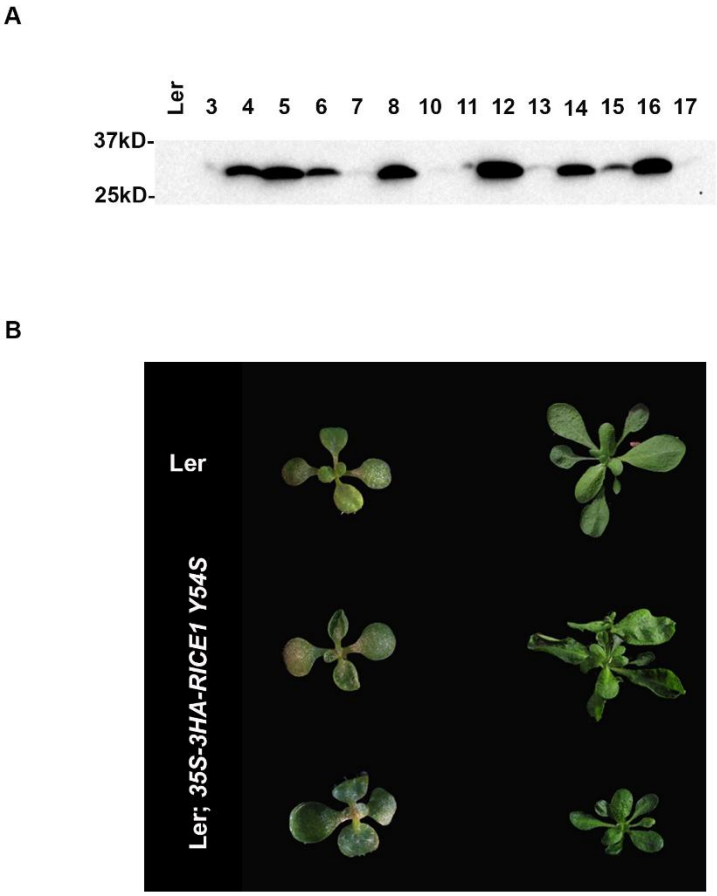

Figure 4- 15 Ectopic expression of RICE1 Y54S mutant protein in wild-type Ler plants causes pleiotropic developmental defects.

(A) Western blot with anti-HA antibody to screen positive transgenic lines. 7-day old seedling samples were collected and ground with liquid nitrogen. Total proteins were extracted by 2XSDS buffer.

(B) Developmental abnormalities observed in T2 transformants. Pictures were taken with both 7-day old seedlings and 3-week old plants grown in soil.

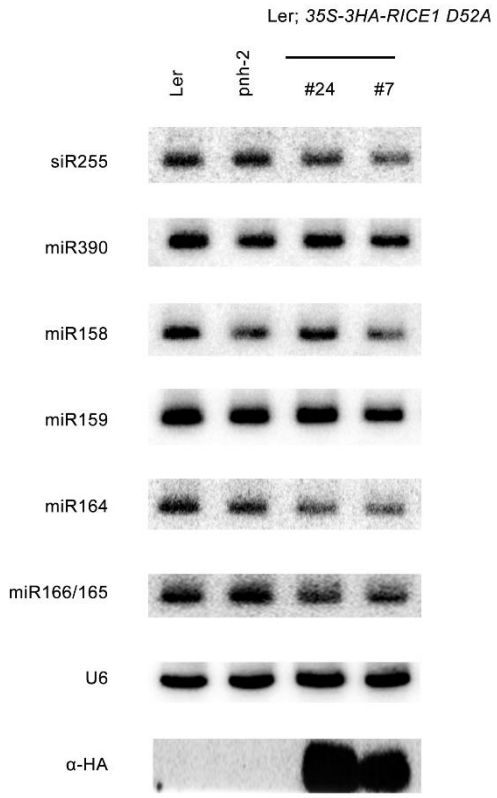

Figure 4- 16 Ectopic expression of RICE1 D52A mutant protein in wild-type Ler plants leads to reduced accumulation of tested sRNAs.

Same membrane was used for probing different sRNAs after stripping. U6 snRNA serves as a loading control.

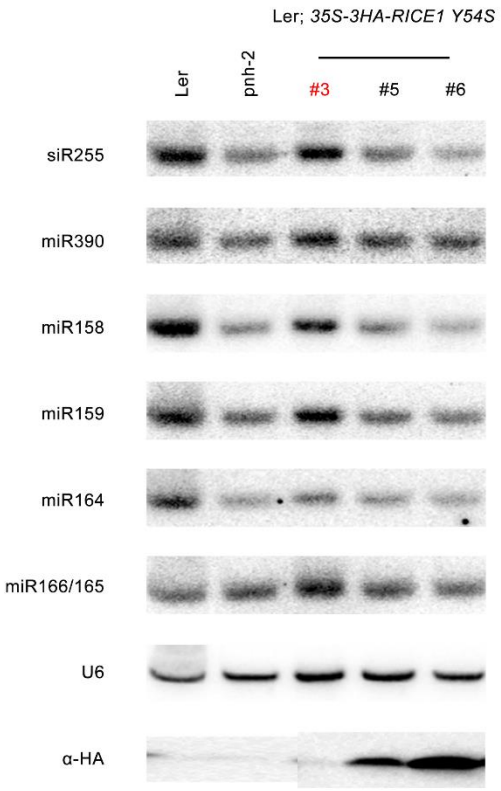

Figure 4- 17 Ectopic expression of RICE1 Y54S mutant protein in wild-type Ler plants leads to reduced accumulation of tested sRNAs.

Same membrane was used for probing different sRNAs after stripping. U6 snRNA serves as a loading control. Note: #3 labeled in red doesn't have transgene expression and serves as a negative sibling control.

These results were reminiscent of the observation in *rice1 rice2* knockdown lines, indicating that catalytic-dead mutations act in a dominant negative manner. These

results further indicated that catalytic activity of RICE1 is essential for its proper function in vivo.

Dimerization is critical for protein integrity in vivo

R47E point mutation abolished the dimerization of RICE1 in my in vitro assay. To examine whether the dimerization was critical for its biological function, I also generated transgenic plants expressing 35S-RICE1 R57E-3HA. Surprisingly, I recovered none of positive transgenic plants by western blot, although Northern blot analysis clearly showed that the transcript levels of this RICE1 variant are comparable with the ones extracted from the plans expressing *35S-3HA-RICE1 D52A/Y54S/K119E*. In line with this, no developmental defects were visible in any of *35S-RICE1 R57E-3HA* transgenic lines (Figure 4-18). Together, these results indicated that disruption of protein dimerization led to instability of this protein.

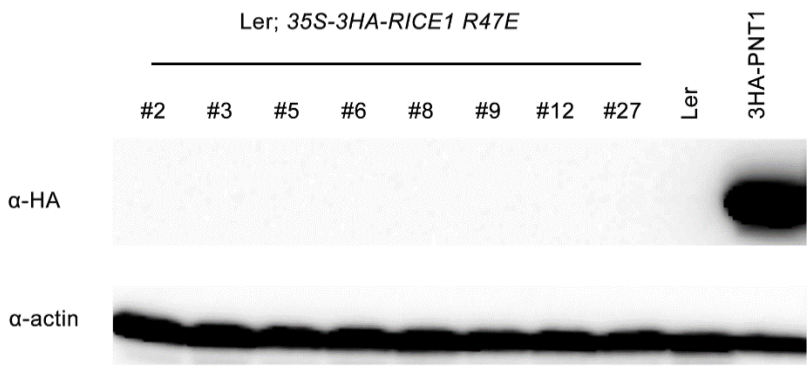

Figure 4- 18 RICE1 R47E doesn't accumulate in *Arabidopsis thaliana*.

Western blot with anti-HA antibody to screen positive transgenic lines. 7-day old seedling samples were collected and ground with liquid nitrogen. Total proteins were extracted by 2XSDS buffer.

Discussion

Compared to siRNA duplexes, the loading of miRNA/* into RISCs are relatively poorly understood. Using Arabidopsis AGO10 as a paradigm, here I reported RICE1 and RICE2, two novel cofactors implanted in RISC, and crystal structures for RICE1. Based on our unbiased biochemical and genetic results, I proposed that these proteins function in clearing miRNA* and promoting loading of miRNA into AGOs, My evidences included: 1) RICE1 resides onto MID domains of AGO proteins, the location in which the 3' end of miRNA* and 5'end of miRNAs are channeled into; 2) RICEs evolve to a 3' to 5' exoribonuclease specifically favoring single strand sRNAs for processing in vitro; 3) Overexpression of *RICEs* causes elevated accumulation of miRNAs while downregulation of *RICE*s decreases miRNA levels; and 4) introduction of catalytic-inactive forms of RICE1 mimics the molecular phenotypes of *rice1 rice2* mutants generated through artificial miRNA strategies. All these results prompted us to hypothesize that RICEs functions to clear the miRNA* upon the loading of miRNA/* duplexes AGO complexes and to activate RISC maturation (Figure 4-26).

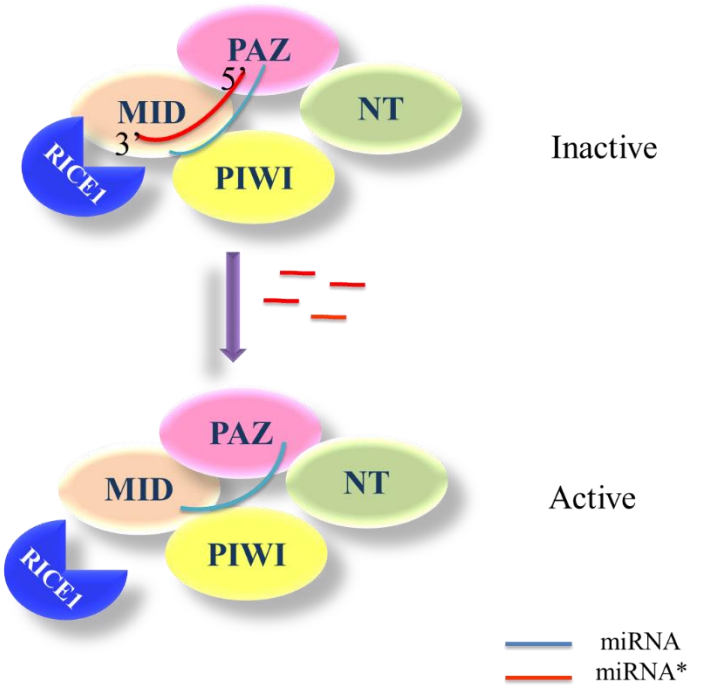

Figure 4- 19 Potential model for RICE1 function.

Functional RICE1 (RICE1-CFP and RICE1-3HA) interacts with the MID domains of AGOs and degrades the miRNAs* in 3' to 5' direction. This process liberates miRNA from the miRNA/* duplexes and leads to subsequent RISC activation. Non-functional RICE1 (3HA-RICE1 D52A, 3HA-RICE1 Y54S, 3HA-RICE1 and amiR-RICEs) cannot fulfill the RISC activator function and it possibly results in RNAi inhibition in vivo.

Biochemical features of RICEs

Structural analysis reveals that RICEs have some unique features. First, RICE harbor some non-canonical residues that are critical for their catalytic function. RICE1 belongs to the DEDD superfamily (also known as DnaQ superfamily) that canonically carry out catalytic functions through the conserved DEDD motif. Besides these four

invariant residues, additional residues also contribute to the catalytic activity of the protein family member, thus the DEDD superfamily can be further grouped into two subfamilies - DEDDh and DEDDy - based on whether the presence of His or Tyr in the catalytic sites (Zuo and Deutscher, 2001a). Notably, RICE1 does not contain the canonical DEDD motif in the putative active site of RICE1, instead, it has three acidic residues, Asp52, Asp114 and Glu187, which correspond to DEDD motif based on structural alignments (Figure 4-9B). The second conserved Glu residue in the catalytic motif is replaced by Tyr54 and there was no additional catalytic His or Tyr in the presumed active site of RICE1. Moreover, D114 appears not be engaged in its enzymatic function. Thus, RICEs seem to evolve to a new catalytic active site. Second, DEDD superfamily proteins share another common catalytic mechanism characterized by the involvement of two metal ions (Zuo and Deutscher, 2001b). Metal ions can be found in all known crystal structures of RICE1 homologs from other organisms such as RNaseT from *E.coli (Zuo et al., 2007),* Ngl3p from *S. cerevisiae* (Feddersen et al., 2012) and WRN from *H. sapiens* (Perry et al., 2006) and it has been demonstrated that the catalytic activities of these proteins are metal cation-dependent. For RICE1, electron density map for Mg^{2+} used in crystallization was not observed around predicated active site. Asp52 and Asp114, two residues that otherwise bind to divalent cations, interact with Lys102 and Arg127 of the other chain. Moreover, EDTA doesn't affect the in vitro enzymatic activity of RICE1 (data not shown). Together, the absence of metal ions in the crystal as well as the unique organization of catalytic active site suggests that RICE1 might possess a novel catalytic mechanism.

Mechanistic uniqueness of RICEs in RISC maturation

Previous two enzymes, C3PO in human (Liu et al., 2009b; Ye et al., 2011) and QIP in *Neurospora* (Maiti et al., 2007), have been previously reported to be involved in loading of siRNAs, but not miRNAs, in other organisms. In *Drosophila* and human, siRNA duplexes are sorted into AGO2 containing RISC complexes (Okamura et al., 2004) where the star strand serves as the first target of RISC and is cleaved by the catalytic active AGO2. C3PO, an Mg^{2+}-dependent endoribonuclease is required for the cleaved passenger strand siRNA removal and subsequent RISC activation (Liu et al., 2009b; Ye et al., 2011). QIP from *Neurospora crassa* is a QDE2 (an AGO in *Neurospora crassa*)-interacting 3' to 5' exoribonuclease that degrades passenger strand siRNA and leads to RISC activation. In *qip* mutant nicked siRNA duplex accumulate and RNAi is compromised (Maiti et al., 2007). The common features for the two nucleases are that both degrade nicked star strands of siRNAs to achieve RISC activation. RICEs functionally differ from the RICEs functionally differ from the above-mentioned QIP. The slicer activity of QDE2 in *Neurospora* is required for generating nicked siRNA duplexes and subsequent QIP function. In our study, RICE1 cannot degrade nicked siRNA star strands. Moreover, catalytic-incompetent AGO recruits miRNAs as efficiently as catalytic-active AGOs, suggesting that the miRNA* is unlikely nicked in plants. Consistently, we did not observe a stable-nicked duplex form in *Arabidopsis thaliana* in *rice1 rice 2* mutants as would expected if RICEs are functionally counterpart for QIP. Moreover, unlike QIP, RICEs are not engaged in siRNA processing, nor miRNA biogenesis (Xue et al., 2012). In addition, unlike QIP (~600 aa)

that contains multiple domains and might have numerous functions, RICEs are relatively small proteins and might evolve to a cognate partner of AGO protein, specifically clearing miRNA*. Given that RICE1 only degrades ssRNAs but not dsRNAs, how would the miRNA* in miRNA/* be accessible to RICE1? We propose that the plant miRNA/* duplexes are fueled into AGO proteins in the duplex form, possibly facilitated by Hsp70/90 and CYP40 (Iki et al., 2012; Iki et al., 2010; Iwasaki et al., 2010; Miyoshi et al., 2010). The two strands of miRNA/* then get separated by AGO protein (Gu et al., 2012; Kwak and Tomari, 2012). The miRNA* will subsequently be channeled to RICEs for degradation and the miRNA-RISC will be activated. The RISC activator function of RICEs are different from previous reported SDNs (Ramachandran and Chen, 2008) which likely function as a downstream to participate in miRNA metabolism and maintenance of miRNA homeostasis. Of a note, the extent of miRNA decrease in *RICE* knockdown lines is much milder than that in transgenic lines overexpressing RICE1 point mutations. One possible reason for this is that the artificial miRNA constructs do not cause complete knockout of *RICE* and the residual protein can still be functional. An alternative explanation is that other unknown RISC activators have redundant function with RICE1 and only knocking down *RICE1* cannot completely inhibit RISC activation. However, in Ler; *35S-3HA-RICE1 D52A* and Ler; *35S-3HA-RICE1 Y54S* lines the overexpressed mutant proteins could act in a dominant negative manner to interfere with the functional RISC activators and as a result we observed a more prevalent effect on miRNA accumulation.

Besides the effects of *RICE*-related transgenes on miRNA accumulation in vivo we also observed that AGO protein levels get affected upon transgene expression. For example, in Ler; *35S-3HA-RICE1* transgenic lines AGO1 protein level decreases (data not shown). We believe that RICE affects AGO1 accumulation at the posttranscriptional level since AGO1 transcripts level is not changed (data not shown). One possible explanation is that inactive RISCs are vulnerable to the degradation pathway and when RISCs cannot get activated they will undergo the decay process. Further study is necessary to test this idea.

AGO10 genetically represses miR166/165 expression and positively regulates the miR166/165 target gene *HD-ZIP III* expression (Liu et al., 2009a; Zhu et al., 2011). In line with this, in situ hybridization shows that *AGO10* co-localizes with *HD-ZIP III* transcripts while displays a complementary expression pattern with that of *MIR*166/165 (McConnell et al., 2001; Tucker et al., 2008), indicating that AGO10-miR166/165 association doesn't result in the cleavage of *HD-ZIP III* transcripts. It is tempting to assume that AGO10 is not assembled in a functional RISC. If this is true, it will be interesting to test the effect of knocking down *RICE1/RICE2* in *AGO10* expression domain.

CHAPTER V

CONCLUSIONS AND FUTURE WORK

RNAi plays pivotal roles in regulating most, if not all, biological processes. Although biochemical framework for RNAi has been schematically outlined, many fundamental issues remain to be explored. One of such issues is to characterize the full composition of protein components that contribute to the regulation of this pathway and to appreciate their underlying molecular mechanism.

My research has been focused on AGO10 in *Arabidopsis*. In this dissertation, I presented the study to reveal a previously unknown function of *Arabidopsis* AGO10 (Chapter II) in RNAi. Moreover, I reported that the N-terminal domain of AGO10 is a key region contributing to the functional specificity of AGO10, especially for SAM regulation (Chapters III). Lastly I demonstrated that identification and characterization of a novel AGO10-interacting protein RICE1 in *Arabidopsis* (Chapter IV). In this chapter, conclusions from these studies and speculations of future directions are described.

To extrapolate how AGO10 regulates SAM development, we performed biochemical studies to isolate AGO10-sRNA complexes and sequenced AGO10-bound sRNA species. Surprisingly, one group of miRNA – miR166/165 is highly represented in AGO10. More astonishingly, genetic studies reveal that AGO10 negatively regulates miR166/165 activity by sequestering miR166/165 from AGO1 and causing its decoy. This is a paradigm-shifting discovery that an AGO protein, which otherwise recruits sRNAs to silence their targets, antagonizes miRNAs and protects their target genes.

The next intriguing question is why AGO10 functions differently from canonical AGOs? I am interested in defining the domain(s) of AGO10 that contribute to its functional uniqueness. Bioinformatics analysis shows that AGO1 and AGO10 are evolutionarily closely related and highly conserved sequence wise, however, the functional modes of these two proteins are entirely different. AGO1 functions as a canonical AGO protein and acts as a master repressor of sRNA target genes by endonucleolytic cleavage and translational repression (Baumberger and Baulcombe, 2005; Bohmert et al., 1998a; Li et al., 2013; Vaucheret et al., 2004). Although AGO10 also has catalytic activity, the silencing function of AGO10 seems to be irrelevant to its role in SAM development in vivo as catalytic-dead forms of AGO10 rescue *ago10* mutant phenotype as efficiently as wild-type AGO10. By swapping domains between AGO1 and AGO10, I discovered that the N-terminal domain of AGO10 was a key region that regulates the function of AGO10. Notably, the sequences of N-terminal domains of AGOs are highly diverse. It is possible that the conformation of AGO10 N-terminal domain determines its special functional mode or some other factors to be identified specifically interacts with AGO10 N-terminal domain and regulates its function.

To this end, the role of AGO10 N-terminal domain awaits further exploration. There are several directions that I propose here that can be helpful to gain more insights of this particular region. First, it needs to be determined whether N-terminal domain contributes to the high binding affinity of AGO10 to miR166/165. Second, it will be helpful to pinpoint critical sequence residues/motifs residing in the N-terminal domain of

AGO10 that are important for its regulatory function. Computational and genetic approaches can be employed for this purpose. Moreover, advances in structural studies of AGO1 and AGO10 in plants will be helpful for understanding the uniqueness of AGO10 N-terminal domain. Lastly, there might be factors that specifically recognize AGO10 N-terminal domain to regulate its function, such factors need further experimental characterization.

To further understand the mechanism of AGO10 it is necessary to investigate how AGO10 complex is assembled in vivo. To this end, RICE1 is identified by proteomics screening of AGO10 interacting proteins. The interaction of AGO10 and RICE1 is characterized by co-IP, split luciferase assay and in vitro pull-down. Biochemical study of RICE1 reveals that it is a 3' to 5'small RNA specific exoribonuclease. Interestingly, RICE1 interacts with AGO10 (and AGO1) MID domain which associates with the 3' termini of sRNAs.

Based on the enzymatic properties of RICE1, we envision two non-mutually exclusive possibilities: 1) RICE1 degrades passenger strands of sRNAs during RISC activation process; and 2) RICE1 degrades AGO-bound sRNAs, in another word, RICE1 induces sRNA release from AGO. I applied to unbiased genetic assays to test these two hypotheses. Overexpression of *RICE1* resulted in elevated levels of sRNAs; while overexpression of catalytic-inactive *RICE1* and higher-order mutants of *rice1 rice2* generated from artificial miRNAs decreased sRNA abundance. These results support the model where RICE1 functions to degrade the star strands of sRNA duplexes during sRNA loading process to activate RISCs. Interestingly, *QIP*, a *Neurospora* ortholog of

RICE1, was known to be involved in both processing and loading of miRNAs. However, in *Neurospora,* miRNA predominantly exist as single strand form while in *qip* mutants miRNA duplex accumulated. We did not observe this scenario in *Arabidopsis*, suggesting mechanistic difference between QIP and RICEs in RISC activation. It would be interesting to examine how RICEs biochemically activate RISC maturation in the future.

Lastly, it will be interesting to see the elution profiles of AGO1/AGO10 and RICE1 by gel filtration. From this result, we can get an idea of how much of RICE1 associates with AGO proteins and also it is interesting to find out whether or not RICE1 can interact with all AGOs in *Arabidopsis thaliana*.

REFERENCES

Hutvágner, G and Zamore, P.D. (2002). RNAi: nature abhors a double-strand. Current Opinion in Genetics & Development *12*, 225–232.

Aboobaker, A.A., Tomancak, P., Patel, N., Rubin, G.M., and Lai, E.C. (2005). Drosophila microRNAs exhibit diverse spatial expression patterns during embryonic development. Proceedings of the National Academy of Sciences of the United States of America *102*, 18017-18022.

Adams, D.R., Ron, D., and Kiely, P.A. (2011). RACK1, A multifaceted scaffolding protein: Structure and function. Cell communication and signaling *9*, 22.

Ahlquist, P. (2002). RNA-dependent RNA polymerases, viruses, and RNA silencing. Science *296*, 1270-1273.

Ameres, S.L., Horwich, M.D., Hung, J.H., Xu, J., Ghildiyal, M., Weng, Z., and Zamore, P.D. (2010). Target RNA-directed trimming and tailing of small silencing RNAs. Science *328*, 1534-1539.

Ameres, S.L., Martinez, J., and Schroeder, R. (2007). Molecular basis for target RNA recognition and cleavage by human RISC. Cell *130*, 101-112.

Anderson, P., and Kedersha, N. (2006). RNA granules. The Journal of cell biology *172*, 803-808.

Ariel, F.D., Manavella, P.A., Dezar, C.A., and Chan, R.L. (2007). The true story of the HD-Zip family. Trends in plant science *12*, 419-426.

Azuma-Mukai, A., Oguri, H., Mituyama, T., Qian, Z.R., Asai, K., Siomi, H., and Siomi, M.C. (2008). Characterization of endogenous human Argonautes and their miRNA partners in RNA silencing. Proceedings of the National Academy of Sciences of the United States of America *105*, 7964-7969.

Barton, M.K. (2010). Twenty years on: the inner workings of the shoot apical meristem, a developmental dynamo. Developmental biology *341*, 95-113.

Barton, M.K., and Poethig, R.S. (1993). Formation of the Shoot Apical Meristem in Arabidopsis-Thaliana - an Analysis of Development in the Wild-Type and in the Shoot Meristemless Mutant. Development *119*, 823-831.

Baulcombe, D. (2004). RNA silencing in plants. Nature *431*, 356-363.

Baumberger, N., and Baulcombe, D.C. (2005). Arabidopsis ARGONAUTE1 is an RNA Slicer that selectively recruits microRNAs and short interfering RNAs. Proceedings of the National Academy of Sciences of the United States of America *102*, 11928-11933.

Behm-Ansmant, I., Rehwinkel, J., Doerks, T., Stark, A., Bork, P., and Izaurralde, E. (2006). MRNA degradation by miRNAs and GW182 requires both CCR4 : NOT deadenylase and DCP1 : DCP2 decapping complexes. Genes & development *20*, 1885-1898.

Bohmert, K., Camus, I., Bellini, C., Bouchez, D., Caboche, M., and Benning, C. (1998). AGO1 defines a novel locus of Arabidopsis controlling leaf development. EMBO J *17*, 170-180.

Bollman, K.M., Aukerman, M.J., Park, M.Y., Hunter, C., Berardini, T.Z., and Poethig, R.S. (2003). HASTY, the Arabidopsis ortholog of exportin 5/MSN5, regulates phase change and morphogenesis. Development *130*, 1493-1504.

Bortolamiol, D., Pazhouhandeh, M., Marrocco, K., Genschik, P., and Ziegler-Graff, V. (2007). The Polerovirus F box protein P0 targets ARGONAUTE1 to suppress RNA silencing. Current biology : CB *17*, 1615-1621.

Brodersen, P., Sakvarelidze-Achard, L., Bruun-Rasmussen, M., Dunoyer, P., Yamamoto, Y.Y., Sieburth, L., and Voinnet, O. (2008). Widespread Translational Inhibition by Plant miRNAs and siRNAs. Science *320*, 1185-1190.

Byrne, M.E. (2006). Shoot meristem function and leaf polarity: the role of class III HD-ZIP genes. PLoS genetics *2*, e89.

Byrne, M.E., Simorowski, J., and Martienssen, R.A. (2002). ASYMMETRIC LEAVES1 reveals knox gene redundancy in Arabidopsis. Development *129*, 1957-1965.

Calderon-Villalobos, L.I., Kuhnle, C., Dohmann, E.M., Li, H., Bevan, M., and Schwechheimer, C. (2005). The evolutionarily conserved TOUGH protein is required for proper development of Arabidopsis thaliana. The Plant cell *17*, 2473-2485.

Capel, B., Swain, A., Nicolis, S., Hacker, A., Walter, M., Koopman, P., Goodfellow, P., and Lovell-Badge, R. (1993). Circular transcripts of the testis-determining gene Sry in adult mouse testis. Cell *73*, 1019-1030.

Carbonell, A., Fahlgren, N., Garcia-Ruiz, H., Gilbert, K.B., Montgomery, T.A., Nguyen, T., Cuperus, J.T., and Carrington, J.C. (2012). Functional analysis of three Arabidopsis ARGONAUTES using slicer-defective mutants. The Plant cell *24*, 3613-3629.

Chapman, E.J., and Carrington, J.C. (2007). Specialization and evolution of endogenous small RNA pathways. Nature Reviews Genetics *8*, 884-896.

Chatterjee, S., and Großhans, H. (2009). Active turnover modulates mature microRNA activity in Caenorhabditis elegans. Nature *461*, 546-549.

Cheloufi, S., Dos Santos, C.O., Chong, M.M., and Hannon, G.J. (2010). A dicer-independent miRNA biogenesis pathway that requires Ago catalysis. Nature *465*, 584-589.

Chen, X. (2004). A MicroRNA as a Translational Repressor of APETALA2 in Arabidopsis Flower Development. Science *303*, 2022-2025.

Chen, X. (2005). MicroRNA biogenesis and function in plants. FEBS letters *579*, 5923-5931.

Chiang, H.R., Schoenfeld, L.W., Ruby, J.G., Auyeung, V.C., Spies, N., Baek, D., Johnston, W.K., Russ, C., Luo, S., Babiarz, J.E., *et al.* (2010). Mammalian microRNAs:

experimental evaluation of novel and previously annotated genes. Genes & development *24*, 992-1009.

Chitwood, D.H., Nogueira, F.T., Howell, M.D., Montgomery, T.A., Carrington, J.C., and Timmermans, M.C. (2009). Pattern formation via small RNA mobility. Genes & development *23*, 549-554.

Chitwood, D.H., and Timmermans, M.C. (2010). Small RNAs are on the move. Nature *467*, 415-419.

Cifuentes, D., Xue, H., Taylor, D.W., Patnode, H., Mishima, Y., Cheloufi, S., Ma, E., Mane, S., Hannon, G.J., Lawson, N.D., *et al.* (2010). A novel miRNA processing pathway independent of Dicer requires Argonaute2 catalytic activity. Science *328*, 1694-1698.

Clough, S.J., and Bent, A.F. (1998). Floral dip: a simplified method for Agrobacterium-mediated transformation of Arabidopsis thaliana. The Plant journal : for cell and molecular biology *16*, 735-743.

Csorba, T., Lozsa, R., Hutvagner, G., and Burgyan, J. (2010). Polerovirus protein P0 prevents the assembly of small RNA-containing RISC complexes and leads to degradation of ARGONAUTE1. The Plant journal : for cell and molecular biology *62*, 463-472.

Czech, B., Zhou, R., Erlich, Y., Brennecke, J., Binari, R., Villalta, C., Gordon, A., Perrimon, N., and Hannon, G.J. (2009). Hierarchical rules for Argonaute loading in Drosophila. Molecular cell *36*, 445-456.

De, N., Young, L., Lau, P.W., Meisner, N.C., Morrissey, D.V., and MacRae, I.J. (2013). Highly complementary target RNAs promote release of guide RNAs from human Argonaute2. Molecular cell *50*, 344-355.

Diederichs, S., and Haber, D.A. (2007). Dual role for argonautes in microRNA processing and posttranscriptional regulation of microRNA expression. Cell *131*, 1097-1108.

Djuranovic, S., Zinchenko, M.K., Hur, J.K., Nahvi, A., Brunelle, J.L., Rogers, E.J., and Green, R. (2010). Allosteric regulation of Argonaute proteins by miRNAs. Nature structural & molecular biology *17*, 144-150.

Dong, Z., Han, M., and Fedoroff, N. (2008). The RNA-binding proteins HYL1 and SE promote accurate in vitro processing of pri-miRNA by DCL1. PNAS *105*, 9970-9975

Dunoyer, P., Schott, G., Himber, C., Meyer, D., Takeda, A., Carrington, J.C., and Voinnet, O. (2010). Small RNA duplexes function as mobile silencing signals between plant cells. Science *328*, 912-916.

Eamens, A.L., Smith, N.A., Curtin, S.J., Wang, M.B., and Waterhouse, P.M. (2009). The Arabidopsis thaliana double-stranded RNA binding protein DRB1 directs guide strand selection from microRNA duplexes. RNA *15*, 2219-2235.

Earley, K., Smith, M., Weber, R., Gregory, B., and Poethig, R. (2010). An endogenous F-box protein regulates ARGONAUTE1 in Arabidopsis thaliana. Silence *1*, 15.

Ebert, M.S., Neilson, J.R., and Sharp, P.A. (2007). MicroRNA sponges: competitive inhibitors of small RNAs in mammalian cells. Nature methods *4*, 721-726.

Elbashir, S.M., Lendeckel, W., and Tuschl, T. (2001a). RNA interference is mediated by 21-and 22-nucleotide RNAs. Genes & development *15*, 188-200.

Elbashir, S.M., Martinez, J., Patkaniowska, A., Lendeckel, W., and Tuschl, T. (2001b). Functional anatomy of siRNAs for mediating efficient RNAi in Drosophila melanogaster embryo lysate. Embo Journal *20*, 6877-6888.

Elkayam, E., Kuhn, C.-D., Tocilj, A., Haase, Astrid D., Greene, Emily M., Hannon, Gregory J., and Joshua-Tor, L. (2012a). The Structure of Human Argonaute-2 in Complex with miR-20a. Cell *150*, 100-110.

Elkayam, E., Kuhn, C.D., Tocilj, A., Haase, A.D., Greene, E.M., Hannon, G.J., and Joshua-Tor, L. (2012b). The structure of human argonaute-2 in complex with miR-20a. Cell *150*, 100-110.

Emery, J.F., Floyd, S.K., Alvarez, J., Eshed, Y., Hawker, N.P., Izhaki, A., Baum, S.F., and Bowman, J.L. (2003). Radial patterning of Arabidopsis shoots by class III HD-ZIP and KANADI genes. Current biology : CB *13*, 1768-1774.

Ender, C., Krek, A., Friedlander, M.R., Beitzinger, M., Weinmann, L., Chen, W., Pfeffer, S., Rajewsky, N., and Meister, G. (2008). A human snoRNA with microRNA-like functions. Molecular cell *32*, 519-528.

Endo, Y., Iwakawa, H.O., and Tomari, Y. (2013). Arabidopsis ARGONAUTE7 selects miR390 through multiple checkpoints during RISC assembly. EMBO reports *14*, 652-658.

Engstrom, E.M., Izhaki, A., and Bowman, J.L. (2004). Promoter bashing, microRNAs, and Knox genes. New insights, regulators, and targets-of-regulation in the establishment of lateral organ polarity in Arabidopsis. Plant physiology *135*, 685-694.

Eshed, Y., Baum, S.F., Perea, J.V., and Bowman, J.L. (2001). Establishment of polarity in lateral organs of plants. Current biology : CB *11*, 1251-1260.

Eshed, Y., Izhaki, A., Baum, S.F., Floyd, S.K., and Bowman, J.L. (2004). Asymmetric leaf development and blade expansion in Arabidopsis are mediated by KANADI and YABBY activities. Development *131*, 2997-3006.

Eulalio, A., Behm-Ansmant, I., and Izaurralde, E. (2007a). P bodies: at the crossroads of post-transcriptional pathways. Nat Rev Mol Cell Bio *8*, 9-22.

Eulalio, A., Behm-Ansmant, I., Schweizer, D., and Izaurralde, E. (2007b). P-body formation is a consequence, not the cause, of RNA-mediated gene silencing. Mol Cell Biol *27*, 3970-3981.

Eulalio, A., Huntzinger, E., and Izaurralde, E. (2008). GW182 interaction with Argonaute is essential for miRNA-mediated translational repression and mRNA decay. Nature structural & molecular biology *15*, 346-353.

Eystathioy, T., Jakymiw, A., Chan, E.K.L., Seraphin, B., Cougot, N., and Fritzler, M.J. (2003). The GW182 protein colocalizes with mRNA degradation associated proteins hDcp1 and hLSm4 in cytoplasmic GW bodies. Rna-a Publication of the Rna Society *9*, 1171-1173.

Faehnle, C.R., Elkayam, E., Haase, A.D., Hannon, G.J., and Joshua-Tor, L. (2013). The making of a slicer: activation of human Argonaute-1. Cell reports *3*, 1901-1909.

Fire, A., Xu, S., Montgomery, M.K., Kostas, S.A., Driver, S.E., and Mello, C.C. (1998). Potent and specific genetic interference by double-stranded RNA in Caenorhabditis elegans. Nature *391*, 806-811.

Forstemann, K., Horwich, M.D., Wee, L., Tomari, Y., and Zamore, P.D. (2007). Drosophila microRNAs are sorted into functionally distinct argonaute complexes after production by dicer-1. Cell *130*, 287-297.

Franco-Zorrilla, J.M., Valli, A., Todesco, M., Mateos, I., Puga, M.I., Rubio-Somoza, I., Leyva, A., Weigel, D., Garcia, J.A., and Paz-Ares, J. (2007). Target mimicry provides a new mechanism for regulation of microRNA activity. Nature genetics *39*, 1033-1037.

Frank, F., Sonenberg, N., and Nagar, B. (2010). Structural basis for 5'-nucleotide base-specific recognition of guide RNA by human AGO2. Nature *465*, 818-822.

Gehrke, S., Imai, Y., Sokol, N., and Lu, B. (2010). Pathogenic LRRK2 negatively regulates microRNA-mediated translational repression. Nature *466*, 637-641.

Ghildiyal, M., Seitz, H., Horwich, M.D., Li, C., Du, T., Lee, S., Xu, J., Kittler, E.L., Zapp, M.L., Weng, Z., *et al.* (2008). Endogenous siRNAs derived from transposons and mRNAs in Drosophila somatic cells. Science *320*, 1077-1081.

Ghildiyal, M., Xu, J., Seitz, H., Weng, Z., and Zamore, P.D. (2010). Sorting of Drosophila small silencing RNAs partitions microRNA* strands into the RNA interference pathway. RNA *16*, 43-56.

Gibbings, D., Mostowy, S., Jay, F., Schwab, Y., Cossart, P., and Voinnet, O. (2012). Selective autophagy degrades DICER and AGO2 and regulates miRNA activity. Nature cell biology *14*, 1314-1321.

Gibbings, D.J., Ciaudo, C., Erhardt, M., and Voinnet, O. (2009). Multivesicular bodies associate with components of miRNA effector complexes and modulate miRNA activity. Nature cell biology *11*, 1143-1149.

Goff, L.A., Davila, J., Swerdel, M.R., Moore, J.C., Cohen, R.I., Wu, H., Sun, Y.E., and Hart, R.P. (2009). Ago2 Immunoprecipitation Identifies Predicted MicroRNAs in Human Embryonic Stem Cells and Neural Precursors. PloS one *4*.

Gregory, B.D., O'Malley, R.C., Lister, R., Urich, M.A., Tonti-Filippini, J., Chen, H., Millar, A.H., and Ecker, J.R. (2008). A link between RNA metabolism and silencing affecting Arabidopsis development. Developmental cell *14*, 854-866.

Grigg, S.P., Canales, C., Hay, A., and Tsiantis, M. (2005). SERRATE coordinates shoot meristem function and leaf axial patterning in Arabidopsis. Nature *437*, 1022-1026.

Gu, S., Jin, L., Huang, Y., Zhang, F., and Kay, M.A. (2012). Slicing-independent RISC activation requires the argonaute PAZ domain. Current biology : CB *22*, 1536-1542.

Gu, S., Jin, L., Zhang, F., Huang, Y., Grimm, D., Rossi, J.J., and Kay, M.A. (2011). Thermodynamic stability of small hairpin RNAs highly influences the loading process of different mammalian Argonautes. Proceedings of the National Academy of Sciences of the United States of America *108*, 9208-9213.

Haley, B., and Zamore, P.D. (2004). Kinetic analysis of the RNAi enzyme complex. Nature structural & molecular biology *11*, 599-606.

Han, B.W., Hung, J.H., Weng, Z., Zamore, P.D., and Ameres, S.L. (2011). The 3'-to-5' exoribonuclease Nibbler shapes the 3' ends of microRNAs bound to Drosophila Argonaute1. Current biology : CB *21*, 1878-1887.

Han, M.H., Goud, S., Song, L., and Fedoroff, N. (2004). The Arabidopsis double-stranded RNA-binding protein HYL1 plays a role in microRNA-mediated gene regulation. Proceedings of the National Academy of Sciences of the United States of America *101*, 1093-1098.

Hansen, T.B., Jensen, T.I., Clausen, B.H., Bramsen, J.B., Finsen, B., Damgaard, C.K., and Kjems, J. (2013). Natural RNA circles function as efficient microRNA sponges. Nature *495*, 384-388.

Hansen, T.B., Wiklund, E.D., Bramsen, J.B., Villadsen, S.B., Statham, A.L., Clark, S.J., and Kjems, J. (2011). miRNA-dependent gene silencing involving Ago2-mediated cleavage of a circular antisense RNA. The EMBO journal *30*, 4414-4422.

Hauptmann, J., Dueck, A., Harlander, S., Pfaff, J., Merkl, R., and Meister, G. (2013). Turning catalytically inactive human Argonaute proteins into active slicer enzymes. Nature structural & molecular biology.

Havecker, E.R., Wallbridge, L.M., Hardcastle, T.J., Bush, M.S., Kelly, K.A., Dunn, R.M., Schwach, F., Doonan, J.H., and Baulcombe, D.C. (2010). The Arabidopsis RNA-Directed DNA Methylation Argonautes Functionally Diverge Based on Their Expression and Interaction with Target Loci. The Plant Cell Online *22*, 321-334.

He, X.J., Hsu, Y.F., Zhu, S., Wierzbicki, A.T., Pontes, O., Pikaard, C.S., Liu, H.L., Wang, C.S., Jin, H., and Zhu, J.K. (2009). An effector of RNA-directed DNA methylation in arabidopsis is an ARGONAUTE 4- and RNA-binding protein. Cell *137*, 498-508.

Heo, I., and Kim, V.N. (2009). Regulating the regulators: posttranslational modifications of RNA silencing factors. Cell *139*, 28-31.

Houseley, J., LaCava, J., and Tollervey, D. (2006). RNA-quality control by the exosome. Nature reviews Molecular cell biology *7*, 529-539.

Hu, H.Y., Yan, Z., Xu, Y., Hu, H., Menzel, C., Zhou, Y.H., Chen, W., and Khaitovich, P. (2009). Sequence features associated with microRNA strand selection in humans and flies. BMC genomics *10*, 413.

Huntzinger, E., and Izaurralde, E. (2011). Gene silencing by microRNAs: contributions of translational repression and mRNA decay. Nature reviews Genetics *12*, 99-110.

Huntzinger, E., Kuzuoglu-Ozturk, D., Braun, J.E., Eulalio, A., Wohlbold, L., and Izaurralde, E. (2013). The interactions of GW182 proteins with PABP and deadenylases are required for both translational repression and degradation of miRNA targets. Nucleic acids research *41*, 978-994.

Hur, J.K., Zinchenko, M.K., Djuranovic, S., and Green, R. (2013). Regulation of Argonaute slicer activity by guide RNA 3' end interactions with the N-terminal lobe. The Journal of biological chemistry *288*, 7829-7840.

Hutvagner, G., and Simard, M.J. (2008). Argonaute proteins: key players in RNA silencing. Nature Reviews Molecular Cell Biology *9*, 22-32.

Ibrahim, F., Rymarquis, L.A., Kim, E.J., Becker, J., Balassa, E., Green, P.J., and Cerutti, H. (2010). Uridylation of mature miRNAs and siRNAs by the MUT68 nucleotidyltransferase promotes their degradation in Chlamydomonas. Proceedings of the National Academy of Sciences of the United States of America *107*, 3906-3911.

Iki, T., Yoshikawa, M., Meshi, T., and Ishikawa, M. (2012). Cyclophilin 40 facilitates HSP90-mediated RISC assembly in plants. The EMBO journal *31*, 267-278.

Iki, T., Yoshikawa, M., Nishikiori, M., Jaudal, M.C., Matsumoto-Yokoyama, E., Mitsuhara, I., Meshi, T., and Ishikawa, M. (2010). In vitro assembly of plant RNA-induced silencing complexes facilitated by molecular chaperone HSP90. Molecular cell *39*, 282-291.

Irvine, D.V., Zaratiegui, M., Tolia, N.H., Goto, D.B., Chitwood, D.H., Vaughn, M.W., Joshua-Tor, L., and Martienssen, R.A. (2006). Argonaute slicing is required for heterochromatic silencing and spreading. Science *313*, 1134-1137.

Iwasaki, S., Kobayashi, M., Yoda, M., Sakaguchi, Y., Katsuma, S., Suzuki, T., and Tomari, Y. (2010). Hsc70/Hsp90 chaperone machinery mediates ATP-dependent RISC loading of small RNA duplexes. Molecular cell *39*, 292-299.

Janas, M.M., Wang, B., Harris, A.S., Aguiar, M., Shaffer, J.M., Subrahmanyam, Y.V., Behlke, M.A., Wucherpfennig, K.W., Gygi, S.P., Gagnon, E., *et al.* (2012). Alternative RISC assembly: binding and repression of microRNA-mRNA duplexes by human Ago proteins. Rna *18*, 2041-2055.

Jaubert, M., Bhattacharjee, S., Mello, A.F., Perry, K.L., and Moffett, P. (2011). ARGONAUTE2 mediates RNA-silencing antiviral defenses against Potato virus X in Arabidopsis. Plant Physiol *156*, 1556-1564.

Ji, L., and Chen, X. (2012). Regulation of small RNA stability: methylation and beyond. Cell research *22*, 624-636.

Jung, J.H., and Park, C.M. (2007). MIR166/165 genes exhibit dynamic expression patterns in regulating shoot apical meristem and floral development in Arabidopsis. Planta *225*, 1327-1338.

Kai, Z.S., and Pasquinelli, A.E. (2010). MicroRNA assassins: factors that regulate the disappearance of miRNAs. Nature Structural & Molecular Biology *17*, 5-10.

Kawamata, T., Seitz, H., and Tomari, Y. (2009). Structural determinants of miRNAs for RISC loading and slicer-independent unwinding. Nature structural & molecular biology *16*, 953-960.

Kennedy, S., Wang, D., and Ruvkun, G. (2004). A conserved siRNA-degrading RNase negatively regulates RNA interference in C. elegans. Nature *427*, 645-649.

Kerstetter, R.A., Bollman, K., Taylor, R.A., Bomblies, K., and Poethig, R.S. (2001). KANADI regulates organ polarity in Arabidopsis. Nature *411*, 706-709.

Khan, A.A., Betel, D., Miller, M.L., Sander, C., Leslie, C.S., and Marks, D.S. (2009). Transfection of small RNAs globally perturbs gene regulation by endogenous microRNAs. Nature biotechnology *27*, 549-555.

Khvorova, A., Reynolds, A., and Jayasena, S.D. (2003). Functional siRNAs and miRNAs exhibit strand bias (vol 115, pg 209, 2003). Cell *115*, 505-505.

Kidner, C.A., and Martienssen, R.A. (2004). Spatially restricted microRNA directs leaf polarity through ARGONAUTE1. Nature *428*, 81-84.

Kidner, C.A., and Martienssen, R.A. (2005). The role of ARGONAUTE1 (AGO1) in meristem formation and identity. Developmental biology *280*, 504-517.

Kim, S., Yang, J.Y., Xu, J., Jang, I.C., Prigge, M.J., and Chua, N.H. (2008). Two cap-binding proteins CBP20 and CBP80 are involved in processing primary MicroRNAs. Plant & cell physiology *49*, 1634-1644.

Kim, V.N. (2008). Sorting out small RNAs. Cell *133*, 25-26.

Kim, V.N., Han, J. and Siomi, M.C. (2009). Biogenesis of small RNAs in animals. *Nat RevMol Cell Biol 10*, 126-139.

Klironomos, F.D., and Berg, J. (2013). Quantitative analysis of competition in posttranscriptional regulation reveals a novel signature in target expression variation. Biophysical journal *104*, 951-958.

Knouf, E.C., Wyman, S.K., and Tewari, M. (2013). The human TUT1 nucleotidyl transferase as a global regulator of microRNA abundance. PloS one *8*, e69630.

Krol, J., Loedige, I., and Filipowicz, W. (2010). The widespread regulation of microRNA biogenesis, function and decay. Nature reviews Genetics *11*, 597-610.

Krutzfeldt, J., Kuwajima, S., Braich, R., Rajeev, K.G., Pena, J., Tuschl, T., Manoharan, M., and Stoffel, M. (2007). Specificity, duplex degradation and subcellular localization of antagomirs. Nucleic acids research *35*, 2885-2892.

Krutzfeldt, J., Rajewsky, N., Braich, R., Rajeev, K.G., Tuschl, T., Manoharan, M., and Stoffel, M. (2005). Silencing of microRNAs in vivo with 'antagomirs'. Nature *438*, 685-689.

Kurihara, Y., and Watanabe, Y. (2004). *Arabidopsis* micro-RNA biogenesis through Dicer-like 1 protein functions. . *Proc Natl Acad Sci USA 101*, 12753-12758.

Kwak, P.B., and Tomari, Y. (2012). The N domain of Argonaute drives duplex unwinding during RISC assembly. Nature structural & molecular biology *19*, 145-151.

Lau, N.C., Lim, L.P., Weinstein, E.G., and Bartel, D.P. (2001). An abundant class of tiny RNAs with probable regulatory roles in Caenorhabditis elegans. Science *294*, 858-862.

Laubinger, S., Sachsenberg, T., Zeller, G., Busch, W., Lohmann, J.U., Rascht, G., and Weigel, D. (2008). Dual roles of the nuclear cap-binding complex and SERRATE in pre-mRNA splicing and microRNA processing in Arabidopsis thaliana. Proceedings of the National Academy of Sciences of the United States of America *105*, 8795-8800.

Lee, Y.S., Pressman, S., Andress, A.P., Kim, K., White, J.L., Cassidy, J.J., Li, X., Lubell, K., Lim do, H., Cho, I.S., *et al.* (2009). Silencing by small RNAs is linked to endosomal trafficking. Nature cell biology *11*, 1150-1156.

Leibfried, A., To, J.P., Busch, W., Stehling, S., Kehle, A., Demar, M., Kieber, J.J., and Lohmann, J.U. (2005). WUSCHEL controls meristem function by direct regulation of cytokinin-inducible response regulators. Nature *438*, 1172-1175.

Leuschner, P.J., Ameres, S.L., Kueng, S., and Martinez, J. (2006). Cleavage of the siRNA passenger strand during RISC assembly in human cells. EMBO reports *7*, 314-320.

Levy, C., Khaled, M., Robinson, K.C., Veguilla, R.A., Chen, P.H., Yokoyama, S., Makino, E., Lu, J., Larue, L., Beermann, F., *et al.* (2010). Lineage-specific transcriptional regulation of DICER by MITF in melanocytes. Cell *141*, 994-1005.

Li, C.F., Pontes, O., El-Shami, M., Henderson, I.R., Bernatavichute, Y.V., Chan, S.W., Lagrange, T., Pikaard, C.S., and Jacobsen, S.E. (2006). An ARGONAUTE4-containing nuclear processing center colocalized with Cajal bodies in Arabidopsis thaliana. Cell *126*, 93-106.

Li, J., Yang, Z., Yu, B., Liu, J., and Chen, X. (2005). Methylation protects miRNAs and siRNAs from a 3'-end uridylation activity in Arabidopsis. Curr Biol *15*, 1501-1507.

Li, S., Liu, L., Zhuang, X., Yu, Y., Liu, X., Cui, X., Ji, L., Pan, Z., Cao, X., Mo, B., *et al.* (2013). MicroRNAs inhibit the translation of target mRNAs on the endoplasmic reticulum in Arabidopsis. Cell *153*, 562-574.

Lima, W.F., Wu, H., Nichols, J.G., Sun, H., Murray, H.M., and Crooke, S.T. (2009). Binding and cleavage specificities of human Argonaute2. The Journal of biological chemistry *284*, 26017-26028.

Lindbo, J.A. (2012). A historical overview of RNAi in plants. Methods in molecular biology *894*, 1-16.

Liu, J., Carmell, M.A., Rivas, F.V., Marsden, C., Thomson, J.M., Song, J., Vachon, S.M., Joshua-Tor, L., and Hannon, G.J. (2004). Argonaute2 Is the Catalytic Engine of Mammalian RNAi. Science.

Liu, J., Rivas, F.V., Wohlschlegel, J., Yates, J.R., 3rd, Parker, R., and Hannon, G.J. (2005a). A role for the P-body component GW182 in microRNA function. Nature cell biology *7*, 1261-1266.

Liu, J., Valencia-Sanchez, M.A., Hannon, G.J., and Parker, R. (2005b). MicroRNA-dependent localization of targeted mRNAs to mammalian P-bodies. Nature cell biology *7*, 719-723.

Liu, N., Abe, M., Sabin, L.R., Hendriks, G.J., Naqvi, A.S., Yu, Z., Cherry, S., and Bonini, N.M. (2011a). The exoribonuclease Nibbler controls 3' end processing of microRNAs in Drosophila. Current biology : CB *21*, 1888-1893.

Liu, Q., Rand, T.A., Kalidas, S., Du, F., Kim, H.E., Smith, D.P., and Wang, X. (2003). R2D2, a bridge between the initiation and effector steps of the Drosophila RNAi pathway. Science *301*, 1921-1925.

Liu, Q., Yao, X., Pi, L., Wang, H., Cui, X., and Huang, H. (2009a). The ARGONAUTE10 gene modulates shoot apical meristem maintenance and establishment of leaf polarity by repressing miR165/166 in Arabidopsis. The Plant journal : for cell and molecular biology *58*, 27-40.

Liu, Q.L., Yao, X.Z., Pi, L.M., Wang, H., Cui, X.F., and Huang, H. (2009b). The ARGONAUTE10 gene modulates shoot apical meristem maintenance and establishment of leaf polarity by repressing miR165/166 in Arabidopsis. Plant Journal *58*, 27-40.

Liu, Y., Tan, H., Tian, H., Liang, C., Chen, S., and Liu, Q. (2011b). Autoantigen La promotes efficient RNAi, antiviral response, and transposon silencing by facilitating multiple-turnover RISC catalysis. Molecular cell *44*, 502-508.

Liu, Y., Ye, X., Jiang, F., Liang, C., Chen, D., Peng, J., Kinch, L.N., Grishin, N.V., and Liu, Q. (2009c). C3PO, an endoribonuclease that promotes RNAi by facilitating RISC activation. Science *325*, 750-753.

Lobbes, D., Rallapalli, G., Schmidt, D.D., Martin, C., and Clarke, J. (2006). SERRATE: a new player on the plant microRNA scene. EMBO reports *7*, 1052-1058.

Long, J.A., and Barton, M.K. (1998). The development of apical embryonic pattern in Arabidopsis. Development *125*, 3027-3035.

Long, J.A., Moan, E.I., Medford, J.I., and Barton, M.K. (1996). A member of the KNOTTED class of homeodomain proteins encoded by the STM gene of Arabidopsis. Nature *379*, 66-69.

Lu, J., Getz, G., Miska, E.A., Alvarez-Saavedra, E., Lamb, J., Peck, D., Sweet-Cordero, A., Ebert, B.L., Mak, R.H., Ferrando, A.A., *et al.* (2005). MicroRNA expression profiles classify human cancers. Nature *435*, 834-838.

Lund, E., Sheets, M.D., Imboden, S.B., and Dahlberg, J.E. (2011). Limiting Ago protein restricts RNAi and microRNA biogenesis during early development in Xenopus laevis. Genes & development *25*, 1121-1131.

Lynn, K., Fernandez, A., Aida, M., Sedbrook, J., Tasaka, M., Masson, P., and Barton, M.K. (1999). The *PINHEAD/ZWILLE* gene acts pleiotropically in *Arabidopsis* development and has overlapping functions with the *ARGONAUTE1* gene. Development *126*, 469-481.

Magnani, E., and Barton, M.K. (2011). A per-ARNT-sim-like sensor domain uniquely regulates the activity of the homeodomain leucine zipper transcription factor REVOLUTA in Arabidopsis. The Plant cell *23*, 567-582.

Maiti, M., Lee, H.C., and Liu, Y. (2007). QIP, a putative exonuclease, interacts with the Neurospora Argonaute protein and facilitates conversion of duplex siRNA into single strands. Genes & development *21*, 590-600.

Mallory, A., Reinhart, B.J., Jones-Rhoades, M.W., Tang, G., Zamore, P.D., Barton, M.K., and Bartel, D.P. (2004). MicroRNA control of PHABULOSA in leaf development importance of pairing to the microRNA 5 region. EMBO Journal *23*, 3356-3364.

Mallory, A., and Vaucheret, H. (2010a). Form, function, and regulation of ARGONAUTE proteins. The Plant cell *22*, 3879-3889.

Mallory, A., and Vaucheret, H. (2010b). Form, Function, and Regulation of ARGONAUTE Proteins. The Plant Cell Online *22*, 3879-3889.

Mallory, A.C., Hinze, A., Tucker, M.R., Bouche, N., Gasciolli, V., Elmayan, T., Lauressergues, D., Jauvion, V., Vaucheret, H., and Laux, T. (2009). Redundant and specific roles of the ARGONAUTE proteins AGO1 and ZLL in development and small RNA-directed gene silencing. PLoS genetics *5*, 1000646.

Mallory, A.C., and Vaucheret, H. (2009). ARGONAUTE 1 homeostasis invokes the coordinate action of the microRNA and siRNA pathways. EMBO reports *10*, 521-526.

Marin-Gonzalez, E., and Suarez-Lopez, P. (2012). "And yet it moves": cell-to-cell and long-distance signaling by plant microRNAs. Plant science : an international journal of experimental plant biology *196*, 18-30.

Martinez de Alba, A.E., Elvira-Matelot, E., and Vaucheret, H. (2013). Gene silencing in plants: A diversity of pathways. Biochimica et biophysica acta *1829*, 1300-1308.

Martinez de Alba, A.E., Jauvion, V., Mallory, A.C., Bouteiller, N., and Vaucheret, H. (2011). The miRNA pathway limits AGO1 availability during siRNA-mediated PTGS defense against exogenous RNA. Nucleic acids research *39*, 9339-9344.

Martinez, N.J., and Gregory, R.I. (2013). Argonaute2 expression is post-transcriptionally coupled to microRNA abundance. RNA *19*, 605-612.

Matranga, C., Tomari, Y., Shin, C., Bartel, D.P., and Zamore, P.D. (2005). Passenger-strand cleavage facilitates assembly of siRNA into Ago2-containing RNAi enzyme complexes. Cell *123*, 607-620.

Matzke, M., Kanno, T., Daxinger, L., Huettel, B., and Matzke, A.J. (2009). RNA-mediated chromatin-based silencing in plants. Current opinion in cell biology *21*, 367-376.

Mayer, K.F., Schoof, H., Haecker, A., Lenhard, M., Jurgens, G., and Laux, T. (1998). Role of WUSCHEL in regulating stem cell fate in the Arabidopsis shoot meristem. Cell *95*, 805-815.

McConnell, J.R., Emery, J., Eshed, Y., Bao, N., Bowman, J., and Barton, M.K. (2001). Role of PHABULOSA and PHAVOLUTA in determining radial patterning in shoots. Nature.

Megraw, M., Baev, V., Rusinov, V., Jensen, S.T., Kalantidis, K., and Hatzigeorgiou, A.G. (2006). MicroRNA promoter element discovery in Arabidopsis. RNA *12*, 1612-1619.

Meister, G., Landthaler, M., Patkaniowska, A., Dorsett, Y., Teng, G., and Tuschl, T. (2004). Human Argonaute2 mediates RNA cleavage targeted by miRNAs and siRNAs. Molecular cell *15*, 185-197.

Meister, G., Landthaler, M., Peters, L., Chen, P.Y., Urlaub, H., Luhrmann, R., and Tuschl, T. (2005). Identification of novel argonaute-associated proteins. Current biology *15*, 2149-2155.

Mi, S., Cai, T., Hu, Y., Chen, Y., Hodges, E., Ni, F., Wu, L., Li, S., Zhou, H., Long, C., *et al.* (2008). Sorting of small RNAs into Arabidopsis argonaute complexes is directed by the 5' terminal nucleotide. Cell *133*, 116-127.

Mica, E., Piccolo, V., Delledonne, M., Ferrarini, A., Pezzotti, M., Casati, C., Del Fabbro, C., Valle, G., Policriti, A., Morgante, M., *et al.* (2009). High throughput approaches reveal splicing of primary microRNA transcripts and tissue specific expression of mature microRNAs in Vitis vinifera. BMC genomics *10*, 558.

Miyashima, S., Honda, M., Hashimoto, K., Tatematsu, K., Hashimoto, T., Sato-Nara, K., Okada, K., and Nakajima, K. (2013). A comprehensive expression analysis of the Arabidopsis MICRORNA165/6 gene family during embryogenesis reveals a conserved role in meristem specification and a non-cell-autonomous function. Plant & cell physiology *54*, 375-384.

Miyashima, S., Koi, S., Hashimoto, T., and Nakajima, K. (2011). Non-cell-autonomous microRNA165 acts in a dose-dependent manner to regulate multiple differentiation status in the Arabidopsis root. Development *138*, 2303-2313.

Miyoshi, K., Tsukumo, H., Nagami, T., Siomi, H., and Siomi, M.C. (2005). Slicer function of Drosophila Argonautes and its involvement in RISC formation. Genes & development *19*, 2837-2848.

Miyoshi, T., Takeuchi, A., Siomi, H., and Siomi, M.C. (2010). A direct role for Hsp90 in pre-RISC formation in Drosophila. Nature structural & molecular biology *17*, 1024-1026.

Montgomery, T.A., Howell, M.D., Cuperus, J.T., Li, D., Hansen, J.E., Alexander, A.L., Chapman, E.J., Fahlgren, N., Allen, E., and Carrington, J.C. (2008a). Specificity of ARGONAUTE7-miR390 Interaction and Dual Functionality in TAS3 Trans-Acting siRNA Formation. Cell *133*, 128-141.

Montgomery, T.A., Howell, M.D., Cuperus, J.T., Li, D., Hansen, J.E., Alexander, A.L., Chapman, E.J., Fahlgren, N., Allen, E., and Carrington, J.C. (2008b). Specificity of ARGONAUTE7-miR390 interaction and dual functionality in TAS3 trans-acting siRNA formation. Cell *133*, 128-141.

Motomura, K., Le, Q.T., Kumakura, N., Fukaya, T., Takeda, A., and Watanabe, Y. (2012). The role of decapping proteins in the miRNA accumulation in Arabidopsis thaliana. RNA biology *9*, 644-652.

Moussian, B., Schoof, H., Haecker, A., Jurgens, G., and Laux, T. (1998a). Role of the ZWILLE gene in the regulation of central shoot meristem cell fate during Arabidopsis embryogenesis. EMBO J *17*, 1799-1809.

Moussian, B., Schoof, H., Haecker, A., rgens, G.J., and Laux, T. (1998b). Role of the ZWILLE gene in the regulation of central shoot meristem cell fate during Arabidopsis embryogenesis. The EMBO journal.

Mukherjee, K., and Burglin, T.R. (2006). MEKHLA, a novel domain with similarity to PAS domains, is fused to plant homeodomain-leucine zipper III proteins. Plant physiology *140*, 1142-1150.

Muller, R., Borghi, L., Kwiatkowska, D., Laufs, P., and Simon, R. (2006). Dynamic and compensatory responses of Arabidopsis shoot and floral meristems to CLV3 signaling. The Plant cell *18*, 1188-1198.

Napoli, C., Lemieux, C., and Jorgensen, R. (1990). lntroduction of a Chimeric Chalcone Synthase Gene into Petunia Results in Reversible Co-Suppression of Homologous Genes *in trans*. The Plant Cell *2*, 279-289.

Noland, C.L., and Doudna, J.A. (2013). Multiple sensors ensure guide strand selection in human RNAi pathways. RNA *19*, 639-648.

Norbury, C.J. (2010). 3' Uridylation and the regulation of RNA function in the cytoplasm. Biochem Soc Trans *38*, 1150-1153.

Nowotny, M., Gaidamakov, S.A., Crouch, R.J., and Yang, W. (2005). Crystal structures of RNase H bound to an RNA/DNA hybrid: substrate specificity and metal-dependent catalysis. Cell *121*, 1005-1016.

Nykanen, A., Haley, B., and Zamore, P.D. (2001). ATP requirements and small interfering RNA structure in the RNA interference pathway. Cell *107*, 309-321.

O'Carroll, D., Mecklenbrauker, I., Das, P.P., Santana, A., Koenig, U., Enright, A.J., Miska, E.A., and Tarakhovsky, A. (2007). A Slicer-independent role for Argonaute 2 in hematopoiesis and the microRNA pathway. Genes & development *21*, 1999-2004.

Okamura, K., Ishizuka, A., Siomi, H., and Siomi, M.C. (2004). Distinct roles for Argonaute proteins in small RNA-directed RNA cleavage pathways. Genes & development *18*, 1655-1666.

Okamura, K., Ladewig, E., Zhou, L., and Lai, E.C. (2013). Functional small RNAs are generated from select miRNA hairpin loops in flies and mammals. Genes & development *27*, 778-792.

Okamura, K., Phillips, M.D., Tyler, D.M., Duan, H., Chou, Y.T., and Lai, E.C. (2008). The regulatory activity of microRNA star species has substantial influence on microRNA and 3 ' UTR evolution. Nature structural & molecular biology *15*, 354-363.

Parent, J.S., Martinez de Alba, A.E., and Vaucheret, H. (2012). The origin and effect of small RNA signaling in plants. Frontiers in plant science *3*, 179.

Parker, J.S. (2010). How to slice: snapshots of Argonaute in action. Silence *1*, 3.

Parker, J.S., Roe, S.M., and Barford, D. (2004). Crystal structure of a PIWI protein suggests mechanisms for siRNA recognition and slicer activity. EMBO J *23*, 4727-4737.

Parker, R., and Song, H.W. (2004). The enzymes and control of eukaryotic mRNA turnover. Nature structural & molecular biology *11*, 121-127.

Pham, J.W., Pellino, J.L., Lee, Y.S., Carthew, R.W., and Sontheimer, E.J. (2004). A Dicer-2-dependent 80s complex cleaves targeted mRNAs during RNAi in Drosophila. Cell *117*, 83-94.

Pinder, B.D., and Smibert, C.A. (2013). microRNA-independent recruitment of Argonaute 1 to nanos mRNA through the Smaug RNA-binding protein. EMBO reports *14*, 80-86.

Ponting, C.P., and Aravind, L. (1999). START: a lipid-binding domain in StAR, HD-ZIP and signalling proteins. Trends in biochemical sciences *24*, 130-132.

Preall, J.B., and Sontheimer, E.J. (2005). RNAi: RISC gets loaded. Cell *123*, 543-545.

Prigge, M.J., Otsuga, D., Alonso, J.M., Ecker, J.R., Drews, G.N., and Clark, S.E. (2005). Class III homeodomain-leucine zipper gene family members have overlapping, antagonistic, and distinct roles in Arabidopsis development. The Plant cell *17*, 61-76.

Qi, H.H., Ongusaha, P.P., Myllyharju, J., Cheng, D., Pakkanen, O., Shi, Y., Lee, S.W., Peng, J., and Shi, Y. (2008). Prolyl 4-hydroxylation regulates Argonaute 2 stability. Nature *455*, 421-424.

Qi, Y., Denli, A.M., and Hannon, G.J. (2005a). Biochemical specialization within Arabidopsis RNA silencing pathways. Molecular cell *19*, 421-428.

Qi, Y., Denli, A.M., and Hannon, G.J. (2005b). Biochemical Specialization within Arabidopsis RNA Silencing Pathways. Molecular Cell *19*, 421-428.

Qi, Y., He, X., Wang, X.J., Kohany, O., Jurka, J., and Hannon, G.J. (2006). Distinct catalytic and non-catalytic roles of ARGONAUTE4 in RNA-directed DNA methylation. Nature *443*, 1008-1012.

Qian, Y., Cheng, Y., Cheng, X., Jiang, H., Zhu, S., and Cheng, B. (2011). Identification and characterization of Dicer-like, Argonaute and RNA-dependent RNA polymerase gene families in maize. Plant cell reports *30*, 1347-1363.

Ramachandran, V., and Chen, X. (2008a). Degradation of microRNAs by a family of exoribonucleases in Arabidopsis. Science *321*, 1490-1492.

Ramachandran, V., and Chen, X. (2008b). Small RNA metabolism in Arabidopsis. Trends in Plant Science *13*, 368-374.

Rand, T.A., Petersen, S., Du, F., and Wang, X. (2005). Argonaute2 cleaves the anti-guide strand of siRNA during RISC activation. Cell *123*, 621-629.

Reddy, G.V. (2008). Live-imaging stem-cell homeostasis in the Arabidopsis shoot apex. Current opinion in plant biology *11*, 88-93.

Reddy, G.V., and Meyerowitz, E.M. (2005). Stem-cell homeostasis and growth dynamics can be uncoupled in the Arabidopsis shoot apex. Science *310*, 663-667.

Reinhardt, D., Pesce, E.R., Stieger, P., Mandel, T., Baltensperger, K., Bennett, M., Traas, J., Friml, J., and Kuhlemeier, C. (2003). Regulation of phyllotaxis by polar auxin transport. Nature *426*, 255-260.

Reinhart, B.J., Liu, T., Newell, N.R., Magnani, E., Huang, T., Kerstetter, R., Michaels, S., and Barton, M.K. (2013). Establishing a framework for the Ad/abaxial regulatory network of Arabidopsis: ascertaining targets of class III homeodomain leucine zipper and KANADI regulation. The Plant cell *25*, 3228-3249.

Ren, G., Chen, X., and Yu, B. (2012a). Uridylation of miRNAs by hen1 suppressor1 in Arabidopsis. Current biology : CB *22*, 695-700.

Ren, G., Xie, M., Dou, Y., Zhang, S., Zhang, C., and Yu, B. (2012b). Regulation of miRNA abundance by RNA binding protein TOUGH in Arabidopsis. Proceedings of the National Academy of Sciences of the United States of America *109*, 12817-12821.

Ren, G., Xie, M., Zhang, S., Vinovskis, C., Chen, X., and Yu, B. (2014). Methylation protects microRNAs from an AGO1-associated activity that uridylates 5' RNA

fragments generated by AGO1 cleavage. Proceedings of the National Academy of Sciences of the United States of America.

Rivas, F.V., Tolia, N.H., Song, J.J., Aragon, J.P., Liu, J., Hannon, G.J., and Joshua-Tor, L. (2005). Purified Argonaute2 and an siRNA form recombinant human RISC. Nature structural & molecular biology *12*, 340-349.

Rogers, K., and Chen, X. (2013a). Biogenesis, turnover, and mode of action of plant microRNAs. The Plant cell *25*, 2383-2399.

Rogers, K., and Chen, X. (2013b). microRNA Biogenesis and Turnover in Plants. Cold Spring Harbor symposia on quantitative biology.

Ruby, J.G., Stark, A., Johnston, W.K., Kellis, M., Bartel, D.P., and Lai, E.C. (2007). Evolution, biogenesis, expression, and target predictions of a substantially expanded set of Drosophila microRNAs. Genome Res *17*, 1850-1864.

Rybak, A., Fuchs, H., Hadian, K., Smirnova, L., Wulczyn, E.A., Michel, G., Nitsch, R., Krappmann, D., and Wulczyn, F.G. (2009). The let-7 target gene mouse lin-41 is a stem cell specific E3 ubiquitin ligase for the miRNA pathway protein Ago2. Nature cell biology *11*, 1411-1420.

Salmena, L., Poliseno, L., Tay, Y., Kats, L., and Pandolfi, P.P. (2011). A ceRNA hypothesis: the Rosetta Stone of a hidden RNA language? Cell *146*, 353-358.

Salzman, J., Gawad, C., Wang, P.L., Lacayo, N., and Brown, P.O. (2012). Circular RNAs are the predominant transcript isoform from hundreds of human genes in diverse cell types. PloS one *7*, e30733.

Scanlon, M.J. (2003). The polar auxin transport inhibitor N-1-naphthylphthalamic acid disrupts leaf initiation, KNOX protein regulation, and formation of leaf margins in maize. Plant physiology *133*, 597-605.

Schirle, N.T., and MacRae, I.J. (2012). The crystal structure of human Argonaute2. Science *336*, 1037-1040.

Schmid, M., Davison, T.S., Henz, S.R., Pape, U.J., Demar, M., Vingron, M., Scholkopf, B., Weigel, D., and Lohmann, J.U. (2005). A gene expression map of Arabidopsis thaliana development. Nature genetics *37*, 501-506.

Schoof, H., Lenhard, M., Haecker, A., Mayer, K.F., Jurgens, G., and Laux, T. (2000). The stem cell population of Arabidopsis shoot meristems in maintained by a regulatory loop between the CLAVATA and WUSCHEL genes. Cell *100*, 635-644.

Schurmann, N., Trabuco, L.G., Bender, C., Russell, R.B., and Grimm, D. (2013). Molecular dissection of human Argonaute proteins by DNA shuffling. Nature structural & molecular biology *20*, 818-826.

Schwarz, D.S., Hutvagner, G., Du, T., Xu, Z.S., Aronin, N., and Zamore, P.D. (2003). Asymmetry in the assembly of the RNAi enzyme complex. Cell *115*, 199-208.

Scott, D.D., and Norbury, C.J. (2013). RNA decay via 3' uridylation. Biochimica et biophysica acta.

Seitz, H. (2009). Redefining microRNA targets. Current biology : CB *19*, 870-873.

Sessa, G., Steindler, C., Morelli, G., and Ruberti, I. (1998). The Arabidopsis Athb-8, -9 and -14 genes are members of a small gene family coding for highly related HD-ZIP proteins. Plant molecular biology *38*, 609-622.

Shen, J., Xia, W., Khotskaya, Y.B., Huo, L., Nakanishi, K., Lim, S.O., Du, Y., Wang, Y., Chang, W.C., Chen, C.H., *et al.* (2013). EGFR modulates microRNA maturation in response to hypoxia through phosphorylation of AGO2. Nature *497*, 383-387.

Siomi, H., and Siomi, M.C. (2009). RISC hitches onto endosome trafficking. Nature cell biology *11*, 1049-1051.

Smibert, P., Yang, J.S., Azzam, G., Liu, J.L., and Lai, E.C. (2013). Homeostatic control of Argonaute stability by microRNA availability. Nature structural & molecular biology *20*, 789-795.

Song, J.J., Smith, S.K., Hannon, G.J., and Joshua-Tor, L. (2004). Crystal structure of Argonaute and its implications for RISC slicer activity. Science *305*, 1434-1437.

Song, L., Han, M., Lesicka, J. and Fedoroff, N. (2007). *Arabidopsis* primary microRNA processing proteins HYL1 and DCL1 define a nuclear body distinct from the Cajal body. *Proc Natl Acad Sci USA 104*, 5437-5442.

Sood, P., Krek, A., Zavolan, M., Macino, G., and Rajewsky, N. (2006). Cell-type-specific signatures of microRNAs on target mRNA expression. Proceedings of the National Academy of Sciences of the United States of America *103*, 2746-2751.

Speth, C., Willing, E.M., Rausch, S., Schneeberger, K., and Laubinger, S. (2013). RACK1 scaffold proteins influence miRNA abundance in Arabidopsis. The Plant journal : for cell and molecular biology *76*, 433-445.

Steiner, F.A., Hoogstrate, S.W., Okihara, K.L., Thijssen, K.L., Ketting, R.F., Plasterk, R.H., and Sijen, T. (2007). Structural features of small RNA precursors determine Argonaute loading in Caenorhabditis elegans. Nature structural & molecular biology *14*, 927-933.

Su, X., Chakravarti, D., Cho, M.S., Liu, L., Gi, Y.J., Lin, Y.L., Leung, M.L., El-Naggar, A., Creighton, C.J., Suraokar, M.B., *et al.* (2010). TAp63 suppresses metastasis through coordinate regulation of Dicer and miRNAs. Nature *467*, 986-990.

Szarzynska, B., Sobkowiak, L., Pant, B.D., Balazadeh, S., Scheible, W.R., Mueller-Roeber, B., Jarmolowski, A., and Szweykowska-Kulinska, Z. (2009). Gene structures and processing of Arabidopsis thaliana HYL1-dependent pri-miRNAs. Nucleic acids research *37*, 3083-3093.

Takeda, A., Iwasaki, S., Watanabe, T., Utsumi, M., and Watanabe, Y. (2008). The mechanism selecting the guide strand from small RNA duplexes is different among argonaute proteins. Plant & cell physiology *49*, 493-500.

Tay, Y., Rinn, J., and Pandolfi, P.P. (2014). The multilayered complexity of ceRNA crosstalk and competition. Nature *505*, 344-352.

Todesco, M., Rubio-Somoza, I., Paz-Ares, J., and Weigel, D. (2010). A collection of target mimics for comprehensive analysis of microRNA function in Arabidopsis thaliana. PLoS genetics *6*, e1001031.

Tomari, Y., Du, T., Haley, B., Schwarz, D.S., Bennett, R., Cook, H.A., Koppetsch, B.S., Theurkauf, W.E., and Zamore, P.D. (2004). RISC assembly defects in the Drosophila RNAi mutant armitage. Cell *116*, 831-841.

Tomari, Y., Du, T., and Zamore, P.D. (2007). Sorting of Drosophila small silencing RNAs. Cell *130*, 299-308.

Tretter, E.M., Alvarez, J.P., Eshed, Y., and Bowman, J.L. (2008). Activity Range of Arabidopsis Small RNAs Derived from Different Biogenesis Pathways. Plant Physiology *147*, 58-62.

Tucker, M.R., Hinze, A., Tucker, E.J., Takada, S., Jurgens, G., and Laux, T. (2008). Vascular signalling mediated by ZWILLE potentiates WUSCHEL function during shoot meristem stem cell development in the Arabidopsis embryo. Development *135*, 2839-2843.

van Wolfswinkel, J.C., Claycomb, J.M., Batista, P.J., Mello, C.C., Berezikov, E., and Ketting, R.F. (2009). CDE-1 affects chromosome segregation through uridylation of CSR-1-bound siRNAs. Cell *139*, 135-148.

Vaucheret, H. (2008). Plant ARGONAUTES. Trends in Plant Science *13*, 350-358.

Vaucheret, H., Mallory, A.C., and Bartel, D.P. (2006). AGO1 homeostasis entails coexpression of MIR168 and AGO1 and preferential stabilization of miR168 by AGO1. Molecular cell *22*, 129-136.

Vaucheret, H., Vazquez, F., Crete, P., and Bartel, D.P. (2004). The action of ARGONAUTE1 in the miRNA pathway and its regulation by the miRNA pathway are crucial for plant development. Genes & development *18*, 1187-1197.

Vazquez, F., Gasciolli, V., Crete, P., and Vaucheret, H. (2004). The nuclear dsRNA binding protein HYL1 is required for MicroRNA accumulation and plant development, but not posttranscriptional transgene silencing. Current Biology *14*, 346-351.

Voinnet, O. (2005). Non-cell autonomous RNA silencing. FEBS letters *579*, 5858-5871.

Voinnet, O. (2009). Origin, Biogenesis, and Activity of Plant MicroRNAs. Cell *136*, 669-687.

Wang, H., Zhang, X., Liu, J., Kiba, T., Woo, J., Ojo, T., Hafner, M., Tuschl, T., Chua, N.-H., and Wang, X.-J. (2011a). Deep sequencing of small RNAs specifically associated

with Arabidopsis AGO1 and AGO4 uncovers new AGO functions. The Plant Journal *67*, 292-304.

Wang, H., Zhang, X., Liu, J., Kiba, T., Woo, J., Ojo, T., Hafner, M., Tuschl, T., Chua, N.H., and Wang, X.J. (2011b). Deep sequencing of small RNAs specifically associated with Arabidopsis AGO1 and AGO4 uncovers new AGO functions. The Plant journal : for cell and molecular biology *67*, 292-304.

Wang, X., Zhao, X., Gao, P., and Wu, M. (2013). c-Myc modulates microRNA processing via the transcriptional regulation of Drosha. Scientific reports *3*, 1942.

Wang, Y., Juranek, S., Li, H., Sheng, G., Wardle, G.S., Tuschl, T., and Patel, D.J. (2009). Nucleation, propagation and cleavage of target RNAs in Ago silencing complexes. Nature *461*, 754-761.

Wienholds, E., Kloosterman, W.P., Miska, E., Alvarez-Saavedra, E., Berezikov, E., de Bruijn, E., Horvitz, H.R., Kauppinen, S., and Plasterk, R.H. (2005). MicroRNA expression in zebrafish embryonic development. Science *309*, 310-311.

Williams, L., Grigg, S.P., Xie, M., Christensen, S., and Fletcher, J.C. (2005). Regulation of Arabidopsis shoot apical meristem and lateral organ formation by microRNA miR166g and its AtHD-ZIP target genes. Development *132*, 3657-3668.

Wilusz, C.J., and Wilusz, J. (2004). Bringing the role of mRNA decay in the control of gene expression into focus. Trends in genetics : TIG *20*, 491-497.

Wyman, S.K., Knouf, E.C., Parkin, R.K., Fritz, B.R., Lin, D.W., Dennis, L.M., Krouse, M.A., Webster, P.J., and Tewari, M. (2011). Post-transcriptional generation of miRNA variants by multiple nucleotidyl transferases contributes to miRNA transcriptome complexity. Genome Res *21*, 1450-1461.

Xie, M., Tataw, M., and Venugopala Reddy, G. (2009). Towards a functional understanding of cell growth dynamics in shoot meristem stem-cell niche. Seminars in cell & developmental biology *20*, 1126-1133.

Xie, Z., Allen, E., Fahlgren, N., Calamar, A., Givan, S.A., and Carrington, J.C. (2005). Expression of Arabidopsis MIRNA genes. Plant physiology *138*, 2145-2154.

Xiong, X., Kurthkoti, K., Chang, K., Lichinchi, G., De, N., Schneemann, A., MacRae, I.J., Rana, T.M., Perrimon, N., and Zhou, R. (2013). Core small nuclear ribonucleoprotein particle splicing factor SmD1 modulates RNA interference in *Drosophila*. Proceedings of the National Academy of Sciences of the United States of America.

Xue, Z., Yuan, H., Guo, J., and Liu, Y. (2012). Reconstitution of an Argonaute-dependent small RNA biogenesis pathway reveals a handover mechanism involving the RNA exosome and the exonuclease QIP. Molecular cell *46*, 299-310.

Yang, J.S., Phillips, M.D., Betel, D., Mu, P., Ventura, A., Siepel, A.C., Chen, K.C., and Lai, E.C. (2011). Widespread regulatory activity of vertebrate microRNA* species. Rna *17*, 312-326.

Yang, L., Huang, W., Wang, H., Cai, R., Xu, Y., and Huang, H. (2006a). Characterizations of a hypomorphic argonaute1 mutant reveal novel AGO1 functions in Arabidopsis lateral organ development. Plant Mol Biol *61*, 63-78.

Yang, L., Wu, G., and Poethig, R.S. (2012). Mutations in the GW-repeat protein SUO reveal a developmental function for microRNA-mediated translational repression in Arabidopsis. Proceedings of the National Academy of Sciences of the United States of America *109*, 315-320.

Yang, Z., Ebright, Y.W., Yu, B., and Chen, X. (2006b). HEN1 recognizes 21-24 nt small RNA duplexes and deposits a methyl group onto the 2' OH of the 3' terminal nucleotide. Nucleic acids research *34*, 667-675.

Ye, R., Wang, W., Iki, T., Liu, C., Wu, Y., Ishikawa, M., Zhou, X., and Qi, Y. (2012). Cytoplasmic assembly and selective nuclear import of Arabidopsis Argonaute4/siRNA complexes. Molecular cell *46*, 859-870.

Ye, X., Huang, N., Liu, Y., Paroo, Z., Huerta, C., Li, P., Chen, S., Liu, Q., and Zhang, H. (2011). Structure of C3PO and mechanism of human RISC activation. Nature structural & molecular biology *18*, 650-657.

Yoda, M., Kawamata, T., Paroo, Z., Ye, X., Iwasaki, S., Liu, Q., and Tomari, Y. (2010). ATP-dependent human RISC assembly pathways. Nature structural & molecular biology *17*, 17-23.

Yuan, Y.-R., Pei, Y., Ma, J.-B., Kuryavyi, V., Zhadina, M., Meister, G., Chen, H.-Y., Dauter, Z., Tuschl, T., and Patel, D.J. (2005). Crystal Structure of A. aeolicus Argonaute, a Site-Specific DNA-Guided Endoribonuclease, Provides Insights into RISC-Mediated mRNA Cleavage. Molecular Cell *19*, 405-419.

Zekri, L., Kuzuoglu-Ozturk, D., and Izaurralde, E. (2013). GW182 proteins cause PABP dissociation from silenced miRNA targets in the absence of deadenylation. The EMBO journal *32*, 1052-1065.

Zeng, Y., Sankala, H., Zhang, X., and Graves, P.R. (2008). Phosphorylation of Argonaute 2 at serine-387 facilitates its localization to processing bodies. The Biochemical journal *413*, 429-436.

Zha, X., Xia, Q., and Yuan, Y.A. (2012). Structural insights into small RNA sorting and mRNA target binding by Arabidopsis Argonaute Mid domains. FEBS letters *586*, 3200-3207.

Zhan, X., Wang, B., Li, H., Liu, R., Kalia, R.K., Zhu, J.K., and Chinnusamy V. (2012). *Arabidopsis* proline-rich protein important for development and abiotic stress tolerance is involved in microRNA biogenesis. Proc Natl Acad Sci U.S.A. *109*, 18198–18203.

Zhang, B.H., Pan, X.P., Wang, Q.L., Cobb, G.P., and Anderson, T.A. (2005). Identification and characterization of new plant microRNAs using EST analysis. Cell research *15*, 336-360.

Zhang, X., Yuan, Y.R., Pei, Y., Lin, S.S., Tuschl, T., Patel, D.J., and Chua, N.H. (2006). Cucumber mosaic virus-encoded 2b suppressor inhibits Arabidopsis Argonaute1 cleavage activity to counter plant defense. Genes & development *20*, 3255-3268.

Zhang, X., Zhao, H., Gao, S., Wang, W.C., Katiyar-Agarwal, S., Huang, H.D., Raikhel, N., and Jin, H. (2011). Arabidopsis Argonaute 2 regulates innate immunity via miRNA393(*)-mediated silencing of a Golgi-localized SNARE gene, MEMB12. Mol Cell *42*, 356-366.

Zhang, Z., and Zhang, X. (2012). Argonautes compete for miR165/166 to regulate shoot apical meristem development. Current opinion in plant biology *15*, 652-658.

Zhao, Y., Yu, Y., Zhai, J., Ramachandran, V., Dinh, T.T., Meyers, B.C., Mo, B., and Chen, X. (2012). The Arabidopsis nucleotidyl transferase HESO1 uridylates unmethylated small RNAs to trigger their degradation. Current biology : CB *22*, 689-694.

Zheng, X., Zhu, J., Kapoor, A., and Zhu, J.-K. (2007). Role of Arabidopsis AGO6 in siRNA accumulation, DNA methylation and translational gene silencing. EMBO J *26*, 1691-1701.

Zhong, R., and Ye, Z.H. (2004). Amphivasal vascular bundle 1, a gain-of-function mutation of the IFL1/REV gene, is associated with alterations in the polarity of leaves, stems and carpels. Plant & cell physiology *45*, 369-385.

Zhou, G.K., Kubo, M., Zhong, R., Demura, T., and Ye, Z.H. (2007a). Overexpression of miR165 affects apical meristem formation, organ polarity establishment and vascular development in Arabidopsis. Plant & cell physiology *48*, 391-404.

Zhou, X., Wang, G., Sutoh, K., Zhu, J.K., and Zhang, W. (2008). Identification of cold-inducible microRNAs in plants by transcriptome analysis. Biochimica et biophysica acta *1779*, 780-788.

Zhou, X., Wang, G., and Zhang, W. (2007b). UV-B responsive microRNA genes in Arabidopsis thaliana. Molecular systems biology *3*, 103.

Zhu, H., Hu, F., Wang, R., Zhou, X., Sze, S.H., Liou, L.W., Barefoot, A., Dickman, M., and Zhang, X. (2011). Arabidopsis Argonaute10 specifically sequesters miR166/165 to regulate shoot apical meristem development. Cell *145*, 242-256.

Zhu, H., Zhou, Y., Castillo-Gonzalez, C., Lu, A., Ge, C., Zhao, Y.T., Duan, L., Li, Z., Axtell, M.J., Wang, X.J., *et al.* (2013). Bidirectional processing of pri-miRNAs with branched terminal loops by Arabidopsis Dicer-like1. Nature structural & molecular biology *20*, 1106-1115.

Zilberman, D., Cao, X., Johansen, L.K., Xie, Z., Carrington, J.C., and Jacobsen, S.E. (2004). Role of Arabidopsis ARGONAUTE4 in RNA-directed DNA methylation triggered by inverted repeats. Curr Biol *14*, 1214-1220.

Zilberman, D., Cao, X.F., and Jacobsen, S.E. (2003). ARGONAUTE4 control of locus-specific siRNA accumulation and DNA and histone methylation. Science *299*, 716-719.

Zuo, J., Niu, Q.W., and Chua, N.H. (2000). Technical advance: An estrogen receptor-based transactivator XVE mediates highly inducible gene expression in transgenic plants. The Plant journal : for cell and molecular biology *24*, 265-273.